

**ISTANBUL TECHNICAL UNIVERSITY ★ ENERGY INSTITUTE**

**DESIGN AND SIMULATION OF  
ELECTRIC VEHICLE FAST CHARGING STATION  
USING SOLAR AND WIND POWER**

**M.Sc. THESIS**

**Taha Nurettin GÜCİN**

**Energy Science and Technology Department  
Energy Science and Technology Programme**

**JANUARY 2013**



**ISTANBUL TECHNICAL UNIVERSITY ★ ENERGY INSTITUTE**

**DESIGN AND SIMULATION OF  
ELECTRIC VEHICLE FAST CHARGING STATION  
USING SOLAR AND WIND POWER**

**M.Sc. THESIS**

**Taha Nurettin GÜCİN  
(301101037)**

**Energy Science and Technology Department  
Energy Science and Technology Programme**

**Thesis Advisor: Prof. Dr. Filiz KARAOSMANOĞLU**

**JANUARY 2013**



**İSTANBUL TEKNİK ÜNİVERSİTESİ ★ ENERJİ ENSTİTÜSÜ**

**ELEKTRİKLİ ARAÇLAR İÇİN RÜZGAR VE GÜNEŞ ENERJİSİ KULLANAN  
HIZLI ŞARJ İSTASYONU TASARLANMASI VE SİMULASYONU**

**YÜKSEK LİSANS TEZİ**

**Taha Nurettin GÜCİN  
(301101037)**

**Enerji Bilim ve Teknoloji Anabilim Dalı**

**Enerji Bilim ve Teknoloji Programı**

**Tez Danışmanı: Prof. Dr. Filiz KARAOSMANOĞLU**

**OCAK 2013**



**Taha Nurettin GÜCİN**, a **M.Sc.** student of **ITU Energy Institute** student ID **301101037** successfully defended the **thesis** entitled “**DESIGN AND SIMULATION OF ELECTRIC VEHICLE FAST CHARGING STATION USING SOLAR AND WIND POWER**”, which he prepared after fulfilling the requirements specified in the associated legislations, before the jury whose signatures are below.

**Thesis Advisor :**      **Prof. Dr. Filiz KARAOSMANOĞLU**      .....

İstanbul Technical University

**Jury Members :**      **Prof. Dr. Metin GÖKAŞAN**      .....

İstanbul Technical University

**Assist. Prof. Dr. Burak BARUTÇU**      .....

İstanbul Technical University

**Date of Submission : 14 December 2012**

**Date of Defense : 24 January 2013**





## **FOREWORD**

I would like to express my deep appreciation and thanks to my supervisor Prof. Dr. Filiz Karaosmanođlu and Assist. Prof. Dr. Kayhan İnce for all the help, guidance and patience during this work. I would also like to thank all my colleagues at the Energy Systems Engineering Department of Yalova University for their constant support. Special thaks to my colleague Mr. Muhammet Biberođlu for showing cooperation and support throughout the process of our thesis work.

I am very very thankful to my dear wife, Nuray, and my fabulous family for supporting and encouraging me in all aspects of my life.

Istanbul, December 2012

Taha Nurettin Gücin  
(Electrical Engineer)



## TABLE OF CONTENTS

	<u>Page</u>
<b>FOREWORD</b> .....	<b>vii</b>
<b>ABBREVIATIONS</b> .....	<b>xi</b>
<b>LIST OF TABLES</b> .....	<b>xiii</b>
<b>LIST OF FIGURES</b> .....	<b>xv</b>
<b>SUMMARY</b> .....	<b>xvii</b>
<b>ÖZET</b> .....	<b>xix</b>
<b>1. INTRODUCTION</b> .....	<b>1</b>
1.1 Structure of the thesis .....	5
<b>2. THEORETICAL PART</b> .....	<b>7</b>
2.1 Renewable Energy Sources .....	7
2.1.1 Sun Power .....	8
2.1.2 Wind Power.....	10
2.2 Electric Vehicles .....	13
2.3 Battery charging .....	20
2.3.1 Constant voltage charging .....	21
2.3.2 Constant current charging .....	22
2.3.3 Constant current – constant voltage charging .....	22
2.3.4 Taper current charging .....	24
2.3.5 Pulsed current charging.....	24
2.4 Power Electronics Interfaces .....	26
2.4.1 Three phase bridge rectifier .....	26
2.4.2 Boost converter .....	27
2.4.3 Buck converter .....	29
2.4.4 Cuk converter .....	31
2.5 Control of Power Electronic Interfaces .....	33
2.5.1 Pulse-width modulation .....	34
2.5.2 PID control.....	34
2.5.3 Maximum power point tracking.....	37
2.5.3.1 MPPT for solar power .....	37
2.5.3.2 MPPT for wind power.....	40
2.6 Electric Vehicle Charging Standards .....	42
2.7 Literature Overview .....	45
<b>3. DESIGN AND SIMULATION PART</b> .....	<b>49</b>
3.1 System Design.....	49
3.1.1 Rectifiers .....	51
3.1.2 Grid side charger model.....	51
3.1.3 PV array model .....	53
3.1.4 Photovoltaic array charger model .....	54
3.1.5 Wind turbine model .....	56
3.1.6 Wind turbine charger model .....	58
3.1.7 Load side charger model .....	58

3.1.8 Battery model .....	59
3.1.9 Calculation of DC/DC converter parameters .....	60
3.1.10 Possible cases .....	61
3.1.11 System controller.....	61
3.2 System Simulation.....	69
3.2.1 Scenario 1 .....	70
3.2.2 Scenario 2 .....	70
3.2.3 Scenario 3 .....	72
3.2.4 Scenario 4.....	74
<b>4. CONCLUSION.....</b>	<b>79</b>
<b>REFERENCES .....</b>	<b>81</b>
<b>CURRICULUM VITAE.....</b>	<b>85</b>

## **ABBREVIATIONS**

<b>AC</b>	: Alternative Current
<b>CC</b>	: Constant Current
<b>CV</b>	: Constant Voltage
<b>CCM</b>	: Continuous Conduction Mode
<b>DC</b>	: Direct Current
<b>DCM</b>	: Discontinuous Conduction Mode
<b>EV</b>	: Electric Vehicle
<b>HCS</b>	: Hill Climb Search
<b>HEV</b>	: Hybrid Electric Vehicle
<b>HRES</b>	: Hybrid Renewable Energy System
<b>ICE</b>	: Internal Combustion Engine
<b>InCond</b>	: Incremental Conductance
<b>ISO</b>	: International Standardization Organization
<b>JARI</b>	: Japan Automotive Research Industry
<b>MPP</b>	: Maximum Power Point
<b>MPPT</b>	: Maximum Power Point Tracking
<b>P&amp;O</b>	: Perturb and Observe
<b>PSF</b>	: Power Signal Feedback
<b>PWM</b>	: Pulse Width Modulation
<b>RES</b>	: Renewable Energy System
<b>SAE</b>	: Society of Automotive Engineers
<b>TSR</b>	: Tip Speed Ratio
<b>VPC</b>	: Voltage per Cell



## LIST OF TABLES

	<u>Page</u>
<b>Table 2.1</b> : Average power and energy requirements of diferent EVs.....	21
<b>Table 2.2</b> : AC charging levels in EU and N.A. ....	44
<b>Table 2.3</b> : DC charging levels defined in J1722 .....	44
<b>Table 3.1</b> : Calculation of DC/DC converter parameters.....	60
<b>Table 3.2</b> : Possible cases.....	62
<b>Table 3.3</b> : Control signals for possible cases. ....	67





## LIST OF FIGURES

	<u>Page</u>
<b>Figure 1.1:</b> World final total energy consumption by fuel (Mtoe).....	1
<b>Figure 1.2 :</b> Share of CO <sub>2</sub> emissions by fuel (Mt) . ....	2
<b>Figure 1.3 :</b> Dependency of energy on sources imported from foreign countries. ....	2
<b>Figure 2.1 :</b> General HRES structure. ....	8
<b>Figure 2.2 :</b> (a) PV Cells connected in series and parallel (b) I-V characteristic for ideal and real PV cells with different irradiance values.....	9
<b>Figure 2.3 :</b> (a)Determining maximum power point of a PV cell (b) Power – Voltage curve of a PV cell .....	10
<b>Figure 2.4 :</b> Wind flowing through wind turbine .....	11
<b>Figure 2.5 :</b> Wind power generation estimation method.....	12
<b>Figure 2.6 :</b> World oil outlook .....	14
<b>Figure 2.7 :</b> BEV Power Train .....	15
<b>Figure 2.8 :</b> EV Power Train.....	16
<b>Figure 2.9 :</b> Possible EV configurations .....	17
<b>Figure 2.10 :</b> Concept of hybrid electric vehicle power train .....	18
<b>Figure 2.11 :</b> Concept of hybrid electric vehicle power train .....	18
<b>Figure 2.12 :</b> Classifications of hybrid electric vehicles (a) series hybrid (b) parallel hybrid (c) series-parallel hybrid (d) complex hybrid system.....	20
<b>Figure 2.13 :</b> Constant voltage charging profile .....	22
<b>Figure 2.14 :</b> Constant current charging profile.....	23
<b>Figure 2.15 :</b> Pseudo-CC charging algorithm .....	23
<b>Figure 2.16 :</b> Taper current charging setup.....	24
<b>Figure 2.17 :</b> Pulsed current charging profile. ....	25
<b>Figure 2.18 :</b> Three-phase bridge rectifier .....	27
<b>Figure 2.19 :</b> Current and voltage waveforms of B6 rectifier.....	27
<b>Figure 2.20 :</b> Boost converter circuit .....	28
<b>Figure 2.21 :</b> Voltage and current waveforms of boost converter .....	28
<b>Figure 2.22 :</b> Buck converter circuit .....	30
<b>Figure 2.23 :</b> Voltage and current waveforms of buck converter .....	31
<b>Figure 2.24 :</b> Cuk converter circuit .....	31
<b>Figure 2.25 :</b> Voltage and current waveforms of boost converter .....	32
<b>Figure 2.26 :</b> (a) Input signal (b) Carrier signal as PWM (c) Output signal .....	35
<b>Figure 2.27 :</b> PWM signal with duty cycle D. ....	35
<b>Figure 2.28 :</b> A PID controller evaluates present, past and future errors.....	36
<b>Figure 2.29 :</b> (a) P (b) PI (c)PID controllers with different values for $k_p$ , $k_i$ and $k_d$ for a process with the transfer function $P(s) = 1/(s+1)^3$ .....	37
<b>Figure 2.30 :</b> I-V characteristic and MPP of a PV array .....	38
<b>Figure 2.31 :</b> P&O Algorithm .....	39
<b>Figure 2.32 :</b> InCond Algorithm .....	39
<b>Figure 2.33 :</b> Maximum power point of wind turbines for different wind speeds....	40
<b>Figure 2.34 :</b> MPPT process for wind turbines .....	41

<b>Figure 2.35</b> : MPPT process with (a) TSR (b) PSF (c) HCS method .....	41
<b>Figure 2.36</b> : Control principle of HCS method.....	42
<b>Figure 2.37</b> : Standards related with EV charging .....	43
<b>Figure 2.38</b> : Charging place distribution estimation.....	45
<b>Figure 3.1</b> : General structure of the designed system. ....	50
<b>Figure 3.2</b> : The structure of GSC.....	52
<b>Figure 3.3</b> : Controller of GSC.....	53
<b>Figure 3.4</b> : Modeling of PV array. ....	53
<b>Figure 3.5</b> : Characteristics of modeled PV array. ....	54
<b>Figure 3.6</b> : General structure of PVC. ....	55
<b>Figure 3.7</b> : MPPT controller of PVC. ....	55
<b>Figure 3.8</b> : Wind Turbine Model. ....	56
<b>Figure 3.9</b> : Wind turbine characteristics. ....	57
<b>Figure 3.10</b> : Wind turbine charger model. ....	58
<b>Figure 3.11</b> : MPPT controller of WTC. ....	58
<b>Figure 3.12</b> : General structure of LSC.....	59
<b>Figure 3.13</b> : Battery Model. ....	59
<b>Figure 3.14</b> : General overview of control system.....	63
<b>Figure 3.15</b> : (a) Wind cut-in & cut-off speed check subsystem (b) solar irradiation check subsystem.....	64
<b>Figure 3.16</b> : Emergency condition.....	64
<b>Figure 3.17</b> : Storage evaluation subsystem.....	65
<b>Figure 3.18</b> : Control logic figured as a tree. ....	68
<b>Figure 3.19</b> : MATLAB code of controller.....	68
<b>Figure 3.20</b> : Results for scenario 1. ....	71
<b>Figure 3.21</b> : Results for scenario 2. ....	73
<b>Figure 3.22</b> : Results for scenario 3. ....	75
<b>Figure 3.23</b> : Results for scenario 4. ....	76

# **DESIGN AND SIMULATION OF ELECTRIC VEHICLE FAST CHARGING STATION USING SOLAR AND WIND POWER**

## **SUMMARY**

The demand for energy has been constantly increasing due to the growth in the population and industrialization. Especially the developing countries, such as Turkey, have a bigger increase rate of energy demand. Since industrial revolution, fossil fuels always have the biggest share between primary energy sources. However, the negative effects caused by the over use of fossil and the fact that these sources are diminishing brought new and renewable options on the agenda. One of the most important solution for the transportation sector is the electrical vehicles. It offers a green solution when the source needed for electrical vehicles is originated from renewable energy sources. On the other hand, these sources, such as wind and solar energy, have some disadvantages too. The costs of production technology and costs needed for adaptation to current system, being less reliable and less available due to the discontinuity of these sources are the disadvantages of these systems that need to be taken into consideration. Such issues stimulate the studies on hybrid renewable energy systems, local/in-situ electricity generation and smart grids, which aim to minimize these disadvantages of these sources. In this work, it is aimed to design an electric vehicle charging station that offers an environment friendly solution for the charging process of electric vehicles, which is one of the most important issues. Thus, the designed station is intended to make use of renewable energy sources. For this purpose, wind power and solar power, are chosen to be used with this hybrid energy system and a fast charging using solar and wind power supported with grid is designed and simulated via Matlab – Simulink. Various possible conditions constituting different cases are taken into account and the system is designed accordingly.



# ELEKTRİKLİ ARAÇLAR İÇİN RÜZGAR VE GÜNEŞ ENERJİSİ KULLANAN HIZLI ŞARJ İSTASYONU TASARLANMASI VE SİMULASYONU

## ÖZET

İnsanoğlu, varoluşundan beri bulunduğu ortamı kendi konfor şartlarına göre düzenleyecek biçimde değiştirme çabası içerisinde. Bu değişiklikleri gerçekleştirebilmek için ise sürekli bir biçimde enerji harcaması gerekmektedir. Daha önceleri kas gücüne dayalı olan bu etkilerin ana kaynağı olan besinler, insanoğlunu tarımsal bir toplum olmaya teşvik etmişti. Sonraları ise, özellikle sanayi devrimi gibi tarihin en önemli mihenk taşlarından biri olan olaylarla, tarım toplumundan sanayi toplumuna doğru bir geçiş yaşanmıştır.

Bu geçiş esnasında en çok kullanılan enerji kaynakları ise kömür ve petrol gibi fosil yakıtlardan oluşmaktaydı. Söz konusu enerji ihtiyacı insan nüfüsü artışı ve endüstrileşme ile sürekli artmaktadır. Türkiye gibi gelişmekte olan ülkelerde bu artış hızı daha da fazladır. Fosil yakıtlar sanayi devriminden beri, birincil enerji kaynakları arasında tüketim açısından en büyük orana sahip olmuştur. Fakat yakın zamanda, dünyamızın hızla artan bu tüketime sandığımız gibi cevap veremediği ve doğal ortamımızın yok olmaya başladığı birçok bilimadamı tarafından iddaa edildi. Bunlara ek olarak da geçmişimizde yaşanan petrol krizleri, fosil kaynakların tükendiği söylentileri ve ekonomik faktörler nedeniyle bu kaynaklara olan ilginin yavaş yavaş başka kaynaklara ve kavramlara kaymasına ve yeni-yenilenebilir çevre dostu seçeneklerin gündeme gelmesine neden oldu. Gündeme gelen bu seçenekler genellikle yenilenebilir enerji kaynakları olarak nitelendirilmişlerdir.

Bunun dışında, bu çalışmanın odak noktasındaki ulaşım sektörü için önemli çözümlerden biri elektrikli taşıtlar olarak lanse edilmektedir. Ulaşım sektörünün enerji ekonomisine katkısı düşünüldüğünde bu alanda yapılacak olan yeniliklerin büyük ölçekte etkileri olacağı aşıkardır. Elektrikli taşıtları tam anlamıyla çevreci bir çözüm olarak nitelendirebilmek için bu taşıtların kullandığı enerjinin, nasıl ve ne şekilde üretildiğine dikkat edilmesi gerekmektedir. Zira, fosil yakıt kullanan elektrik santrallerinde üretilmiş bir elektrikle şarj edilen bir aracın tam anlamı ile “çevreci” olduğu iddaa edilemez.

Bu bağlamda, çalışmanın konusu yenilenebilir enerji kaynakları ile elektrikli taşıtların etkileşiminin artırılması hedeflenerek belirlenmiştir. Bu düşünce sonucunda elektrikli taşıtların büyük sorunlarından biri olan şarj etme sürecini yenilenebilir kaynaklardan yararlanarak sağlayan bir sistem dizayn edilmesine karar verilmiştir. Zira, Türkiye gibi enerji konusunda dış kaynaklara had safhada bağımlı olan ülkeler için bu tarz sistemlerin daha da önem taşıdığı söylenebilir.

Ancak, bu çalışmada Türkiye'nin potansiyeli gözetilip de vurgu yapılmış olan güneş, rüzgar gibi yenilenebilir kaynakların bazı dezavantajları da mevcuttur. Bu kaynakların üretim teknolojisi ve mevcut sistemin bu kaynaklara adaptasyonu için gerekli olan maliyetlerin yüksek olması, kaynakların süreksizliği nedeni ile

güvenilirlik ve emre amadeliklerinin daha düşük olması dikkkate alınması gereken dezavantajlardır. Böylesi sorunlar, yenilenebilir kaynakların dezavantajlarını en aza indirmeye yönelik hibrit enerji sistemleri, yerel-yerinde enerji üretimi ve akıllı şebekeler gibi konulardaki araştırmalara yoğunlaşma yaratmıştır.

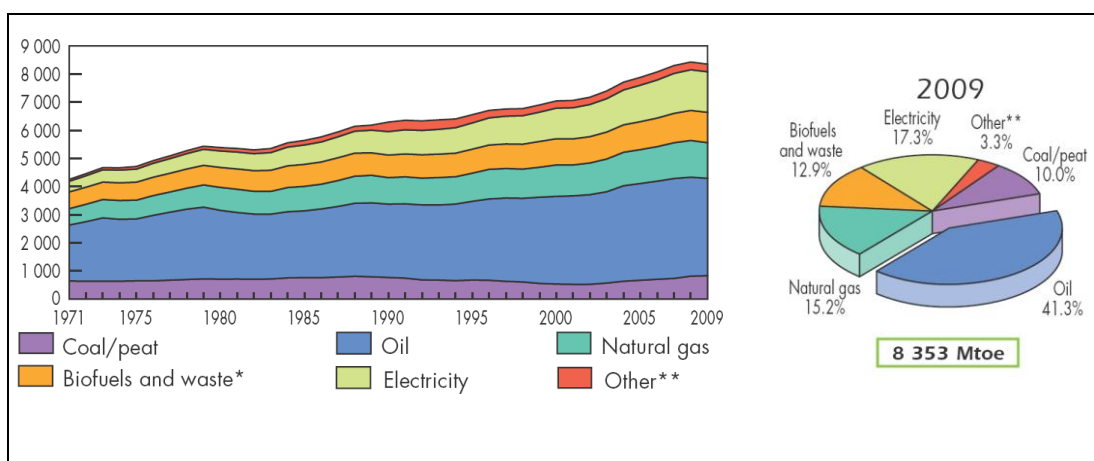
Sonuç olarak, bu tez çalışmasında elektrikli taşıtların en önemli sorunlarından biri olan şarj etme aşaması için çevre dostu bir çözüm sunan bir şarj istasyonu sistemi tasarlanması ve tasarlanan şarj istasyonunun yenilenebilir enerji kaynaklarından faydalanması hedeflenmiştir. Güneş ve rüzgar kaynakları hibrit enerji sistemi için seçilmiş ve elektrikli araçlar için güneş ve rüzgar elektriği kullanan ve şebeke ile desteklenen bir şarj istasyonu tasarlanarak Matlab-Simulink ile simulasyon yapılmıştır. Çalışmada dikkat edilen tasarım noktaları ve sistem bileşenleri detaylı bir biçimde açıklanmıştır. Bunun dışında, çalışmada çoklu koşullar tarafından oluşturulan durumlar ele alınarak sistem bu durumlara cevap verebilecek nitelikte sunulmuştur. Sistemin bu durumlara cevap verip veremediği son bölümde oluşturulan dört farklı senaryo ile test edilip sonuçlar sunulmuştur.

## 1. INTRODUCTION

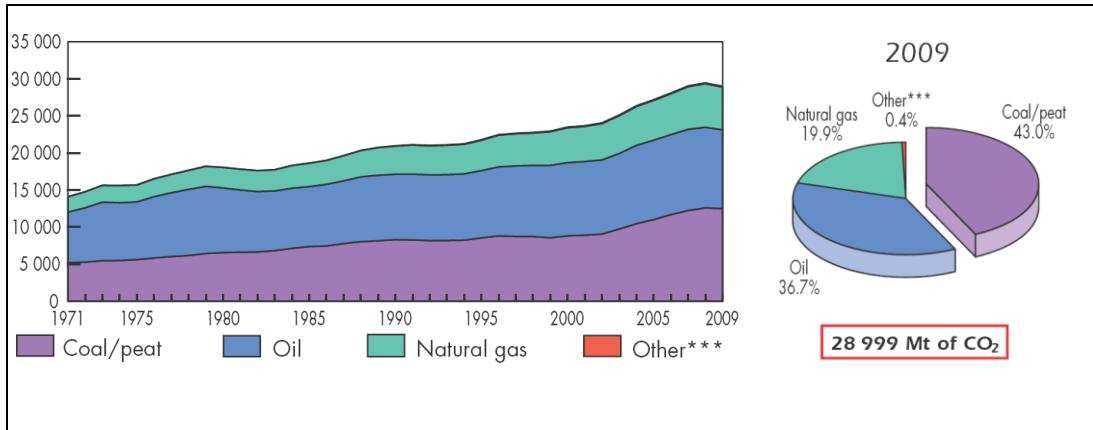
Since their existence, human beings are in effort to make the environment adopt their conditions. However, all these changes require a certain amount of energy. Formerly this energy was supplied mostly by the power of muscles, making foods the main energy source and leading human beings to be agrarian society. Afterwards, the industrial revolution, which is a milestone in human history that changed the focus point of energy sources, led human beings to be an industrial society.

Figure 1.1 shows the values of global total energy consumption since 1971 to 2009 according to fuels. As it is seen from the figure the energy consumption always has the trend to increase, which has a bigger increase rate in developing countries such as Turkey. Also it is obvious that the biggest share has always been oil, which was 41.3% in 2009 [1].

One of the biggest drawbacks of fossil fuels is the CO<sub>2</sub> emissions caused by combustion process of these fuels. Figure 1.2 shows the amount of CO<sub>2</sub> emissions from 1971 to 2009 by fuel. While coal has the biggest share with 43%, oil has a share of 36.7% and the smallest share is by natural gas with 19.9%. CO<sub>2</sub> emissions caused by other sources are almost neglectable with 0.4% [1].



**Figure 1.1:** World final total energy consumption by fuel (Mtoe) [1].



**Figure 1.2 :** Share of CO<sub>2</sub> emissions by fuel (Mt) [1].

When the energy balance in Turkey is interpreted, it can be seen that the transportation sector plays a big role in both energy balance and economy in the country. The energy demand of primary energy sources is equal to 114480.2 Toe, whereas the energy consumption is 86962.2 Toe. The Figure 1.3 shows the rate of energy production depending on the imported sources from foreign countries [2]. The transportation sector constitutes nearly 20% of the total consumption [3]. In addition to that, the share of transportation in energy imports is 62.11%, which is equal to 20.50 billion dollars. This means that 8.5% of total imports is caused by the transportation sector alone [4].

According to the strategic plans of Ministry of Energy and Natural Resources, it is aimed to increase the share of renewables and domestic sources in energy production and to decrease the dependence on imported sources [2]. The investments for renewable energy in Turkey are constantly increasing. Currently, geothermal energy, solar energy, wind energy and hydraulic energy are in focus. The installed capacities of these sources are sequentially 81.6 MW, 6 MW and 1512 MW and 17699.5 MW whereas the total installed power is 52911 MW [2,3].

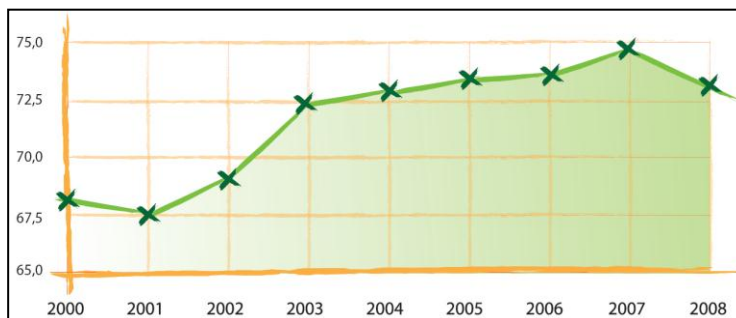


**Figure 1.3 :** Dependency of energy on sources imported from foreign countries [2].



Due to the facts mentioned above, the renewable energy sources, such as wind, sun and biofuels have been popular. The importance of the renewable energy can be conceived from the actual trends in the global energy policies.

Year 2010, European Union (EU) noticed some transformations in Europe and decided to take action by taking precautions and set a few social, economical and energy related targets. When these targets are interpreted in scope of the thesis, the “20/20/20” climate/energy goals are the ones that should be paid attention. These “20/20/20” goals state that greenhouse gas emissions should be lowered by 20%, the share of renewable energy sources should be increased by 20% and the overall energy efficiency should be increased by 20% [5].

Also recently, the United Nations (UN) has set three goals to be achieved by 2030, called “Sustainable Energy for All”: supplying modern energy systems, doubling the increase in the energy efficiency and doubling the percentage of renewable energy usage. For this purpose UN stated 2012 as the “International Year of Sustainable Energy for All” [6].

In other words, importance placed on renewable energy is continuously rising. The whole world is trying to produce and use energy in more environmental friendly and efficient ways. However, growth of renewable energy sources bring its own challenges along. One of these challenges is that the current electricity network infrastructure needs to be modified and expanded in order to make better use of renewable energy sources. This challenge results in the concept of smart grids, which is defined as an electricity grid that utilizes advanced technologies with the aim of tracking and organizing the transmission of electrical energy from sources to the end users that have varying energy demands. The main advantage of smart grids is that it enables energy producers and end users to organize their needs and potentials in real-time [7].

A second result of these challenges is the concept of distributed/decentralized electricity generation. The distributed/decentralized electricity generation means that the energy demand of a small region is met by a small scaled electricity generation facility that makes use of the region’s favorable energy source. When all the concepts of renewable energy production, distributed/decentralized generation and smart grids are considered together, a better and more efficient use of energy is

possible which will enable people to produce energy from a large variety of energy sources, lower transmission losses and provide a better reliability of electricity [8]. Another advantageous result is that even small investors will be able to access the energy market [8].

27.35 % of worldwide energy consumption is due to transportation[1], which is 95% dependent on oil products. This means that almost a half of the global oil consumption is caused by transportation sector [9], resulting in approximately 14% of global greenhouse gas emissions [10]. These numbers are proving that the transport sector has a very big effect on the global energy issues.

Considering these facts and the environmental problems, electric vehicles (EVs) have become the focus point of debates concerning energy issues. Although the fact that electric vehicles seem to be a new topic, in reality the concept of electric vehicles has a long history.

Since a few years, EVs have been gaining popularity once again, as their advantages have become more important than ever. EVs seem to be the future of transportation; a research done by Center for Entrepreneurship & Technology University of California, Berkeley forecasts that by 2030 EVs will be an important part of U.S. light-vehicle fleet covering 24% of the fleet and 64% of light-vehicle sales [11]. This prediction may become true even earlier if the disadvantages of EVs such as energy storage and high costs can be eliminated.

When the whole EV infrastructure considered there are more challenges to overcome despite all the advantages of EVs. A recent study of the Joint Research Centre of the European Commission projects that the peak electrical power demand would increase approximately 30% if EVs comprise 25% of vehicle fleet [12]. Also some researches show that if the share of the EVs is bigger than 10% of all vehicles, charging regulation mechanisms must be constructed so that the line voltage value does not surpass the minimum limit allowed [13]. Such issues again lead to concept of smart grids and distributed/decentralized electricity production using renewables sources, which is also a popular topic. This thesis aims to design a electric vehicle fast charging station using solar and wind power so that it offers a more environment friendly solution for EV charging issues, where such systems are possible to build. A simulation will be performed and the results will be evaluated.

## **1.1 Structure of the thesis**

Chapter 1 emphasizes the importance of renewable energy sources and discusses the wide application areas of these sources. The energy statistics of transportation, which plays a big role in the global energy trends, are given and it is pointed out that renewable energy applications can be used for transportation systems. Chapter 2 focuses on the theoretical aspects of the thesis; a brief summary of the system configuration prepared for this thesis is given and all of the necessary components and control basics are explained in detail. At the end of the Chapter 2, a literature overview of the current researches done on similar topics is to find. This overview will be interpreted in three subtopics; charging station standards and applications, battery management strategies and finally hybrid renewable power systems. Chapter 3 is the design and simulation part of the thesis. The design considerations and methods are explained. Every component of the simulation is described in detail. After then, the simulation results for different scenarios are discussed. This chapter also examines the liability and evaluates the advantages and disadvantages of the proposed system. The final chapter, Chapter 4, is the conclusion, where the important aspects of the work are mentioned and some suggestions for future work are given.



## **2. THEORETICAL PART**

In this section, it is aimed to give the fundamental knowledge about the components and control basics that are used in charging stations and similar systems. Since such systems involve lots of components, they can be interpreted in six stages; renewable energy sources, electric vehicles, charging methods, power electronics interfaces, control theory and charging station standards. The electric vehicles and battery charging methods will also be mentioned. At the end of the chapter, a literature overview concerning the subjects of the work will be given.

### **2.1 Renewable Energy Sources**

Nowadays, renewable energy sources such as solar energy, wind energy and biomass energy have been popular topics due to increasing need for effective and environment friendly energy consumption. However the penetration of systems, which benefit from such sources, is somehow limited because of the disadvantages of these sources. The biggest disadvantage of such systems, especially the ones that include solar energy or wind energy, is the reliability of these systems due to their unpredictable natures. For example, the PV panels and wind turbines alone are not able to produce energy for significant portion of throughout the year. This may lead to fact that the system components probably need to be oversized which results in expensive system designs. Although methods including the prediction of these sources have been intensely studied, the idea of combining such sources within a system so that they compensate the disadvantages of each other seems to be a very convenient strategy. Such systems are called hybrid renewable energy systems (HRES) [14,15].

The topic of HRES, where multiple energy sources are used together to improve the reliability, are currently very popular. These energy sources that are included in such systems may be the combination of a few renewable energy sources and some conventional energy sources so that the reliability of the system is increased even further [14,15]. This thesis concentrates on solar and wind energy which have wide

application areas. Thus, these two sources will be interpreted in scope of the thesis. Figure 2.1 gives the general structure of hybrid renewable energy systems.

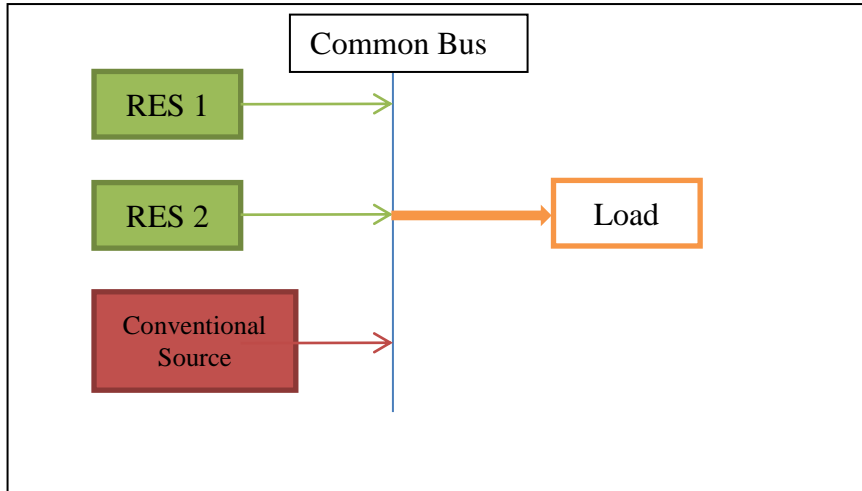


**Figure 2.1 :** General HRES structure.

### 2.1.1 Sun Power

The sun provides for the energy needed to maintain the life for our solar system. The fusion reaction of hydrogen converting to helium on the surface of sun produces a mass amount of energy. This energy radiates away from sun in form of sunlight. The solar energy received within an hour is almost equal to the energy consumption of whole world throughout the year [16]. It is possible to produce energy directly from sunlight by using photovoltaic cells. These cells typically produce nearly 3 watts at nearly 0.5 Volts. Thus, for larger power systems it is essential to connect these cells in series or parallel to receive the projected power and voltage/current limits, as it is showed in Figure 2.2. The typical I-V characteristics of an ideal and real PV cell can be seen in Figure 2.2. As seen in the figure the current produced from the cell varies as the produced voltage changes.

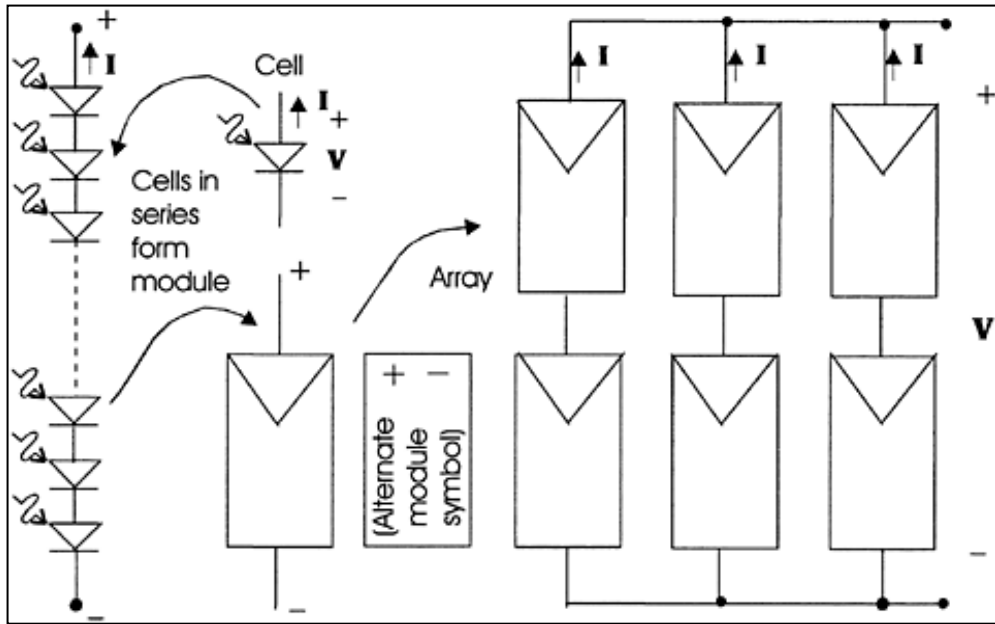
The equation of the I-V characteristic for an ideal PV is given below [16]:

$$I = I_l - I_0 \left( e^{\frac{qV}{kT}} - 1 \right) \quad (2.1)$$

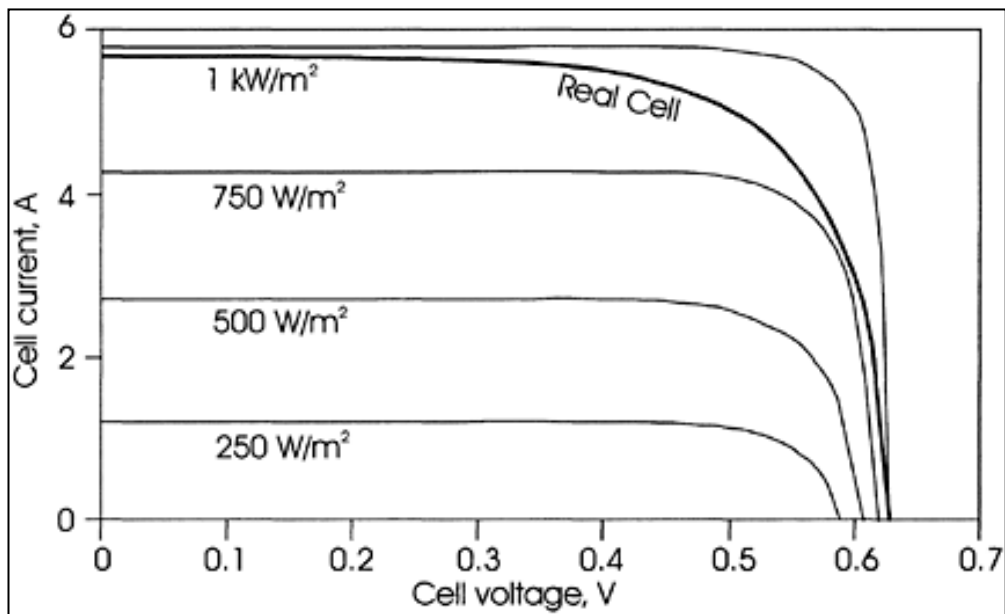
Thus, a maximum power point is to be determined. Figure 2.3 shows that hyperbolas defined as  $IV=\text{constant}$  helps to find the maximum power point (MPP) of a cell.

This feature of PV cells requires that a control method is to be used within the system so that the PV array delivers the maximum available amount of power. This

process is called “Maximum Power Point Tracking” (MPPT), which will be mentioned later.



(a)



(b)

**Figure 2.2 :** (a) PV Cells connected in series and parallel (b) I-V characteristic for ideal and real PV cells with different irradiance values [16].

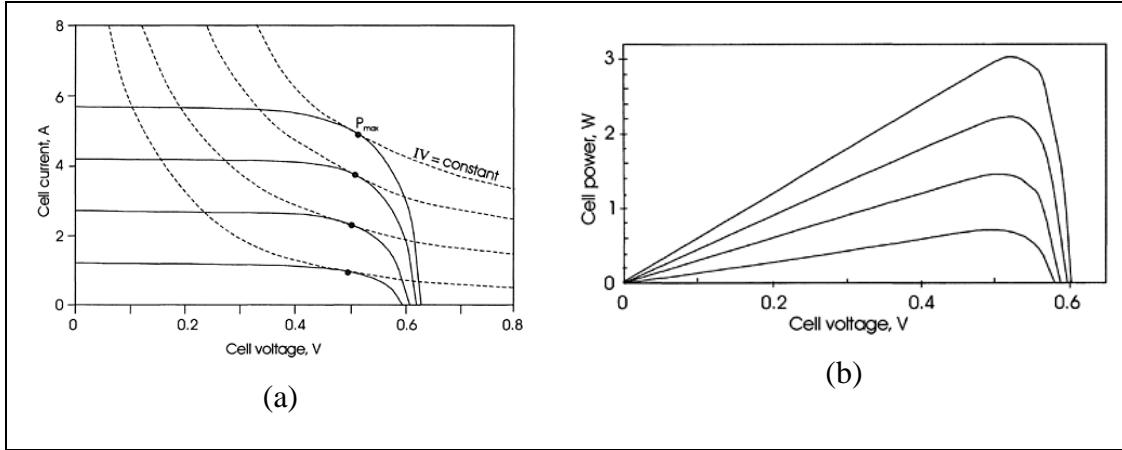


**Figure 2.3 :** (a) Determining maximum power point of a PV cell (b) Power – Voltage curve of a PV cell [16].

### 2.1.2 Wind Power

Wind energy has been used for a long time. Until 20<sup>th</sup> century, wind energy was mainly used for grain milling or water pumping. However technological developments and new designs provided electricity generation using wind energy. After the oil crisis in 1970s there were many research programs focused on wind energy, which resulted in a revolution in wind energy systems. Currently, wind power is most progressing renewable energy source. The investments made in wind power has surpassed all prediction as the annual grow rate of wind power in recent years has averaged more than 30% [17].

In general, the energy of the moving air, wind, is converted into electrical energy using a wind turbine and a generator. The kinetic energy of a moving mass can be defined by the following formula, where  $m$  is mass and  $V$  is the speed:

$$\text{Kinetic Energy} = \frac{1}{2} \cdot m \cdot V^2 \text{ joules} \quad (2.2)$$

In order to apply this formula for wind, the mass of moving air must be defined with the following formula:

$$P = \frac{1}{2} \cdot (\rho AV) \cdot V^2 = \frac{1}{2} \cdot \rho AV^3 \text{ watts} \quad (2.3)$$

Where,

$P$  = mechanical power in the moving air

$\rho$  = air density,  $\text{kg/m}^3$



$A$  = area swept by the rotor blades,  $m^2$

$V$  = velocity of the air,  $m/s$

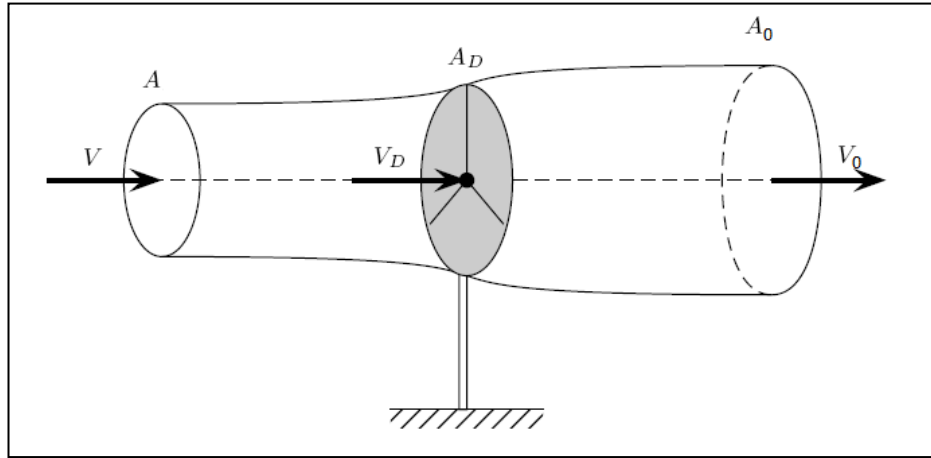


**Figure 2.4 :** Wind flowing through wind turbine [17].

This equation gives the energy carried by the wind within the swept area of the wind turbines. The wind speed and the area, which the wind passes through, change after the wind passes through the turbine.

The power extracted from the wind by the turbine can be defined as below, using the difference of the wind speed:

$$P_0 = \text{mass flow rate per second} \cdot \{V^2 - V_0^2\} \quad (2.4)$$

Where,

$P_0$  = mechanical extracted by the rotor, the turbine output power

$V$  = upstream wind velocity at the entrance of the rotor blades

$V_0$  = downstream wind velocity at the exit of the rotor blades

mass flow rate =  $\rho \cdot A \cdot (V + V_0) / 2$

Thus the final can be expressed as:

$$\begin{aligned} P_0 &= \frac{1}{2} \left[ \rho \cdot A \cdot \frac{(V + V_0)}{2} \right] \cdot (V^2 - V_0^2) \\ &= \frac{1}{2} \cdot \rho \cdot A \cdot V^3 \cdot \frac{\left(1 + \frac{V_0}{V}\right) \left[1 - \left(\frac{V_0}{V}\right)^2\right]}{2} \end{aligned} \quad (2.5)$$

Finally, the fraction of the upstream wind power captured by rotor blades can be defined as:

$$C_P = \frac{\left(1 + \frac{V_0}{V}\right) \left[1 - \left(\frac{V_0}{V}\right)^2\right]}{2} \quad (2.6)$$

Which gives [18]:

$$P_0 = \frac{1}{2} \cdot \rho \cdot A \cdot V^3 \cdot C_P \quad (2.7)$$

So, the power produced by a wind turbine can be calculated if the  $C_p$  of the turbine is known. There are also other approximations. One of this approximation divides the power curve of the wind turbine in a few parts as shown in Figure 2.5 and expresses each part with different polynomial equations [19].

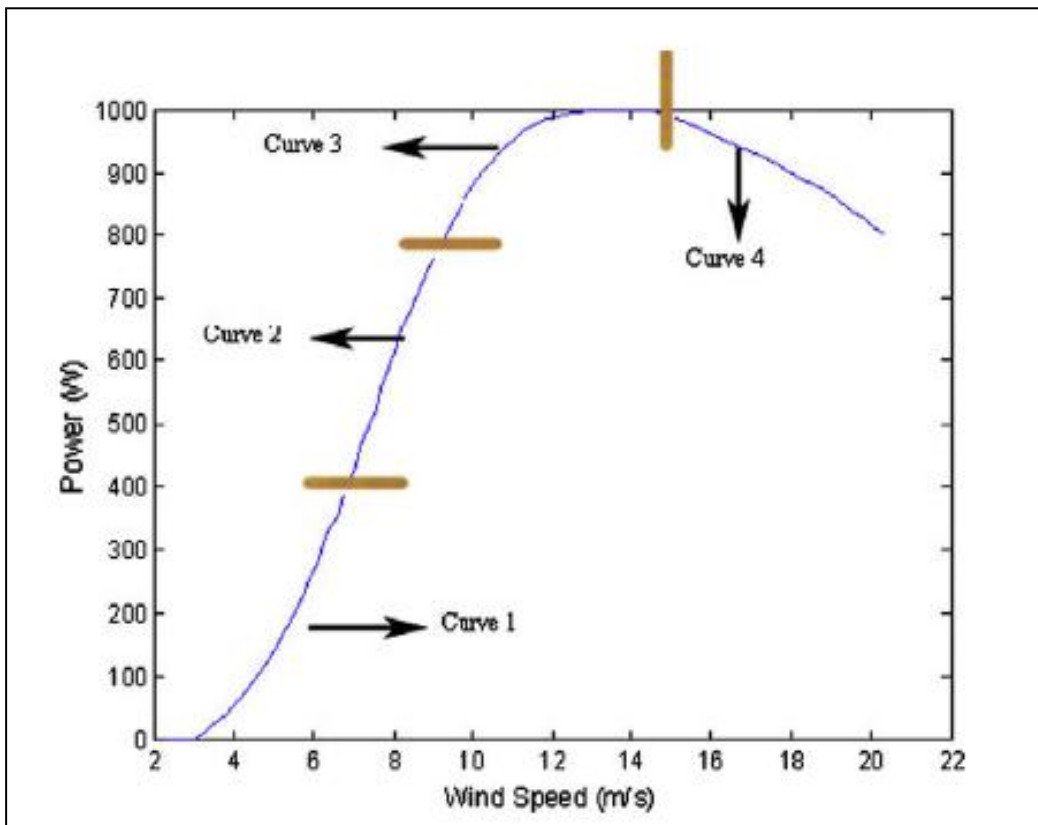


**Figure 2.5 :** Wind power generation estimation method [19].

The graph above can be expressed as [19]:

$$P_W = \begin{cases} 0, & V \leq V_{ci} \text{ or } V \geq V_{co} \\ a_1 V^3 + b_1 V^2 + c_1 V + d_1, & V_{ci} < V < V_1 \\ a_2 V^3 + b_2 V^2 + c_2 V + d_2, & V_1 < V < V_2 \\ \dots \\ a_n V^3 + b_n V^2 + c_n V + d_n, & V_{n-1} < V < V_r \\ V_r, & V_r < V < V_{co} \end{cases} \quad (2.8)$$

Where,

a,b,c,d = Polynomial coefficients

$P_w$  = Output power of wind turbine

$P_r$  = Rated power of wind turbine

$V_i$  = Cut-in speed of wind turbine

$V_r$  = Rated speed of wind turbine

$V_{co}$  = Cut-off speed of wind turbine

One other approximation is using the formula below [20]:

$$P_W = \begin{cases} P_r [(V^2 - V_{ci}^2)/(V_r^2 - V_{ci}^2)], & V_{ci} \leq V \leq V_r \\ P_r, & V_r \leq V \leq V_{co} \\ 0, & \text{Otherwise} \end{cases} \quad (2.9)$$

## 2.2 Electric Vehicles

The discovery of internal combustion engines (ICE) is one of the greatest discoveries of all times. The ICE has contributed a lot in the progress of modern society by all means. On the other hand, the overuse of ICEs has caused some very serious environmental damages such as the climate change. Statistical facts, which were emphasizing the influence of transportation sector on environment, were given at Chapter 1. In addition to these facts, the overuse of fossil fuels caused the depletion of the petroleum products and the continuous rise of oil prices. Studies have shown that the world faces the probability of the oil reserves to extinct by year 2038, on which the whole global economy depends. The Figure 2.6 shows that the reserves that are being discovered decreases year by year, while the consumption is increasing with a higher rate [22].

Such issues lead the researches on transportation to be focused more efficient and clean solutions. One such solution is to increase the share of EVs in transportation sector. Unlike the general impression, EVs are not a new topic. The history of EVs

starts in 17<sup>th</sup> century, when Gustave Trouve built a tricycle consisting of a 0.1 hp DC motor and lead-acid batteries in 1881. From this time to early 1920s, the EVs have competed with vehicles using combustion engines. When New York in 1903 is observed, a different situation is noticed: there were nearly 4000 vehicles registered that consist of 53% steam-powered vehicles, 27% ICE vehicles and 20% EVs. The EVs outsold the both vehicle types in 1899-1900 in USA.

There were also charging stations built. Some of these stations were conventional stations, where the driver deposited the coins and the EV was charged in-place. On the other hand, some of them were using fast battery swapping system, where the battery of the EV was changed with a charged one. After 1900s, HEVs were demonstrated, which made use of advantages of both ICEs and EVs. However these vehicles mostly disappeared during the First World War. From this time on, the popularity of EVs and HEVs increased only in the times of oil crises. This is due to the rapid development of ICEs and the technological limitations of EVs and HEVs, such as the driving range and costs [22].

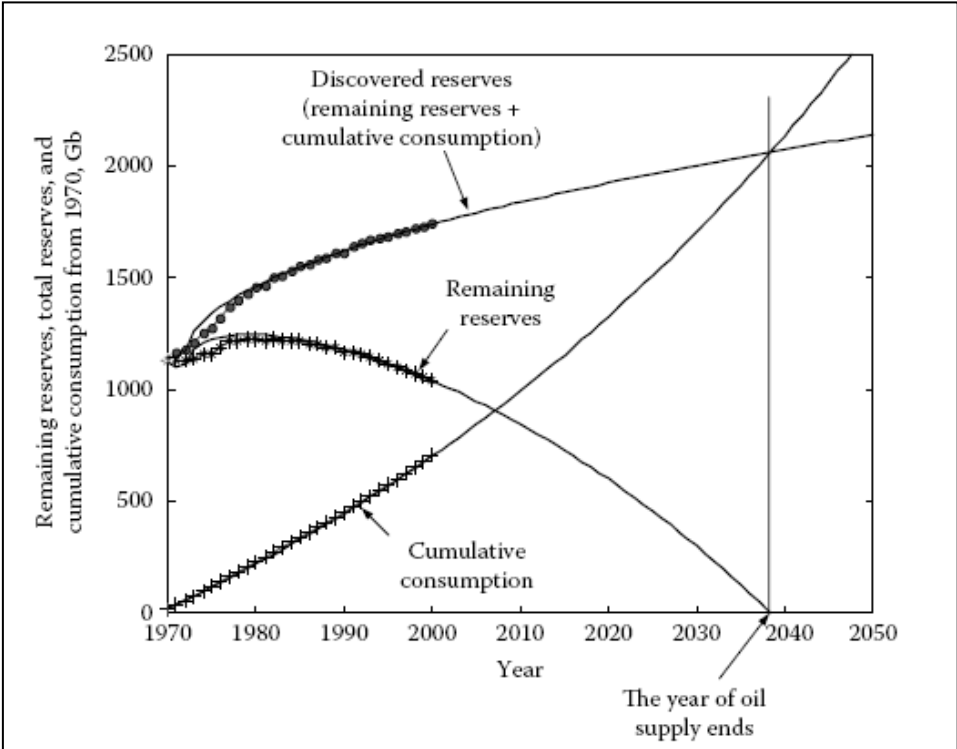


**Figure 2.6 :** World oil outlook [22].

Basically, there are two types of EVs. The first type is fuel cell EVs, where electrical energy is instantly generated on place. The second type EVs are the ones which are equipped with battery used for energy storage. In the scope of this thesis, the focus

will be on hybrid EVs equipped with batteries, where a charging procedure is in question.

Formerly, EVs was constructed just by replacing the ICE and fuel tank with an electric motor and battery pack, so that an ICE vehicle was converted to an EV. As showed in Figure 2.7. However, these vehicles suffered from heavy weight, low flexibility and weak performance. The modern purposely built, EVs, shown in Figure 2.8, have three subsystems; electric propulsion, energy source and auxiliary.

The electric propulsion subsystem consists of a vehicle controller, power electronic converters, electric motor and mechanical transmission. The energy source subsystem comprised of an energy source, energy refueling unit and energy/battery management unit. The auxiliary unit involves power steering unit, climate control unit and auxiliary power supply [22].

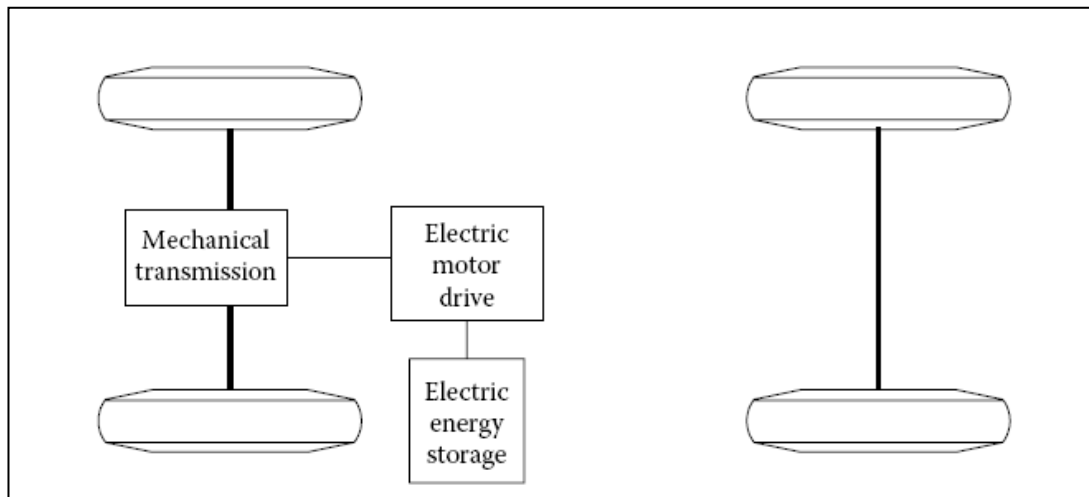


**Figure 2.7 : BEV Power Train [22].**

According to the signals from the brake and accelerator inputs, the power converter adjusts the system to react appropriately so that it regulates the power flow between electric motor and energy source. This includes the regenerative braking, where the power flow is from the electric motor to energy source. During the whole process, the vehicle controller and energy/battery management unit works together. The auxiliary unit supplies energy to all other auxiliaries that have different voltage levels. Modern BEVs have a few configurations [22]:

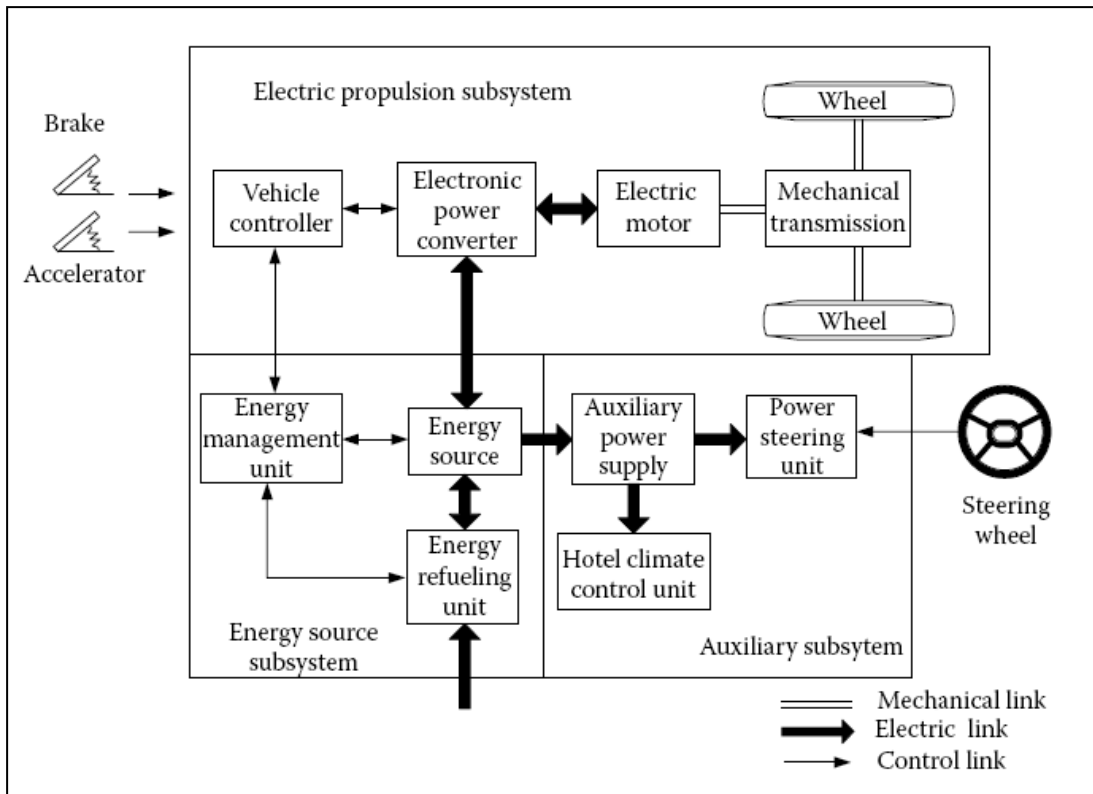


**Figure 2.8 :** EV Power Train [22].

- The first configuration represents the case, where the ICE of a vehicle is replaced with electric propulsion. The vehicle comprised of an electric motor, a gearbox, a clutch and a differential. It is also possible that an automatic gear is used with this configuration. The gearbox enables the driver to choose the most suitable gear ratio for the load requirement. The motion on a curved path requires the wheels on both sides to rotate at different speeds. The differential provides for this motion.
- The remaining configurations are derived from the previous ones; in the second configuration, the gearbox is replaced with a fixed gearing so that the need for multispeed gearbox and clutch is prevented. However, this configuration is suitable for vehicles that use an electric motor, which has a constant power for wide speed ranges.
- The third configuration, where fixed gearing, electric motor and differential is converted in a single assembly, provides a much simpler and compact drive train.
- One other configuration consists of a drive train where wheels on both sides are driven by different electric motors. The control of the vehicle is more

complicated because these motors need to be driven at different speeds when driving along a curved path. However, the drive train is much simpler.

- e) At this configuration, the electric motors are placed in the wheels. Thus, this configuration is also called “In-wheel Drive”. For this configuration, a thin planetary gear may be used.
- f) The last configuration provides the simplest drive train; the configuration does not involve any mechanical gearing. The electric motors are directly connected to the wheels. However, special electric motors, which have high torques to start and accelerate, need to be used with this configuration.

These configurations are summarized in Figure 2.9.

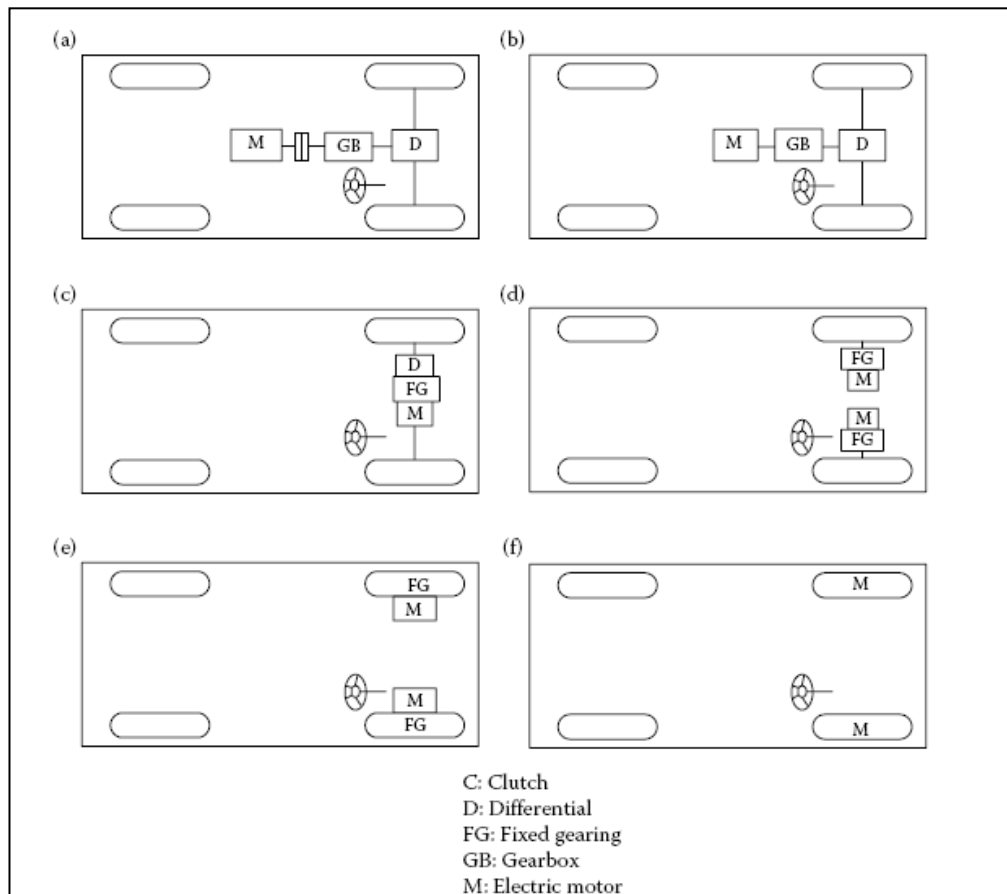


**Figure 2.9 :** Possible EV configurations [22].

In addition to the conventional EVs mentioned above, there are also modified EVs which make use of both electrical motors and ICEs in the propulsion system. Any such vehicle that combines two or more power trains is called hybrid electric vehicle (HEV), as shown in Figure 2.10. Generally, a HEV consists of two power trains, because more power trains would make the vehicle too much complicated. HEVs

aim to combine the advantages of both ICEVs and BEVs; efficiency of electric motor, regenerative braking ability, more stable fuel prices, less effects on environment, long range and good performance. If the HEV has a plug, which can connect an external electrical source so that the energy storage of the vehicle is charged, this vehicle is called plug-in hybrid electric vehicle (PHEV).

The power demand of the vehicles varies randomly due to the conditions of the route. As shown in Figure 2.11 this random power demand can be expressed as two functions, where one function is steady and the other one is dynamic. These are expressed as average and dynamic power in Figure 2.11. The HEVs supply the average power demand by the source that is favorable for steady state operation; the ICE power train. On the other hand, the dynamic power demand is covered by electric motor [22].

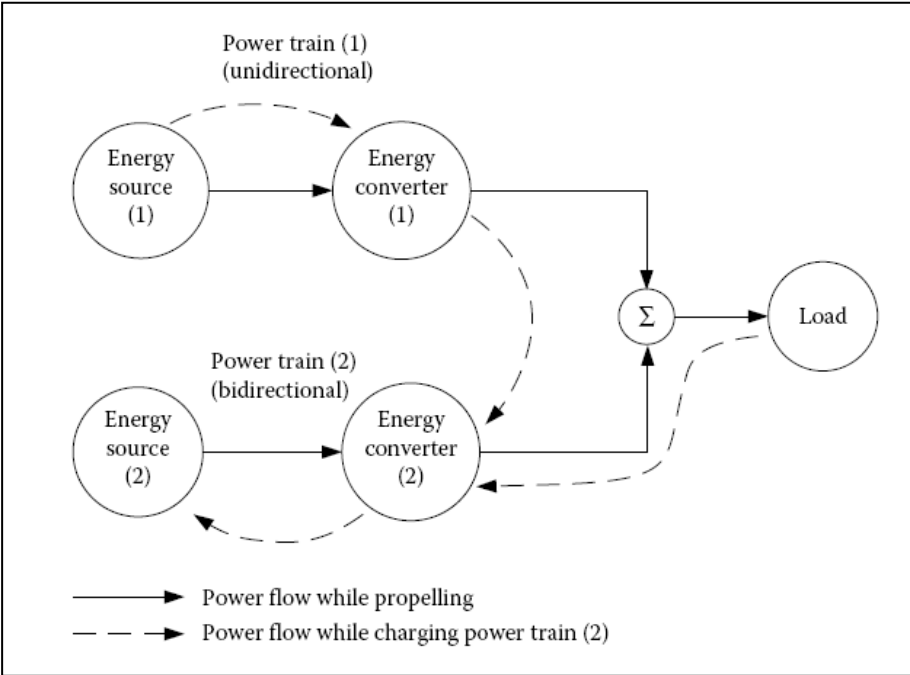


**Figure 2.10 :** Concept of hybrid electric vehicle power train [22].

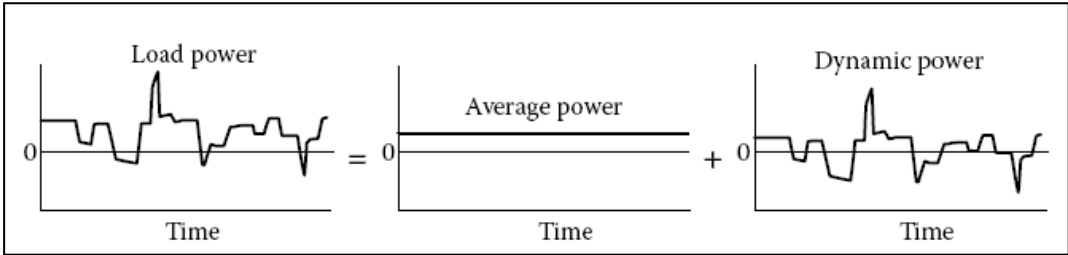


**Figure 2.11 :** Concept of hybrid electric vehicle power train [22].



There are four general configurations for HEVs [23]:

- **Series Hybrid System:** This configuration is the simplest one, where the system basically consists of ICE and electric motor connected in series and a battery bank. Using the ICE and the generator electrical power is produced. This produced energy can either be used to charge the battery bank or it can be used to propel the wheels by powering up the electric motor. This configuration can be defined as “ICE assisted EV”. Although the system is very simple, the systems involves three propulsion machines; ICE, generator and electric motor. In addition to that disadvantage, all of these propulsion machines needs to be sized according to the maximum power demand due to fact that these machines are connected in series and are not able the share the load.
- **Parallel Hybrid System:** Opposite to the series system configuration, parallel system both ICE and electric motor can deliver power directly to the wheels. The propulsion may be provided by only ICE, by only electric motor or by both of them. This design can be called “Electric Motor Assisted ICEV”. The electric motor can charge the battery bank by regenerative braking. The system involves two propulsion machines, which is a big advantage compared to series system configuration. Another big advantage is that these propulsion machines can be chosen to be smaller due to fact that they can share the load demand.
- **Series-Parallel Hybrid System:** This system involves features of both series and parallel system. This is obtained by adding a mechanical coupler and shaft between ICE and transmission so that the ICE can directly deliver power to the wheels. While this system includes an extra mechanical link compared with the series system, it has also again more propulsion machines compared to parallel system. Therefore, the system is more complicated and more costly.
- **Complex System:** The complex system is similar to the series-parallel system. The decisive difference is that the unidirectional generator in series-parallel system is replaced with bidirectional electric motor, which can either operate as a generator or motor. The system becomes much more complex, however

this system offers more driving modes. There are examples of new HEVs using this system adopting for dual axis propulsion.

These configurations are summarized in Figure 2.12.

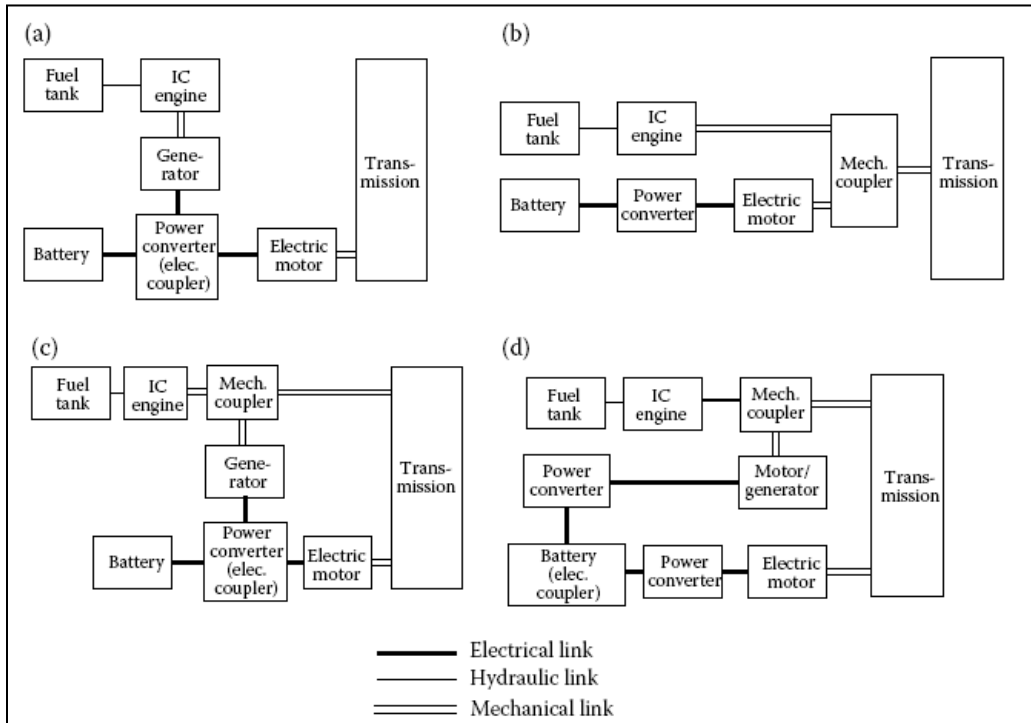


**Figure 2.12 :** Classifications of hybrid electric vehicles (a) series hybrid (b) parallel hybrid (c) series-parallel hybrid (d) complex hybrid system [22].

### 2.3 Battery charging

All electric vehicles include a battery bank. The type and size of this battery bank is chosen considering the needs of the vehicle. Table 2.1 summarizes the average values of battery bank sizes needed for EV types. Until recently, the nickel-metal hydride (NiMH) batteries and valve regulated lead acid (VRLA) batteries were the most used battery types for EVs. However, with the emergence of lithium ion (Li-ion) batteries, it seems that this type will be the most common for EV applications. The Li-Ion batteries provide a very good energy density, making them favorable for EV applications. Recent EVs such as Renault Fluence and Nissan Leaf use Li-ion batteries. Here, most common ones of these methods will be mentioned. It should be noted that there are many topologies for battery charging, which are derived from different applications of the methods mentioned below.

**Table 2.1** : Average power and energy requirements of different EVs [24].

EV type	Power range (kW)	Energy range (kWh)	Voltage range (V)
Micro-HEV	2.5 - 5	0.5	12 - 36
Mild-HEV	15 - 30	1	120 - 160
Full HEV	30 - 50	2 - 3	200 – 350
Fuel Cell Vehicle	25 - 30	1 - 2	220
PHEV	30 – 100 (Van)	5 - 15	200 – 350
BEV	35 – 70 (Van)	25 - 40	200 – 350

### 2.3.1 Constant voltage charging [25]

There are several charging techniques for batteries type. One such charging method is constant voltage (CV) charging where the charger voltage is set to a fixed point, which doesn't allow a current that will damage the battery. This is also called IU charging in Europe. Figure 2.13 shows an example for one such charging process for a 200 Ah VRLA battery at 2.23 Voltage per Cell (VPC) and at 2.4 VPC. As seen from figure, at first the voltage is limited by a current rating. After a while, as current decreases the voltage reaches the voltage set point and it is kept at this value. At this transition point, approximately at 2.7 hours, almost 60% of the battery is charged for the charging set point with lower limit. As the current continues to decrease, the energy delivered falls so much that the last 15% of the battery capacity requires almost 15 hours to be charged.

The advantages of the CV charging are as follows:

- The overcharge possibility is minimized
- The voltage and current limits can be adjusted for slow or fast charge

The disadvantages of CV charging can be summarized as:

- Long durations for full charging, caused by the rapid decrease of charging current.
- Undercharging is possible.
- Equalization, meaning the synchronization of each cell SOC level, is not likely to happen.

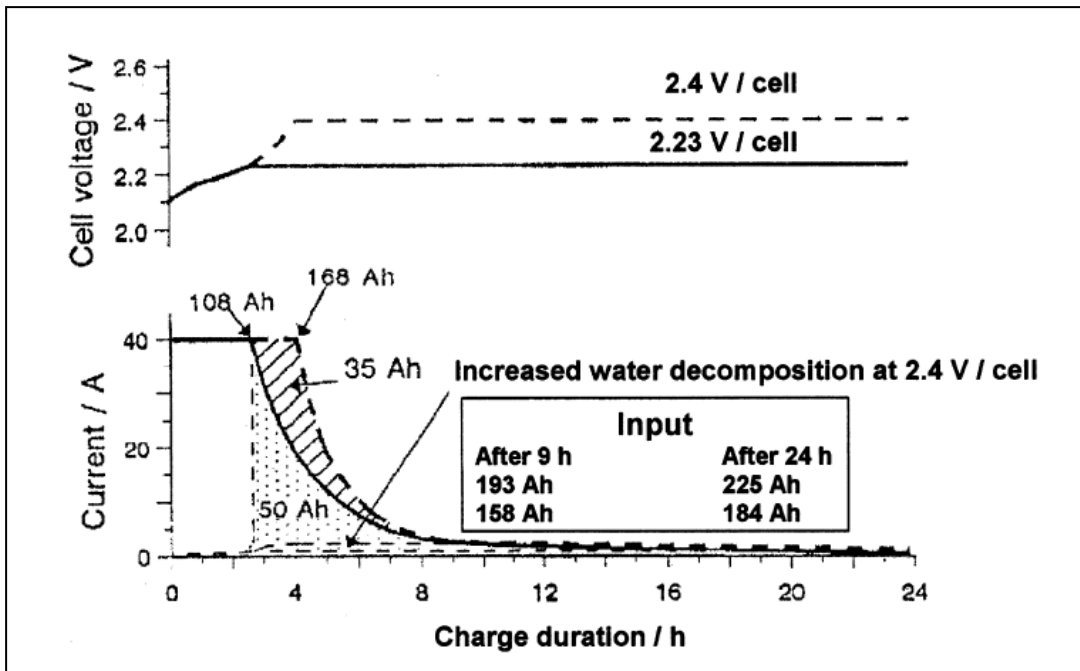


**Figure 2.13 :** Constant voltage charging profile [25].

### 2.3.2 Constant current charging [25]

One other method is to apply a constant current (CC) to the battery, called CC charging. Generally this constant current is applied in more steps. This method has a few advantages:

- CC chargers are mostly inexpensive.
- It enables rapid charging.
- Undercharging is not likely to occur.
- Equalization occurs on every charging cycle.

However it has also some drawbacks:

- A CC charging at a single level may cause to overcharge, resulting in shortened lifetime.
- The voltage is uncontrolled and high voltage may cause corrosion and gassing in the batteries, which again shortens the lifetime.

### 2.3.3 Constant current – constant voltage charging [26]

One common method is the combination of both CC and CV methods. The CC-CV method, which is summarized in Figure 2.14, gives an example for CC-CV charging of a lithium-ion battery. Generally, a constant current with a value of 1 C is applied

until a certain voltage limit is reached. (Here, 1 C is defined as the constant current that will charge the battery in one hour; for example 1 C current of a 100 Ah battery is equal to 100 A) After then, the control algorithm switches to constant voltage. As the voltage of the battery approaches to the maximum the current drops to a value of approximately 0.03 C and the charging is terminated.

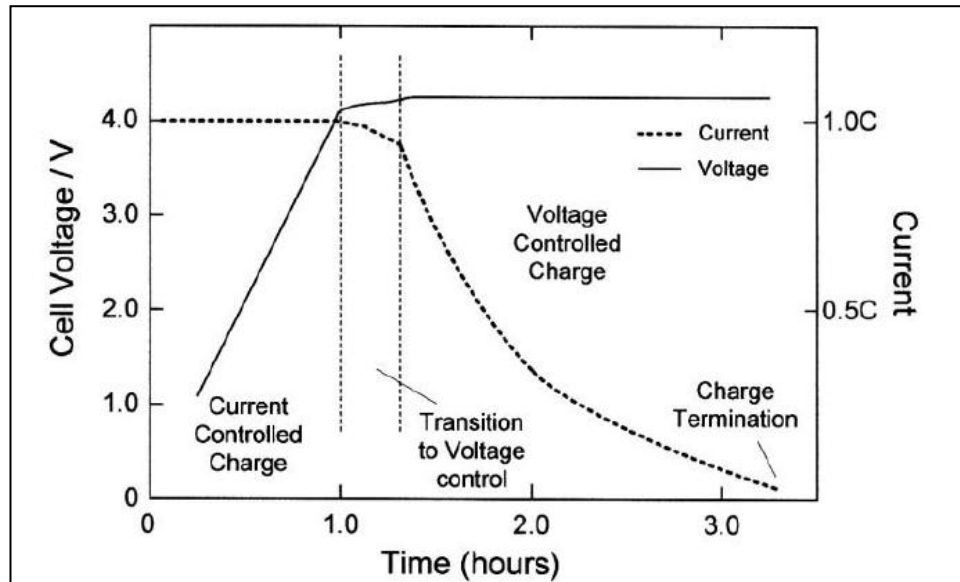


**Figure 2.14 :** Constant current charging profile [26].

Modifications of this method are available. The constant current stage may be done in more steps with mostly decreasing current levels, so that the voltage of the battery will not reach to dangerous levels. It is also possible to apply a short CC finishing step, enabling cell-to-cell charge equalization. One such algorithm called “pseudo-CC” algorithm is presented in figure below. This method offers a more efficient charging method compared to both CC and CV charging.

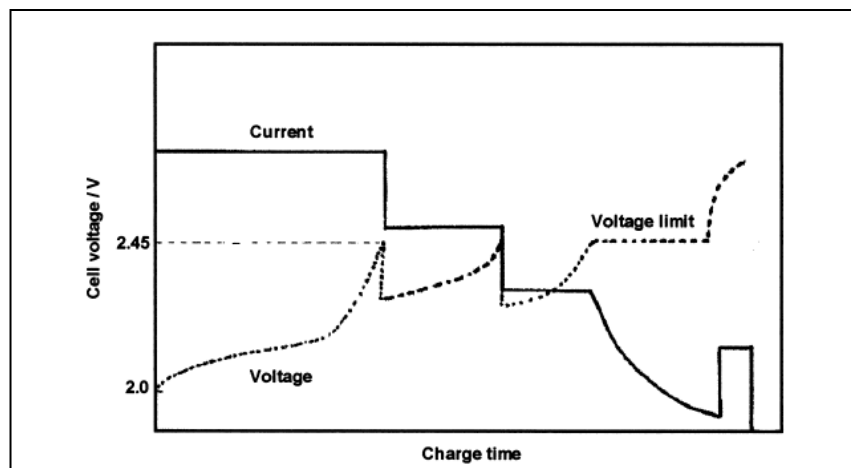


**Figure 2.15 :** Pseudo-CC charging algorithm [26].

### 2.3.4 Taper current charging [25]

Taper current (TC) charging is a very simple method, where neither the voltage nor the current is controlled. In this method a power supply connected in series with resistor and battery provides the energy. The value of the current depends on the value of the resistor and the voltage difference between the power supply and the battery. A typical TC charger circuit is given in the figure below.

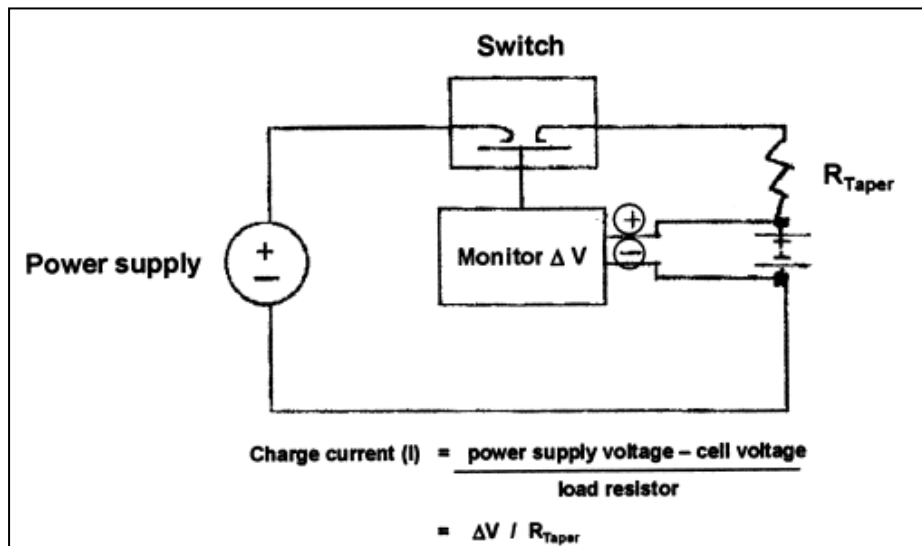


**Figure 2.16 :** Taper current charging setup.

During the charging process the charging current decreases as the voltage difference between power supply and battery decreases. The advantages of this method are as follows:

- These chargers are inexpensive.
- If the values of resistor and power supply are properly chosen, the undercharging is very unlikely to occur.
- The method is suitable for fast charging.

However, there are several disadvantages of this method:

- The levels of noises, such as ripple and harmonics, may be significant.
- The probability of high overcharge is possible.

### 2.3.5 Pulsed current charging [25]

The pulsed current (PC) is an effective method; there are very efficient applications of this method. This method is mostly used for fast charging. The most used

approaches, which are showed in figure below, are either to apply a charging current with constant period and decreasing magnitude, or to apply a current with constant magnitude and decreasing period. The decreasing of the period or magnitude causes the average input of energy to be decreased, which results in minimizing the overcharge and gassing.

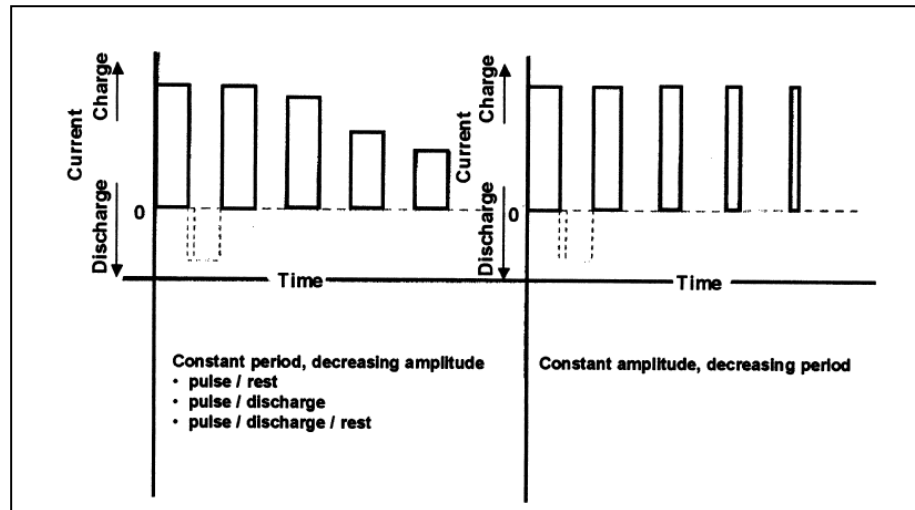


**Figure 2.17 :** Pulsed current charging profile.

The advantages of this method are:

- The “off periods”, where no current is applied, enables heat dissipation and liquid diffusion so that the efficiency of the process is increased.
- The method is available for fast charging.

The main disadvantage of the method is that the control is much more complex; applying a square wave current is not easy, as an exact square wave form current is almost impossible.

In conclusion, a constant current charging method is chosen to be applied for this work. This is due to fact that the work mainly aims to provide a fast charging. However studies on some batteries have shown that the constant current charging with 1 C rate may charge the battery to nearly 75% SOC, where the pressure of the battery rises so high that the charging must be terminated [27]. In order to prevent such effects, there are multistep constant charging methods suggested in the literature [28,29].

There are also intense studies aiming to develop charging related issues of batteries. A recent study states that a special Li-ion battery, called the “18650” battery,

maintains its' full capacity even after 20.000 charging and discharging cycle with a 10 C (6 minutes) charge and 5 C (12 minutes) discharge rate [30]. Commercialization of such efficient batteries will resolve the most of battery related problems of EVs and it will also enable very fast charging processes.

## **2.4 Power Electronics Interfaces [31]**

While the photovoltaic cells produce direct current (DC), wind turbines might produce alternative current (AC) or DC, depending on the generator type. The network all around the world usually runs on AC. Also, different components of such systems require different voltage and current levels. Thus, power conversion is needed within such power systems. This is provided by the power electronics circuits. Here, the needed circuits will be mentioned.

There are mainly four types of power electronic circuits:

1. AC – AC Converters: These circuits provides interaction between two AC systems with different frequency, form or amplitude.
2. AC – DC Converters: These converters enable to convert AC energy to DC energy where it is needed. These circuits are also called rectifiers.
3. DC – DC Converters: These circuits used to meet different voltage and current criterias required within DC systems. They can also be used for isolation and protection.
4. DC – AC Converters: These converters, also known as inverters, are used to convert DC energy to AC energy.

In this chapter, only the ones that will be used in designing and simulation part will be used so that the work is not congested with unnecessary details.

### **2.4.1 Three phase bridge rectifier**

Rectifiers are used to convert the AC energy to DC energy. This circuitis can either be single phase or multi phase. Mostly, three phase circuits used for interaction with grid. Three phase bridge rectifier, also known as B6 rectifier, is a basic rectifier circuit. The schematic of the B6 rectifier can be found in Figure 2.18. The B6 rectifier is an uncontrolled circuit, it mainly consists of six diodes. Because of the nature of the diodes, each diode is in conduction mode for  $2\pi/3$  angle, considering



one period is  $2\pi$ . As it can be seen in Figure 2.19, there are always 2 diodes in conduction mode throughout the process.

The average output voltage  $V_{dc}$  and output root mean square (RMS) voltage  $V_L$  can be calculated via following formulas:

$$V_{dc} = \frac{6}{2\pi} \int_{\pi/3}^{2\pi/3} \sqrt{3}V_m \sin \theta d\theta = V_m \frac{3\sqrt{3}}{\pi} = 1.645V_m \quad (2.10)$$

$$V_L = \sqrt{\frac{9}{\pi} \int_{\pi/3}^{2\pi/3} (V_m \sin \theta)^2 d\theta} = V_m \sqrt{\frac{3}{2} + \frac{9\sqrt{3}}{4\pi}} = 1.655V_m \quad (2.11)$$

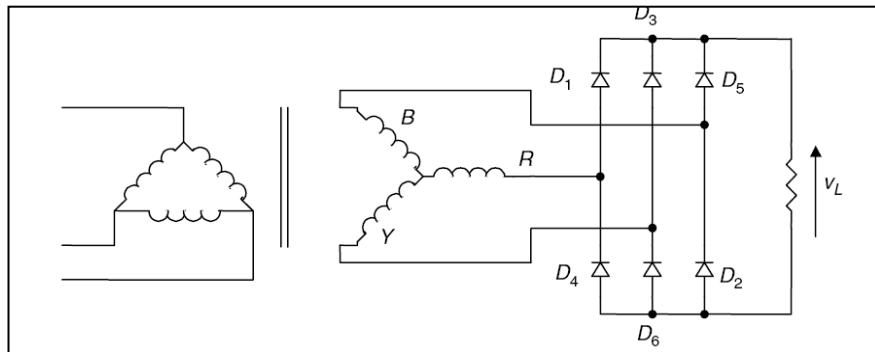


**Figure 2.18 :** Three-phase bridge rectifier [31].

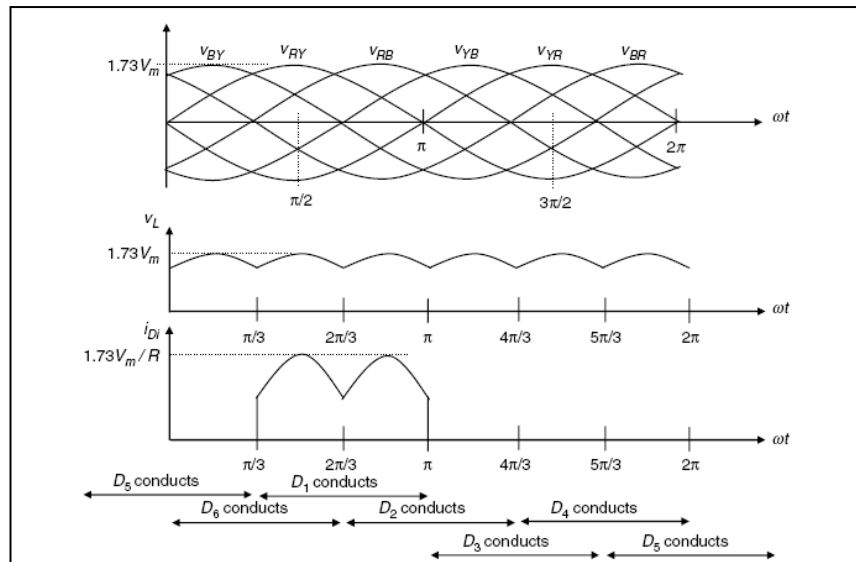


**Figure 2.19 :** Current and voltage waveforms of B6 rectifier [31].

## 2.4.2 Boost converter

Boost converter is a DC/DC converter used to increase the input voltage at the output of the circuit. Figure 2.20 shows the basic boost converter circuit and Figure 2.21

shows the voltage and current waveforms. When the switch is on, the voltage source feeds the inductor L and the inductor current  $I_L$  increases linearly. When the switch is off, the current passes through the diode D, the capacitor C and the load. The duty cycle D is defined same as the duty cycle of cuk converter. Similar to the calculations of cuk converter, when the

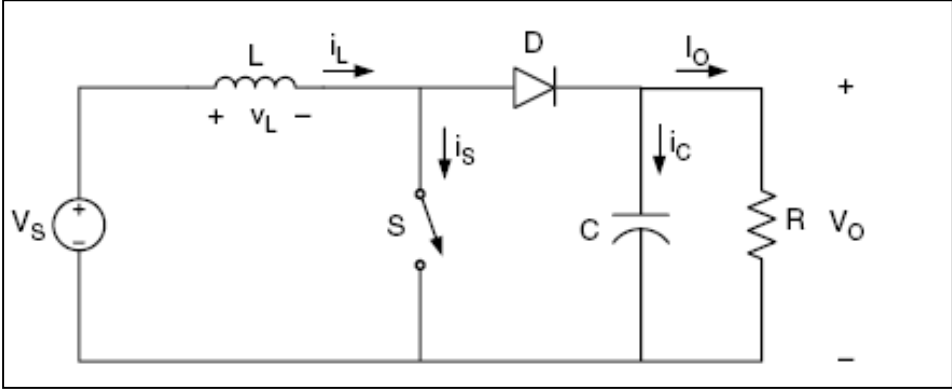


Figure 2.20 : Boost converter circuit [31].

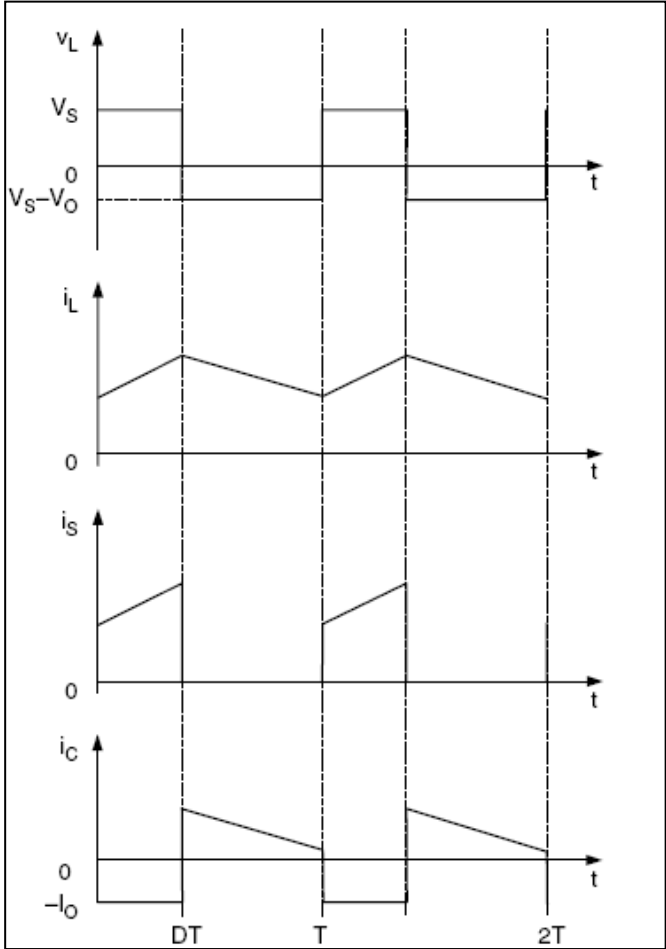


Figure 2.21 : Voltage and current waveforms of boost converter [31].

Faraday's Law, stating that the volt-seconds product of the inductor over a period is zero, is applied, the equation 2.12 is derived:

$$V_S DT = (V_O - V_S)(1 - D)T \quad (2.12)$$

Again, the proportion of output voltage  $V_O$  to input voltage source  $V_S$  can be defined by simple calculations:

$$\frac{V_O}{V_S} = \frac{D}{1 - D} \quad (2.13)$$

The equation 2.14 gives the boundary inductor value between DCM and CCM:

$$L_b = \frac{(1 - D)^2 DR}{2f} \quad (2.14)$$

Finally the last design parameter, capacitor value  $C$ , can be derived from the voltage ripple value  $V_r$ :

$$C_{min} = \frac{DV_O}{V_r R f} \quad (2.15)$$

PV charger circuit will use a MPPT algorithm that will enable the PV cells to produce all the available energy. The algorithm and design will be explained later.

### 2.4.3 Buck converter

Buck converter is also a DC/DC converter. Opposite to boost converter, the buck converter is used to decrease the input voltage at the output. Figure 2.22 shows the circuit of a basic buck converter and Figure 2.23 shows the voltage and current waveforms of this circuit.

When the switch is on, the diode  $D$  is reverse biased, thus the current flows through inductor  $L$ , capacitor  $C$  and load. When the switch is off, the diode allows current to pass and the inductor  $L$  supplies current for the load.

The equation 2.16 is again the implementation of Faraday's Law for steady state conditions.

$$(V_S - V_O)DT = -V_O(1 - D)T \quad (2.16)$$

The equation 2.16 leads to equation 2.17 via simple calculations:

$$\frac{V_O}{V_S} = D \quad (2.17)$$

As it can be seen from the working principles of the buck converter, the load is always supported by either voltage source  $V_S$  or the inductor  $L$ . If the current supplied by inductor is so high that the load current never falls to zero, the buck converter is in continuous conduction mode (CCM). Otherwise, if the load current falls to zero the buck converter is in discontinuous conduction mode (DCM). Mostly CCM is preferred due to fact that it is more efficient. The boundary inductor value  $L_b$  which is the boundary between CCM and DCM, is given by the equation 2.18, where  $f$  is the frequency of the switching:

$$L_b = \frac{(1 - D)DR}{2f} \quad (2.18)$$

Another design parameter of the buck converter is the determination of the capacitor value  $C$ . This value is chosen regarding to the desired voltage ripple value  $V_r$ .

$$C_{min} = \frac{(1 - D)V_O}{8V_rLf^2} \quad (2.19)$$

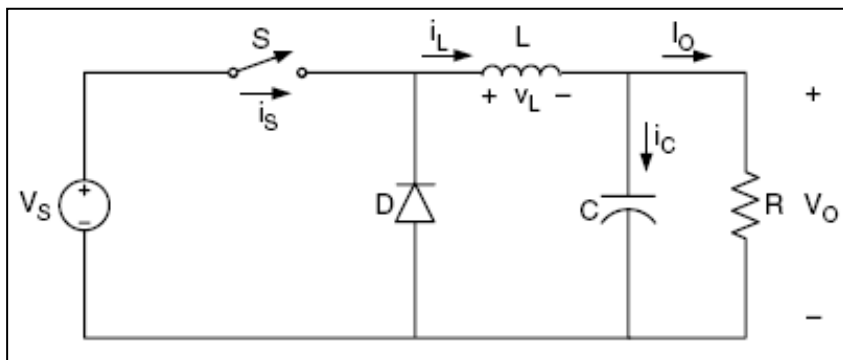


**Figure 2.22** : Buck converter circuit [31].

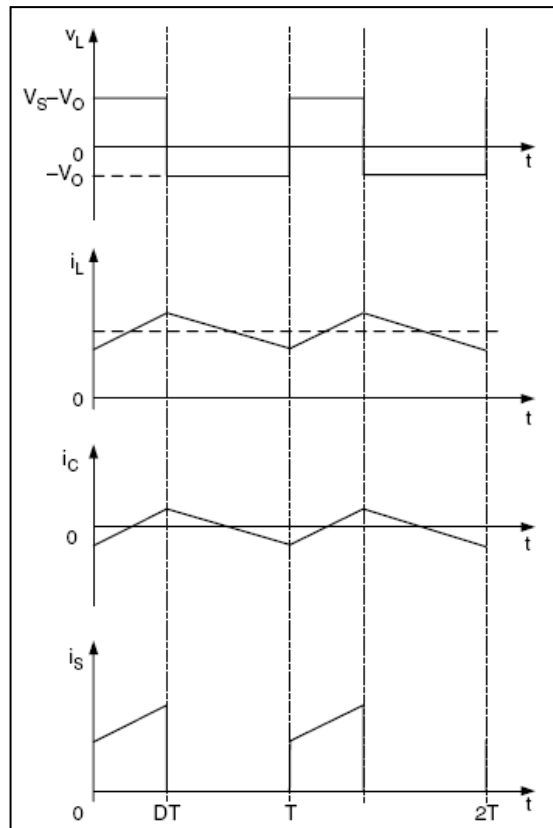


**Figure 2.23** : Voltage and current waveforms of buck converter [31].

#### 2.4.4 Cuk converter

Cuk converter is again a DC/DC converter, which is used either to decrease the or increase the input voltage at the output. Figure 2.24 is the circuit of a basic cuk converter, which consists of two inductances, two capacitors, a diode and a switching element.  $V_S$  is input voltage source,  $L_1$  is input inductor,  $C_1$  is energy transfer capacitor,  $L_2$  is filter inductor and  $C$  is filter capacitor.

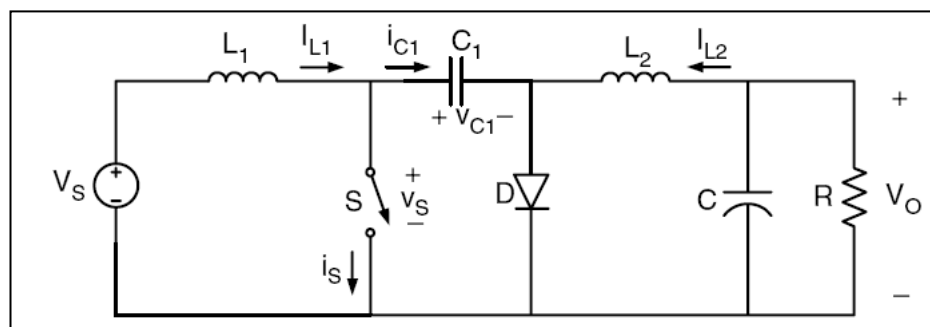


**Figure 2.24** : Cuk converter circuit [31].

The operation cycle of cuk converter can be seen at Figure 2.25. Basically, when the switch is on, the diode current is zero and the capacitor  $C_1$  is discharged by the current of filter inductance  $L_2$ . On the other hand when the switch is off, the diode

allows current of  $L_1$  and  $L_2$  to pass through and the capacitor  $C_1$  is charged by the current of  $L_1$ .

In order to derive the transfer function of the cuk converter, it is assumed that the steady state average current through a capacitor is zero and the values  $L_1$  and  $L_2$  is so large that the ripples can be ignored. The steady state conditions of Faraday's Law for capacitor  $C_1$  can be written as follows:

$$I_{L2}DT = I_{L1}(1 - D)T \quad (2.20)$$

The proportion of the time the switch is on to the time the switch is off is defined as duty cycle,  $D$ . If it is assumed that the converter is lossless, the power can be expressed as follows:

$$P_S = V_S I_{L1} = -V_O I_{L2} = P_O \quad (2.21)$$

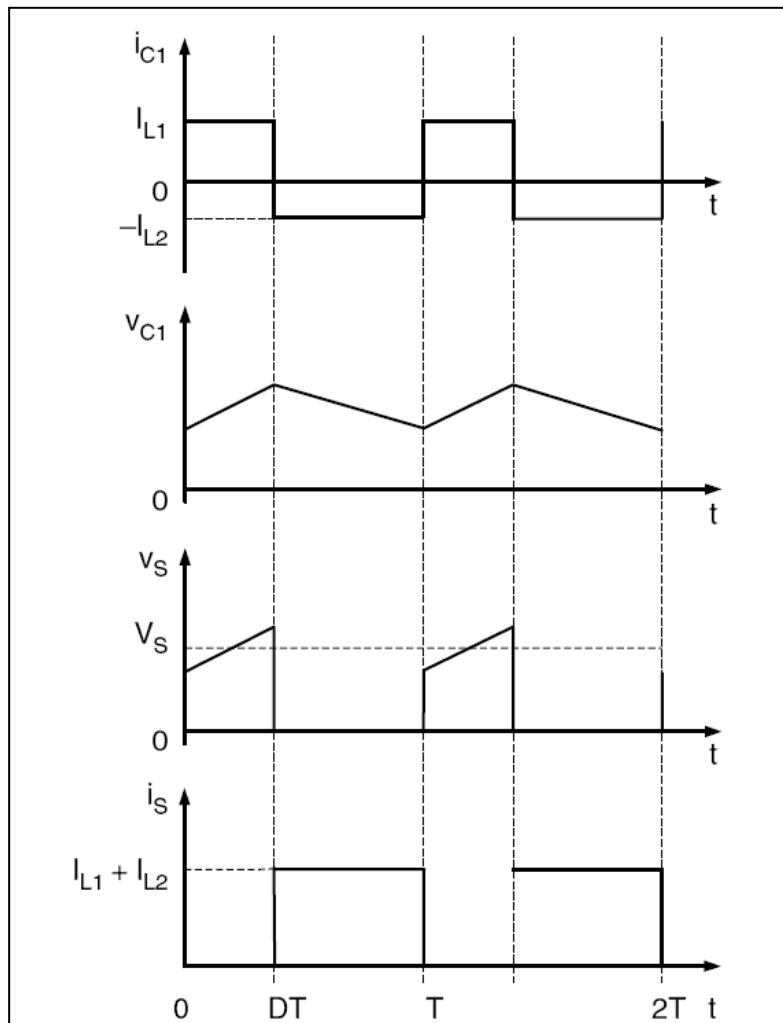


**Figure 2.25** : Voltage and current waveforms of boost converter [31].

Where  $P_S$  is the power supplied by source and  $V_O$  is output power. Combining both equations gives the transfer function of the converter:

$$M_V = \frac{V_O}{V_S} = -\frac{D}{1-D} \quad (2.22)$$

The values of the inductors and the capacitors are important design parameters for converters. Depending on these parameters and the switching frequency, the converter can work either in continuous conduction mode (CCM) or discontinuous conduction mode (DCM): CCM means that the output current of the converter never drops to zero and energy is continuously supplied to the load, whereas DCM means that the output current of the converter drops to zero each cycle. In order to calculate these parameters, the current ripple, voltage ripple and CCM boundaries are taken into account. The two equations below are CCM boundary equations used for calculating necessary minimum values of inductances:

$$L_{b1} = \frac{(1-D)R}{2Df} \quad (2.23)$$

$$L_{b2} = \frac{(1-D)R}{2f} \quad (2.24)$$

The value of the capacitors  $C_1$  and  $C_2$  are calculated using the voltage ripples  $V_r$  and  $V_{r1}$  value with the equation below:

$$C_{2,min} = \frac{(1-D)V_O}{8V_rDL_2f^2} \quad (2.25)$$

$$C_{1,min} = \frac{DV_O}{V_{r1}Rf} \quad (2.26)$$

The grid side charger will use a PID controller that will keep the charging current for a desired value. The theoretical background and details of PID controller will be explained in later chapters.

## 2.5 Control of Power Electronic Interfaces

The control of power electronics components is of big importance since all the required voltage and current levels are adjusted with the help of these control

systems. In this chapter, basic theoretical knowledge about the control strategies used for the simulation of this work will be mentioned.

### 2.5.1 Pulse-width modulation

Pulse-width modulation (PWM) is one of the most common modulation methods used for sampling. Figure 2.26 shows the usage of PWM for sampling. However, in the topic of power electronics the PWM method is mostly used for regulating the switching elements of the circuits.

The main idea is to constantly adjust the conduction period of switching elements  $t_{on}$  by applying square wave signals. This way the output voltage can be regulated. As mentioned before, the duty cycle,  $D$ , can be defined as the percentage of the period  $T$  that the switch is on:

$$d = \frac{t_{on}}{T} = \frac{t_{on}}{t_{on} + t_{off}} \quad (2.27)$$

Adjusting  $t_{on}$  or  $t_{off}$  gives the ability to regulate duty cycle  $D$ , shown in Figure 2.27. These PWM regulators can either run at fixed frequency or variable frequency, whereas fixed frequency regulators are the most common ones.

Most of switching elements are controlled by a voltage or current signal applied to the gate of the switching element, which changes the conduction mode of these elements.

As mentioned earlier, the duty cycle of controlled power electronic circuits determine the output voltage or current. Thus, controlling duty cycle, with the use of PWM method applied to the gates of switching elements, enables to meet the required parameters by the system.

### 2.5.2 PID control

PID control is the most common way of getting feedback from systems and they have a very large application area. The name of PID control comes from “Proportional”, “Integral” and “Derivative”. Basically, a PID controller calculates the present, past and prediction of future errors from the reference value.



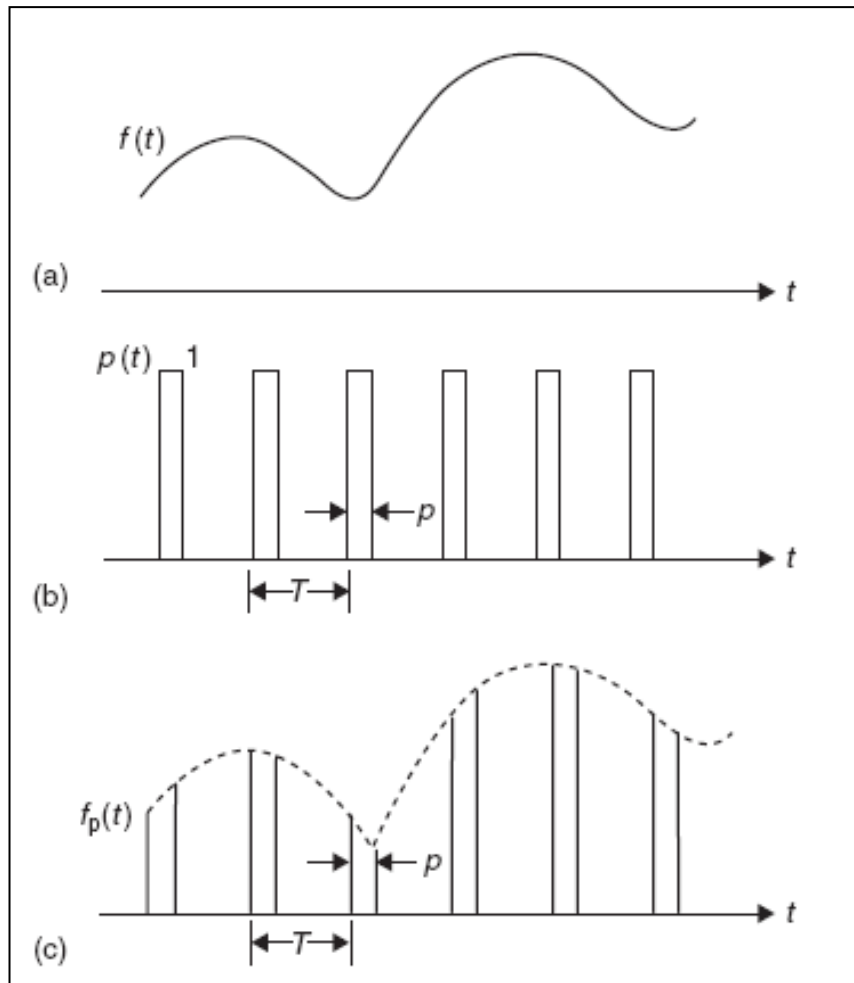


**Figure 2.26 :** (a) Input signal (b) Carrier signal as PWM (c) Output signal [32].

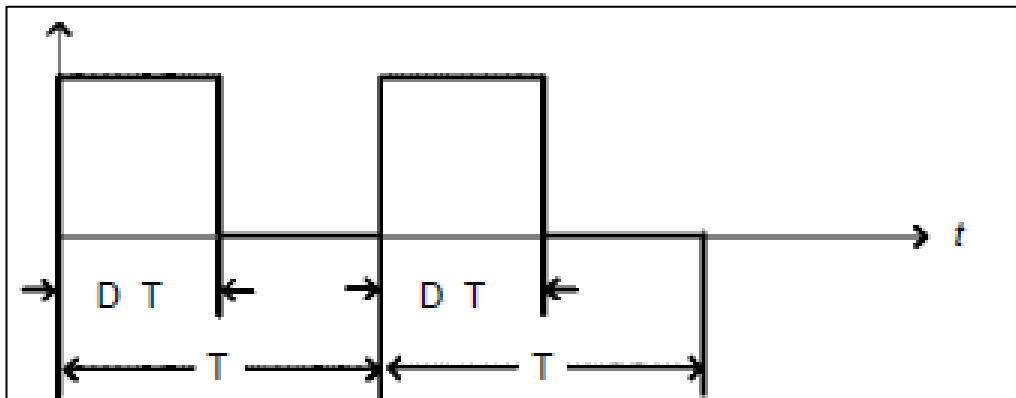


**Figure 2.27 :** PWM signal with duty cycle D.

The basic formula of a PID controller is given below [33]:

$$u(t) = k_p e(t) + k_i \int_0^t e(\tau) d\tau + k_d \frac{de}{dt} \quad (2.28)$$

Where  $e(t)$  = error signal

$u(t)$  = control signal

$k_p$  = proportional gain

$k_i$  = integral gain

$k_d$  = derivative gain

Here, the error signal  $e(t) = r - y$  is the the difference between actual value of controlled parameter,  $y$ , and desired value,  $r$ . The equation consists of three components; proportional, integral and differential components. The equation can be written with the use of derivative time constant  $T_d$  and integral time constant  $T_i$ :

$$u(t) = k_p \left( e(t) + \frac{1}{T_i} \int_0^t e(\tau) d\tau + T_d \frac{de}{dt} \right) \quad (2.29)$$

As shown in figure below, the proportional part represents the present error, the integral represents the past errors and the derivative can be understood as the prediction of future errors.

Some of the gains  $k_p$ ,  $k_i$  and  $k_d$  may be equal to zero, which results in the elimination of the related part. Thus, there are some combinations of PID control such as P and PI control. Depending on the application P, PI and PID control strategy can be preferred. In Figure 2.29 you can interpret the effects of different combinations of P, PI and PID controllers on the change of control signal,  $u$ , and the actual value of the controlled parameter,  $y$ .

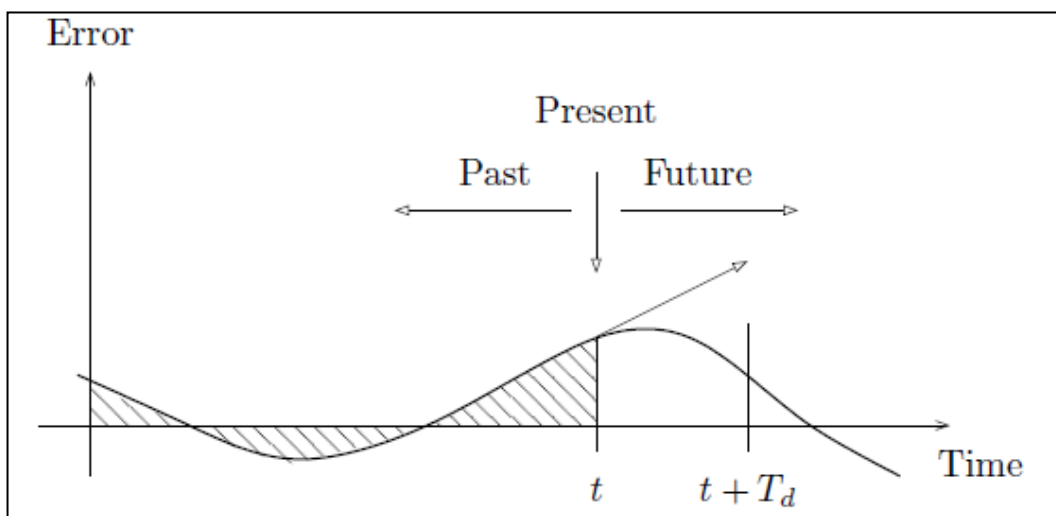


**Figure 2.28 :** A PID controller evaluates present, past and future errors [33].

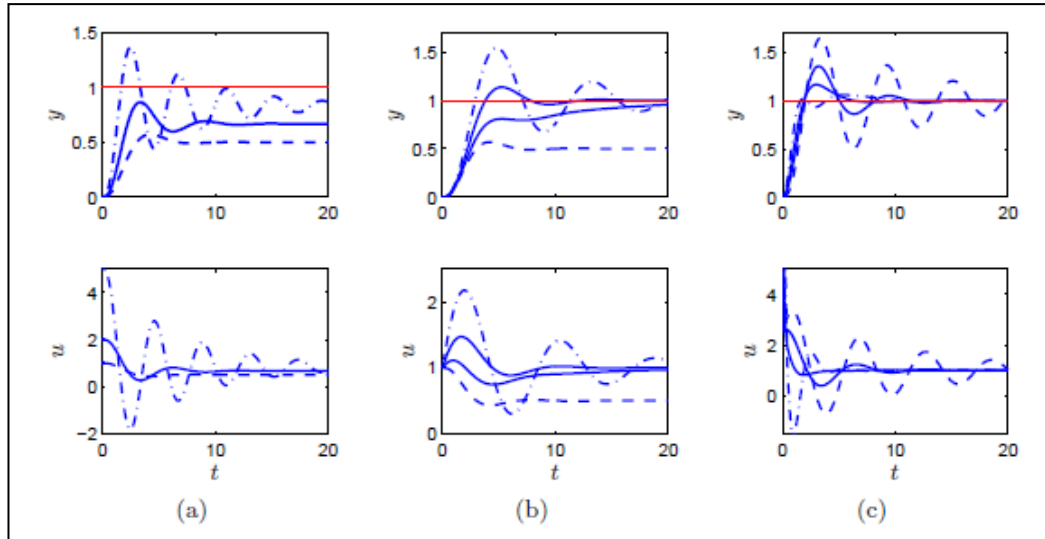


**Figure 2.29 :** (a) P (b) PI (c) PID controllers with different values for  $k_p$ ,  $k_i$  and  $k_d$  for a process with the transfer function  $P(s) = 1/(s+1)^3$  [33].

### 2.5.3 Maximum power point tracking

As mentioned before, the MPPT enables to produce the most of the available power from renewable energy sources. Such methods are needed due to the characteristics of these sources. This thesis focuses on solar and wind energy. Thus, the MPPT methods for these sources will be explained.

#### 2.5.3.1 MPPT for solar power

The I-V characteristics of PV cells explained before, require that a MPPT method needs to be used with PV power systems. There are various such algorithms but so called “Hill-Climbing Methods” are the most common ones. The basic idea of hill-climbing methods is to move the operation point of the array in the direction where the power production is increasing. In this chapter, two of these methods will be interpreted; perturb and observe (P&O) method and incremental conductance (InCond) method.

PV cells are generally connected to a power converter which feeds the load. The P&O method basically aims to change the operating voltage of the power converter in the direction where the generated power is increasing. The main idea is to apply a perturbation and observe the outcome, which is generated power. If the power is increased the perturbation is kept in the same direction. On the other hand, if there is a decrement in the power, then the next perturbation is in the opposite direction. When the MPP is reach the P&O method oscillates around the MPP, which is the

main problem of the method. The P&O algorithm can be seen in the Figure 2.31 [34].

InCond method makes use of power vs voltage curve, where the slope of the curve is equal to zero at MPP, which is shown in Figure 2.30. While the slope of this curve is positive at the left side of the MPP, the slope is negative at the right side. It can be summed as [34]:

- $\Delta V/\Delta P=0$  ( $\Delta I/\Delta P=0$ ) at the MPP
- $\Delta V/\Delta P=0$  ( $\Delta I/\Delta P<0$ ) on the left
- $\Delta V/\Delta P=0$  ( $\Delta I/\Delta P>0$ ) on the right

The basic algorithm is given at Figure 2.32. As mentioned before the first disadvantage of these methods is the algorithm keeps oscillating around the MPP. The second disadvantage is that the sudden changes of the solar irradiation may cause these methods to lose track [34]. There are many modifications for these methods aiming to eliminate these disadvantages. These modifications are very related with the type of battery and the chemical reactions in the charging process. However, in this work only the basic algorithms will be mentioned.

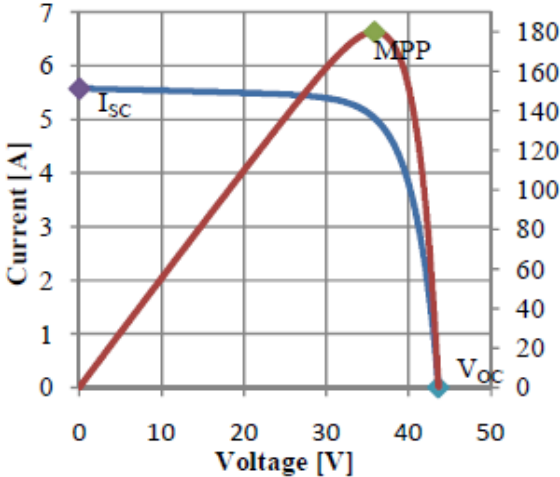


**Figure 2.30 :** I-V characteristic and MPP of a PV array [34].

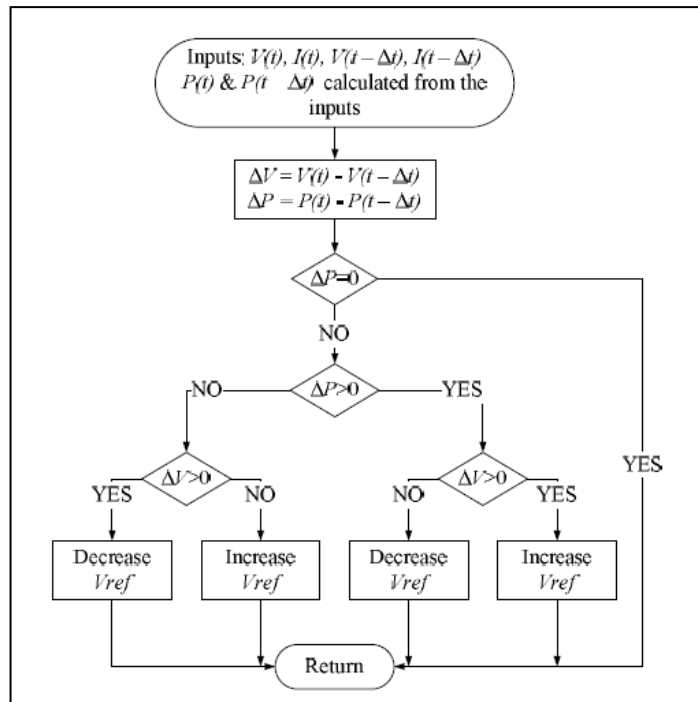


**Figure 2.31 :** P&O Algorithm [34].

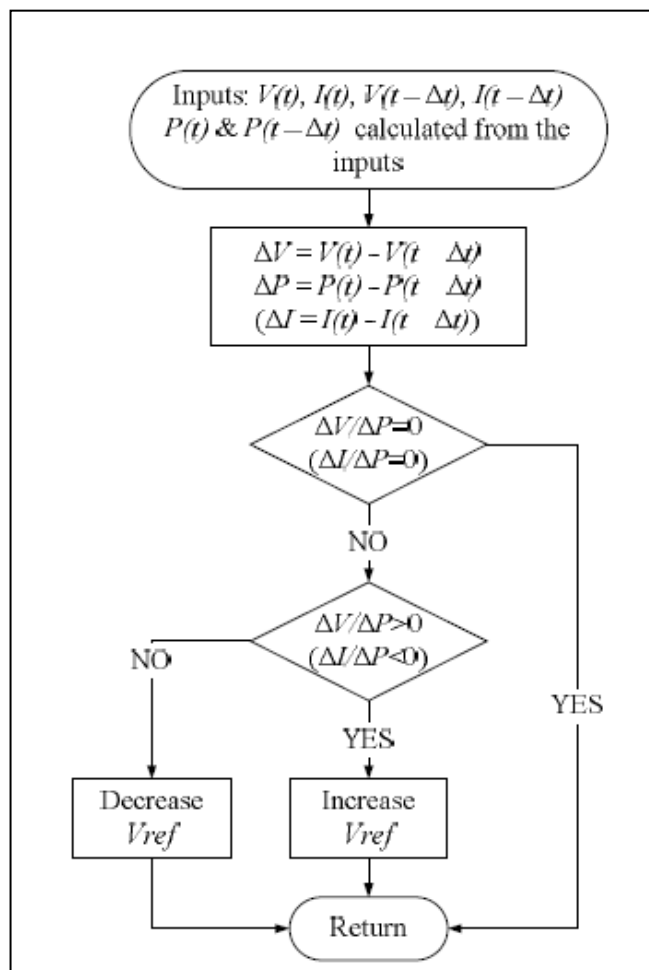


**Figure 2.32 :** InCond Algorithm [34].

Other than hill-climbing methods there are lots of methods making use of computational methods and different techniques such as neural networks, fuzzy logic and current sweep.

### 2.5.3.2 MPPT for wind power

As it can be seen from the Figure 2.33, the power extracted from the wind varies with the wind speed and the shaft speed of the generator. Thus, the operating point must always be controlled, similar to PV power systems, as shown in Figure 2.34.

There are mainly three MPPT methods for wind energy conversion systems; tip speed ratio (TSR), power signal feedback (PSF) and hill-climb search (HCS) [35]. The TSR method, as seen in Figure 2.35, aims to adjust the rotational speed of the generator so that the maximum power can be extracted from the wind. This method requires the knowledge about the optimum TSR of the turbine, wind speed and turbine speed measurement. PSF method, as seen in Figure 2.35, uses the knowledge about the turbine's power curve, where these curves must be gained using simulations or experiments with the individual turbine. The HCS method, as seen in Figure 2.35, is very similar to hill-climbing methods for PV power system. The basic idea, which is summed up at Figure 2.36, and the disadvantages are the same. The two different algorithms mentioned at Chapter 2.3.3.1 (P&O and InCond) are also valid for wind power systems.

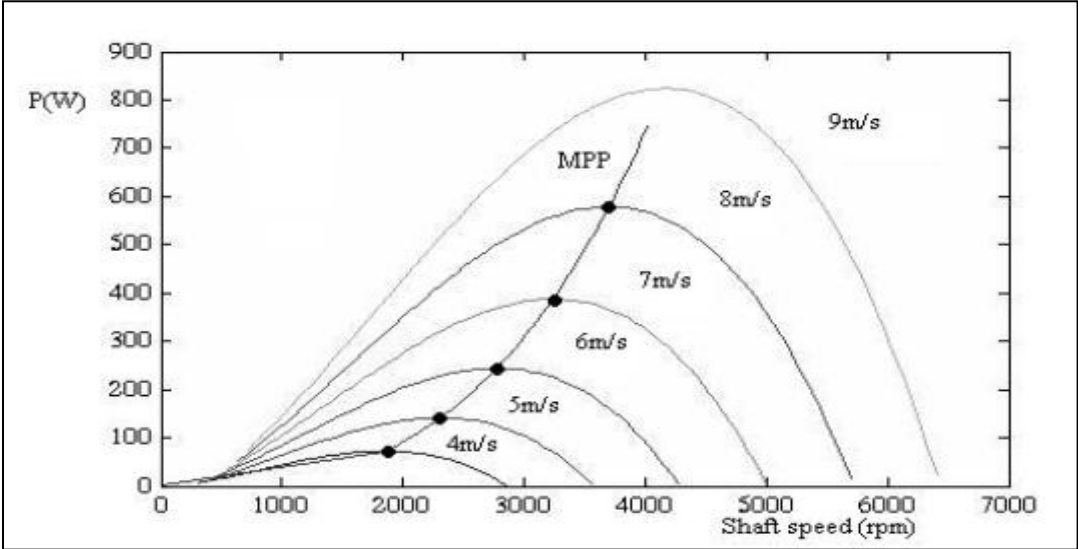


Figure 2.33 : Maximum power point of wind turbines for different wind speeds [21].

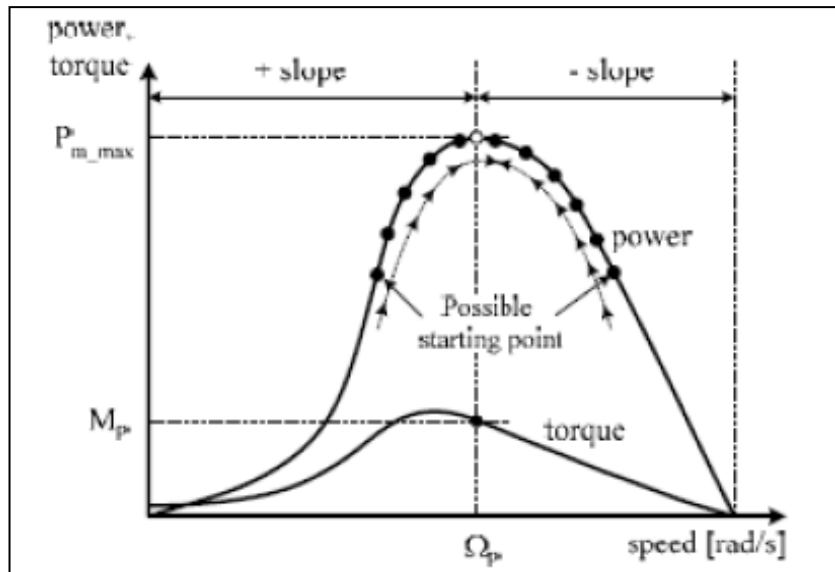
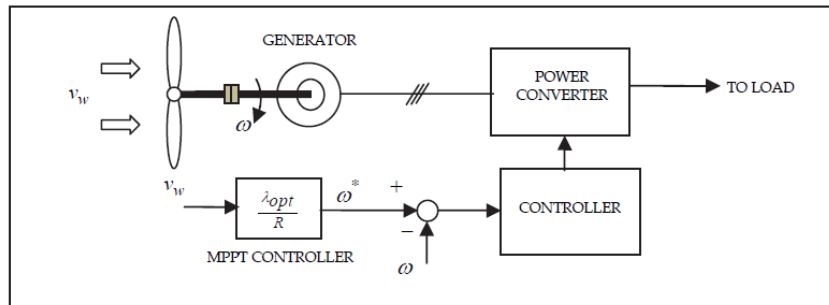
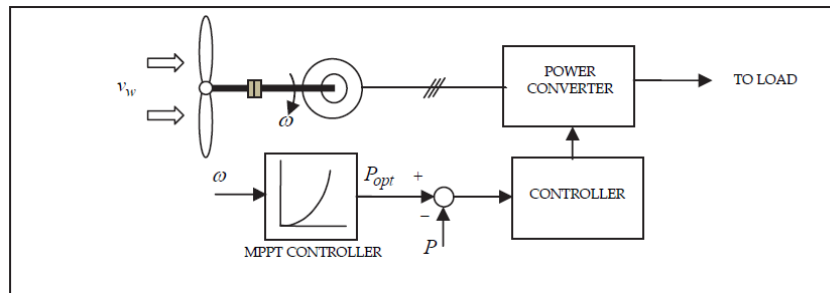


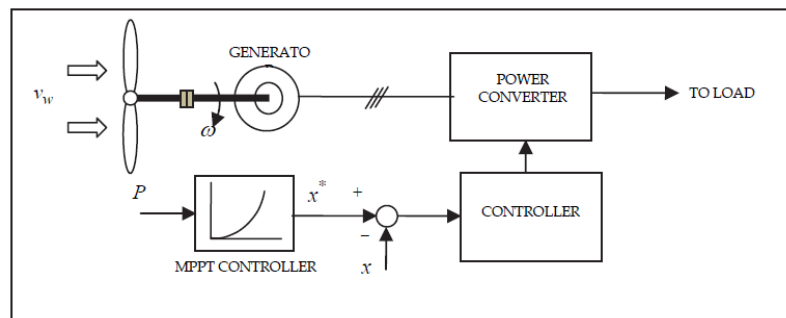
Figure 2.34 : MPPT process for wind turbines [21].



(a)



(b)



(c)

Figure 2.35 : MPPT process with (a) TSR (b) PSF (c) HCS method [35].

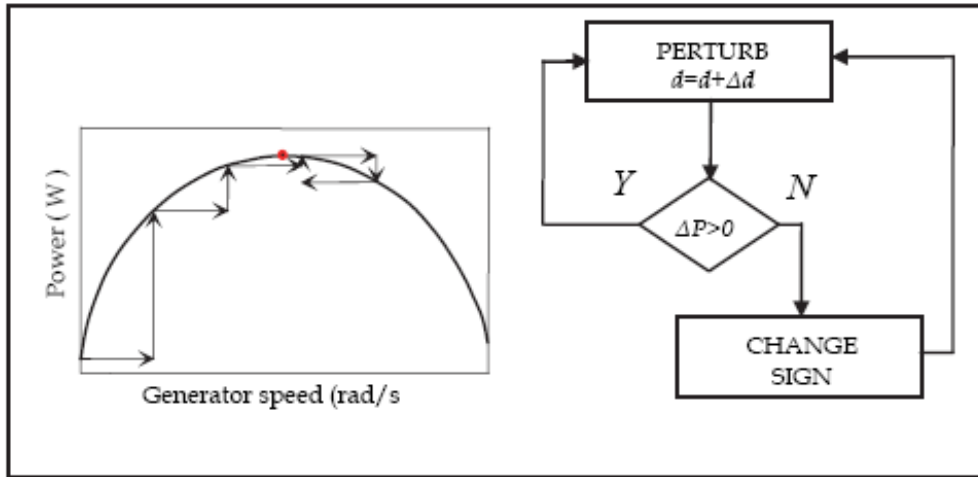


**Figure 2.36 :** Control principle of HCS method[35].

## 2.6 Electric Vehicle Charging Standards

One of the big challenges concerning EVs is the standardization of the infrastructure and the charging components of the EVs. Biggest authorities of standardization of EV charging systems are Society of Automotive Engineers (SAE), Japan Automotive Research Institute (JARI) and International Organization of Standardization (ISO). Right now, the standardization works carried out by SAE has been the most regarded ones. There are lots of standards concerning different fields of EVs and charging stations. The figure below shows the standards related to EV charging stations [36]. Figure 2.37 summarizes some of the most important standards.

These standards define the safety procedures, charging topologies, communication processes and components of charging stations such as connectors, wirings etc. Among these standards, there are defined charging types and levels by SAE J1772. These are divided in two types; AC charging and DC charging. AC charging implies that the car is directly connected to AC grid and an on-board charger system regulates the charging process, while DC charging means that an off-board charger system outside of the vehicle, which supplies DC, is regulating the charging process. There are also levels defined according to voltage, current and power delivered to the EV by the charger. These levels also directly affect the charging speed.



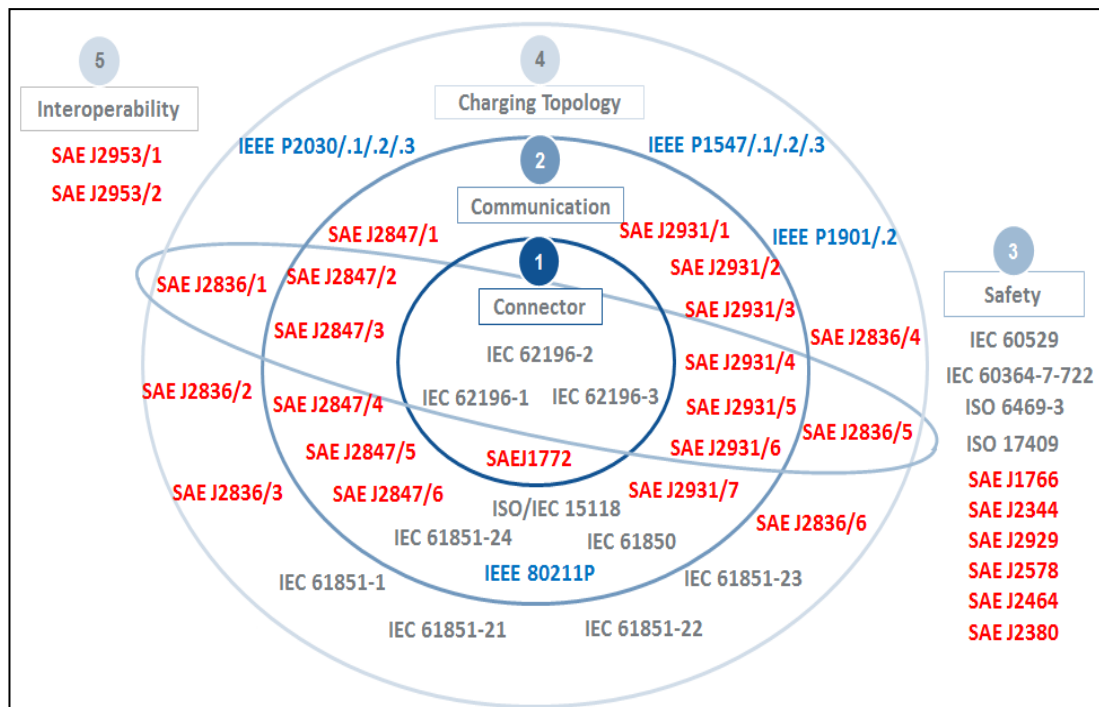


**Figure 2.37 :** Standards related with EV charging [36].

The basic level is called “Standard/Normal” and it corresponds to “Level 1” charging in United States. These charging limits are mostly chosen by the power outlet limitations of the countries. However, nominal values of the grid are different in North America (N.A.) and European Union (EU).

In addition to that, the allowed current levels differ at each country; in EU, this limit is equal to 16 Amperes at 230 Volts in residential areas, while in United Kingdom (UK) it is limited to 13 Amperes and in Switzerland to 10 Amperes. In North America the standard power output is 15 Amperes at 120 Volts. Thus the standards vary in N.A. and EU [37,38,39].

The second level is “Semi-fast” charging, which corresponds to “Level 2” charging in United States. This charging level provides a faster charge. However, it has again differences due to different power outlet standards defined by countries. The defined levels in EU and N.A. are given in the Table 2.2 [37,38,39].

Also it should be noted that, AC charging standards are almost completed, whereas DC charging standardization is still in process. The DC Charging is mostly used for fast charging. The power levels defined by SAE J1722 Standards are given in the Table 2.3.

**Table 2.2 :** AC charging levels in EU and N.A. [37,38,39].

<b>Level</b>	<b>Phases</b>	<b>Maximum Voltage</b>	<b>Maximum Current</b>	<b>Approximate Power Level</b>
<b>N.A. – Level 1</b>	1	120 V	15 A	1.8 kW
<b>N.A. – Level 2</b>	1	240 V	30/80 A	7.2/19.2 kW
<b>EU Standard</b>	1	230 V	16 A	3.7 kW
<b>EU Semi-fast</b>	1	230 V	32 A	7.4 kW
<b>EU Semi-fast</b>	3	400 V	16 A	11.1 kW
<b>EU Semi-fast</b>	3	400 V	32 A	22.2 kW

**Table 2.3 :** DC charging levels defined in J1722 [37,38].

<b>Type &amp; Level</b>	<b>Maximum Voltage</b>	<b>Maximum Current</b>	<b>Maximum Power Level</b>
<b>DC – Level 1</b>	450	80	36 kW
<b>DC – Level 2</b>	450	200	80 kW
<b>DC – Level 3</b>	600	400	160 kW

Another topic on charging stations that worth mentioning is the types of areas where these stations are supposed to be built. This is directly related with the people’s preference of where they want to charge their EVs. The figure below shows the estimated distribution of charging locations. According to the figure it is expected that people will most likely prefer to charge their EVs at home. The second preferable location is expected to be the workplaces, where people spend a lot of time during the day. The least preferable charging place is estimated to be public places. As it is obvious these preferences are in close relationship with the charging time; this leads to fact that people mainly prefers to charge their EVs where they spend the most of their time. This is briefly summarized in Figure 2.38.



**Figure 2.38** : Charging place distribution estimation [40].

## 2.7 Literature Overview

This chapter is organized in such way that the chosen works are overviewed under three steps. This is due to fact that the topic of this thesis involves many subtopics within itself. First of all, a brief overview of the works on hybrid renewable energy systems (HRES) is presented. The second step is the overview of the literature on power management strategies of similar energy systems. Lastly, actual works concerning charging stations and concepts are introduced.

There are many works on hybrid renewable energy systems in the literature. Here, the ones that involve similar platform with the thesis are presented. Bajpai and Dash published a detailed review of HRES especially for standalone applications. In this work they described the reasons for emergence of such systems, reviewed the optimization, design, control and modeling of various HRES types [14]. Another study focusing on the modeling of HRES is done by Deshmukh and Deshmukh where they interpreted the modeling of the HRES components and trends in the HRES for both standalone and grid-integrated applications [15]. Bernal-Agustin and Dufo-Lopez explained the design and control strategies for wind and/or PV and/or diesel hybrid systems with batteries or fuel cells as energy storage components [41].

Although this work does not include the optimization of HRES, it is worth mentioning that there are also important studies focusing on the optimization process

of HRES, where sizing and control of separate components are a big problem. Fadaee and Radzi researched the multi-objective optimization methods for standalone HRES by using evolutionary algorithms [42]. Hafez and Bhattacharya investigated the optimization problem of HRES by using HOMER, which is a simulation program [43]. Erdinc and Uzunoglu prepared a detailed review of different approaches for optimization of HRES, where they especially focused on sizing problems [44].

As seen from the works above, HRES is a very important type of power system, which can either be used as standalone system or can be integrated to the grid. This thesis aims to apply such systems for the charging process of electric vehicles.

Power management system, which regulate the power conditions of the system and provide the power flow, is the heart of HRES. Thus, this important topic attracts the attention of many researches. There are many works for power management systems of HRES in the literature. One such work is published by Gupta et al.; in this work they offered a power management strategy for a HRES consisting of renewable AC and DC generators, diesel generator and battery banks [45].

Kohsri and Plangklang discussed power management and control system of a standalone power unit consisting of PV, diesel generator and battery bank feeding a variable AC load, which has the profile similar to daily energy consumption of an average house [46].

Jeong et al. proposed another hybrid system consisting of a fuel cell system and battery that feeds an AC load [47]. The controller checked the parameters of battery and used fuzzy logic to control the fuel cell system and DC/DC converter.

Tofighi and Kalantar worked on a PV – battery hybrid system feeding DC loads. The controller system regulated DC/DC converters to control the whole system [48].

As a result it can be said that the power management of such systems are of big importance. There are various types of HRES; every system has specific features and specific parameters to be controlled. Thus, every system needs to be specifically designed and controlled considering the characteristics of the system.

As mentioned before, studies on charging stations and concepts are to be mentioned. One of the publications about the charging stations for EVs is studied by Benysek and Jarnut, which describes the development and the trends of the EV charging

infrastructure in Poland. They also discussed the development of EV market and influence of EVs on the grid in Poland [49].

Another work on EV charger is published by Li-wei and Dian-long, which focuses on the digital charger. They used digital signal processor (DSP) for the control system, which has benefits such as high frequencies, large data processing capacity and short instruction cycles. They also used the soft switching technique, which enables them to increase the efficiency and stability [50].

In addition to works above, Gallardo-Lozano et al. designed an on-board EV charger that is compatible with smart grids. They designed a novel control system which enables the charger to operate bi-directionally, meaning that EV can either draw energy from the grid or it can supply energy to grid with no harmonics [51].

As mentioned before, this thesis aims to combine the topics of HRES and EV charging stations. One of the works combining renewable energy sources and charging stations is published by Dunbar P. Birnie, which represents the idea of solar powered charging stations. Birnie analyzed the advantages of solar charging and made the conclusion that daytime charging at workplace parking lots are the best option for plug-in electric and hybrid vehicles [52].

Another study that involves one of the renewable energy sources is done by Suppes. The study offers a charging station for plug-in hybrid vehicles, which makes use of a regenerative fuel cell (RFC) stack as charger [53].

Besides the works above, there are also studies that offering whole new concepts of charging operation. One such work is published by Villa et al., where they pointed out that electrification of public transport vehicles, such as bus, are not yet feasible due to the extra weight caused by batteries. They offered a new charging procedure, which involves charging these vehicles at bus stops along the route by using an inductive coupling power transfer (ICPT) system [54].



### **3. DESIGN AND SIMULATION PART**

At this chapter, the electrical and control background of charging station for EVs, which makes use of solar and wind power supported with grid network, is designed and simulated for different cases. The simulation is performed using MATLAB - Simulink which is a simulation program with wide application area.

#### **3.1 System Design**

Every power system aims to supply energy to a given load. In this thesis, the electrical vehicle to be charged is referred as the load. The designed system aims to supply electrical energy for electrical vehicles where it is beneficial for consumers to produce electrical energy using photovoltaic panels and wind turbines. The system is an on-grid hybrid power system, which makes use of the electrical grid network in the case of an emergency.

In the scope of this thesis, the focus point is the DC charging concept. The designed system works within the limits of Level 2 DC Charging Standards. The designed system is basically a fast charging station, which makes it preferable to use in public places or workplaces. On the other hand, the ability of the designed system to charge the EVs using renewable sources, where it uses MPPT algorithms to extract the most available power, makes it also preferable to use at residential areas. The system provides a “fast charging” using a multistep constant current charging method. Briefly, this algorithm charges the EV in two steps: at the first step the EV is charged with 100 amperes if the SOC is less than 70%, once this level is reached the second steps begins, where the charging current is set to be 37.5 volts which provides a safe charge. It can also provide a slow charging by using the maximum available amount of renewable energy sources, if the EV doesn't need to be fast charged: this method is referred as MPPT charging throughout the thesis. The method aims to charge the EV in 1 to 2 hours depending on the capacity of the vehicle. For example, the Renault Fluence has a 22 kWh Li-ion battery. A battery with such size at nearly 300 Volts, would have nearly 75 Ah capacity, meaning that 70% of the battery would be

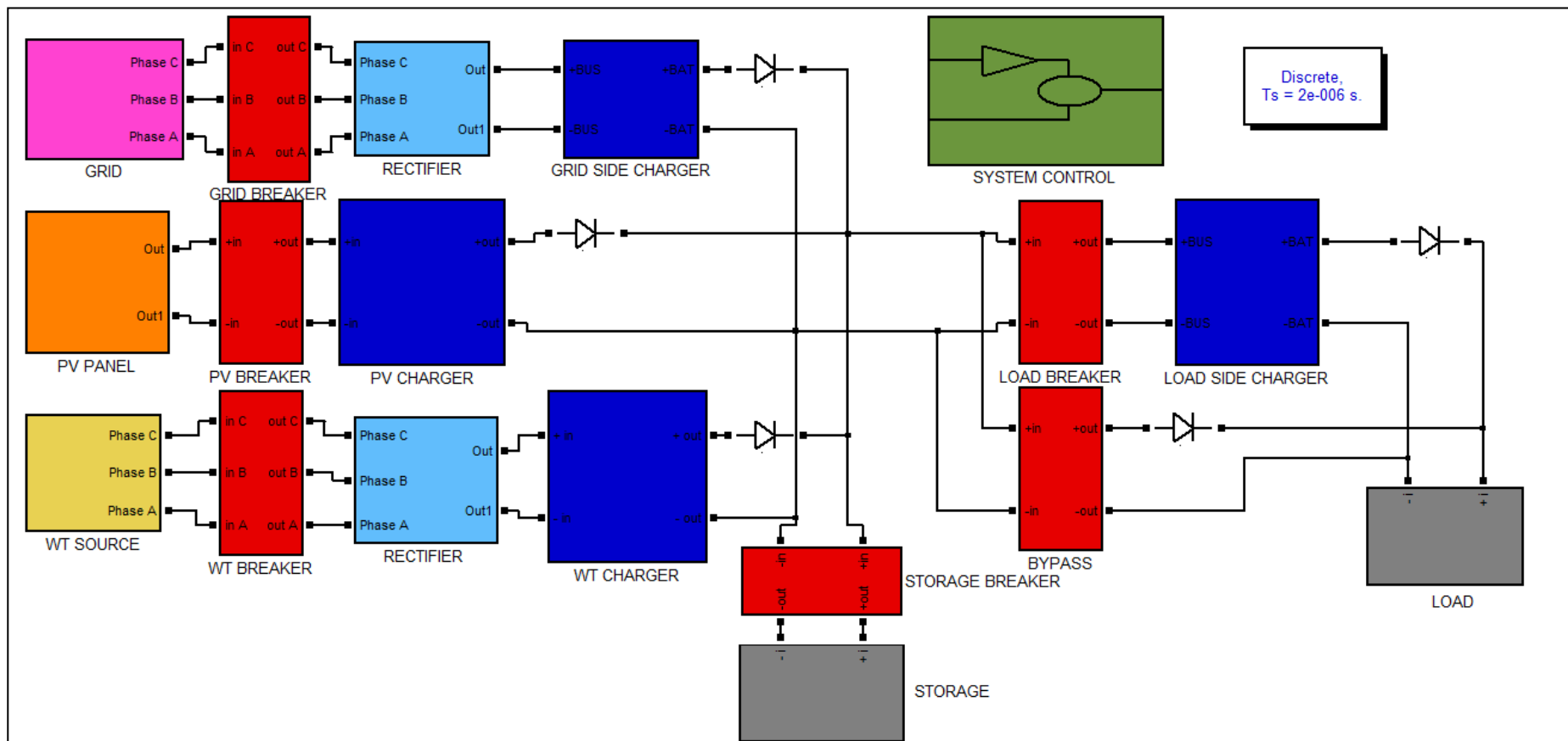


**Figure 3.1** : General structure of the designed system.



charged within around 32 minutes and the second step of the method would require nearly 36 minutes to charge the battery to full capacity.

As seen in the Figure 3.1, the system basically consists of a PV array, wind turbine, grid, battery bank (storage), breakers and power converters that are used to adjust the system parameters according to voltage and current requirements. These power converters are “Grid Side Charger”, “Photovoltaic Charger”, “Wind Turbine Charger”, “Load Side Charger” and two rectifiers. The PV array and wind turbine produce energy when the environmental conditions are convenient for renewable energy generation. The battery bank is used to store the produced renewable energy so that it can be used when an electrical vehicle is to be charged.

However it is an engineer’s responsibility to consider some unexpected emergency cases. In this case following situations are considered: the possibility of an error on the solar power and wind energy branch or simply the fact that the energy demand might exceed the stored energy. Thus, the system is adapted to use electrical grid in cases of emergency.

### **3.1.1 Rectifiers**

Renewable sources can be used either standalone or with grid. The designed system mainly act as a standalone system, whereas in case of an emergency the grid is put into use. One such emergency is the case where no resources are available and the batteries are discharged to unwanted limits, where the life time of batteries is shortened. Thus, the grid, which runs on AC, must be connected to the system that runs on DC. For this purpose, a three-phase bridge rectifier, which is also known as B6 rectifier, is used. A second rectifier with same type is also used to convert generated AC energy from wind turbine to DC energy. The schematics of these components are given in Figure 2.18.

### **3.1.2 Grid side charger model**

The grid steps in emergency cases to charge the battery. However certain voltage and current conditions must be met in order to charge the battery. The rectifier used to rectify the AC is an uncontrolled circuit. Thus, the output cannot be adjusted for the requested conditions. Therefore a DC/DC converter to meet the requirements is used.

The grid side charger (GSC) is used when the load demands a fast charge and neither the battery bank nor the renewable energy sources are able to supply the required energy. Considering that the input voltage of the grid side charger is the peak line voltage, which is around 325 Volts, and the voltage levels of the storage and load are different, the voltage either needs to be increased or decreased depending on the conditions.

Another emergency situation is that when the state of charge (SOC) of the battery bank used as storage is so low that the expected life cycle of the battery bank decreases. In this situation the GSC steps in to supply 100 Amperes to the storage to increase the SOC value to a safe level.

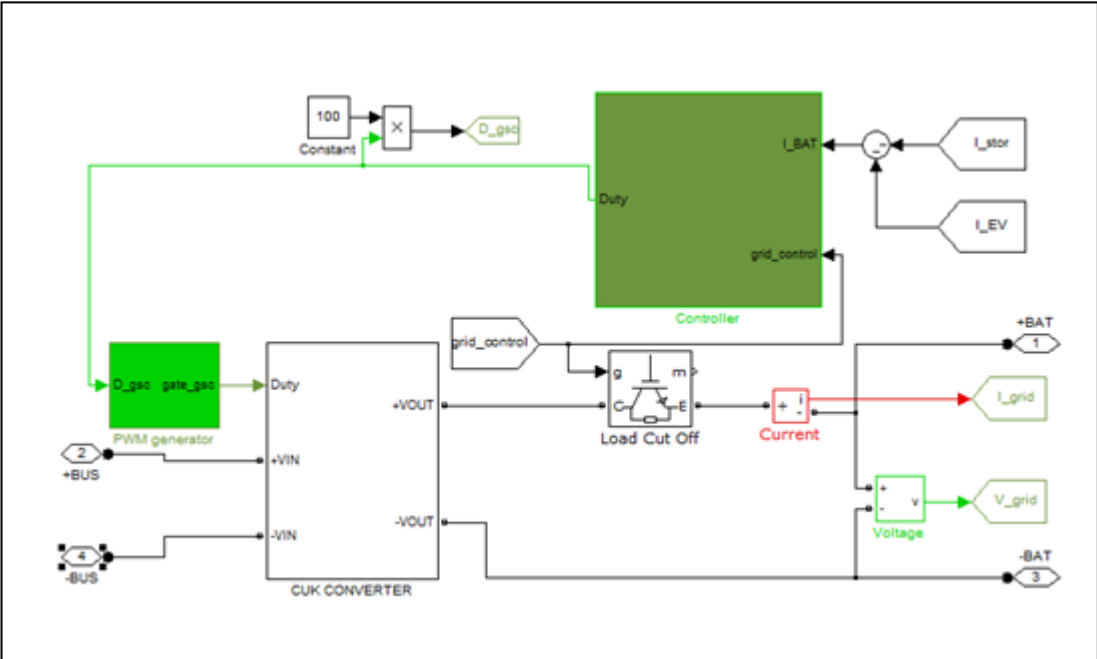


**Figure 3.2 :** The structure of GSC.

As seen in the Figure 2.2 GSC is basically a cuk converter. The input voltage of the GSC, which is the line voltage, is approximately 320 volts at peak. The nominal voltage of the load is assumed to be 300 volts, whereas the nominal voltage of the battery banks used for storage is 150 volts. Therefore, during the charging process the voltage may either need to be increased or decreased. For this reason a cuk converter, which can either increase or decrease the input voltage, is used within the GSC. The controller is a basic PID controller that regulates the output current to be a constant value. If GSC is used to increase the SOC value of the storage, it supplies 100 amperes, which is the default current value. If GSC is used to charge the EV the

controller applies the multistep constant current algorithm. In the first step the EV is charged with 100 Amperes until the SOC value reaches the 70%. Above this value, the GSC charges the EV with 37.5 Amperes. Figure 3.3 shows the PID controller, where the constant “Step 1 Ref” is defined as the default reference current value, 100 Amperes. The switch enables the system to switch to the second step of constant current charging, where the value of the current is set to be 37.5 Amperes.

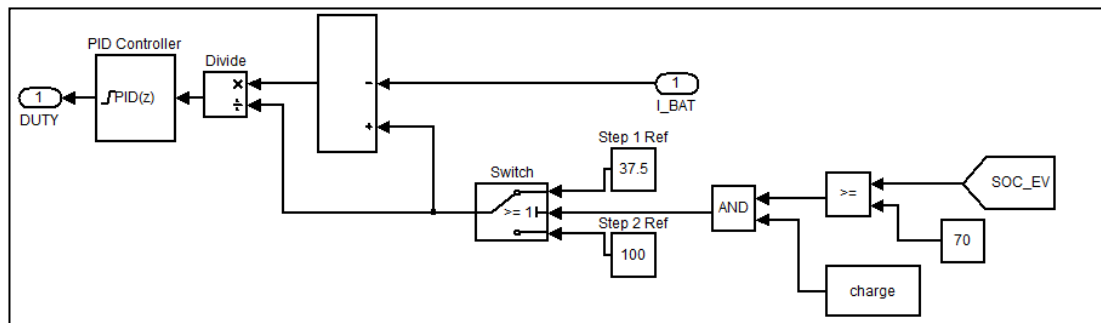


**Figure 3.3 :** Controller of GSC.

### 3.1.3 PV array model

The I-V characteristic of a PV cell was mentioned before. A PV array model coherent with this characteristic must be built. Here, basically a controlled current source is used to model the PV array. The control signal of the current source is provided from a lookup table, where the I-V characteristic behavior under different irradiation levels is defined.

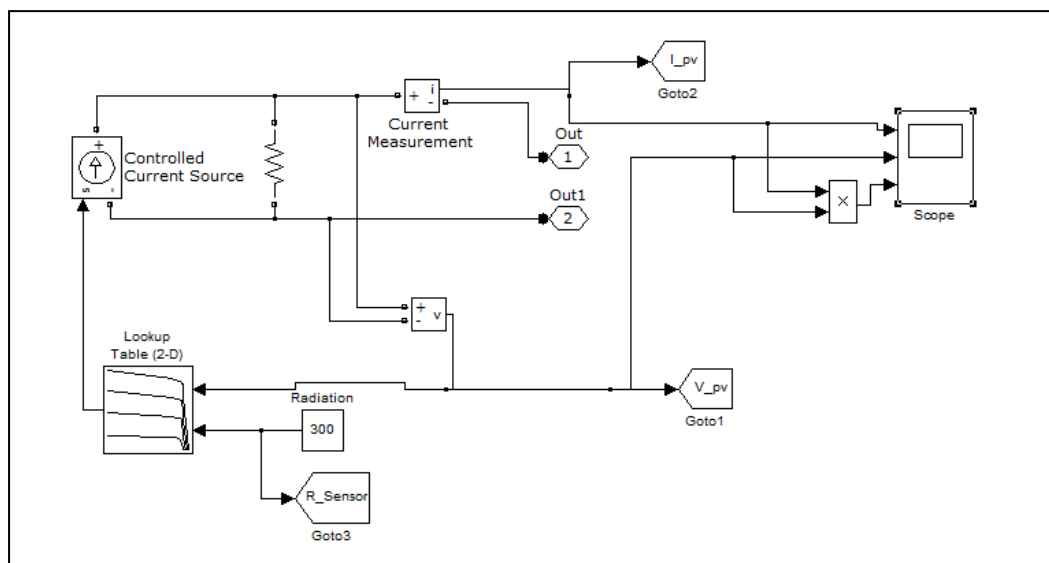


**Figure 3.4 :** Modeling of PV array.

The modeled PV array has the following parameters;  $V_{OC}= 130$  Volts,  $I_{SC}= 85$  Amperes,  $P_{MAX} \cong 8750$  Watts at 1000 Watts/m<sup>2</sup> irradiation level.

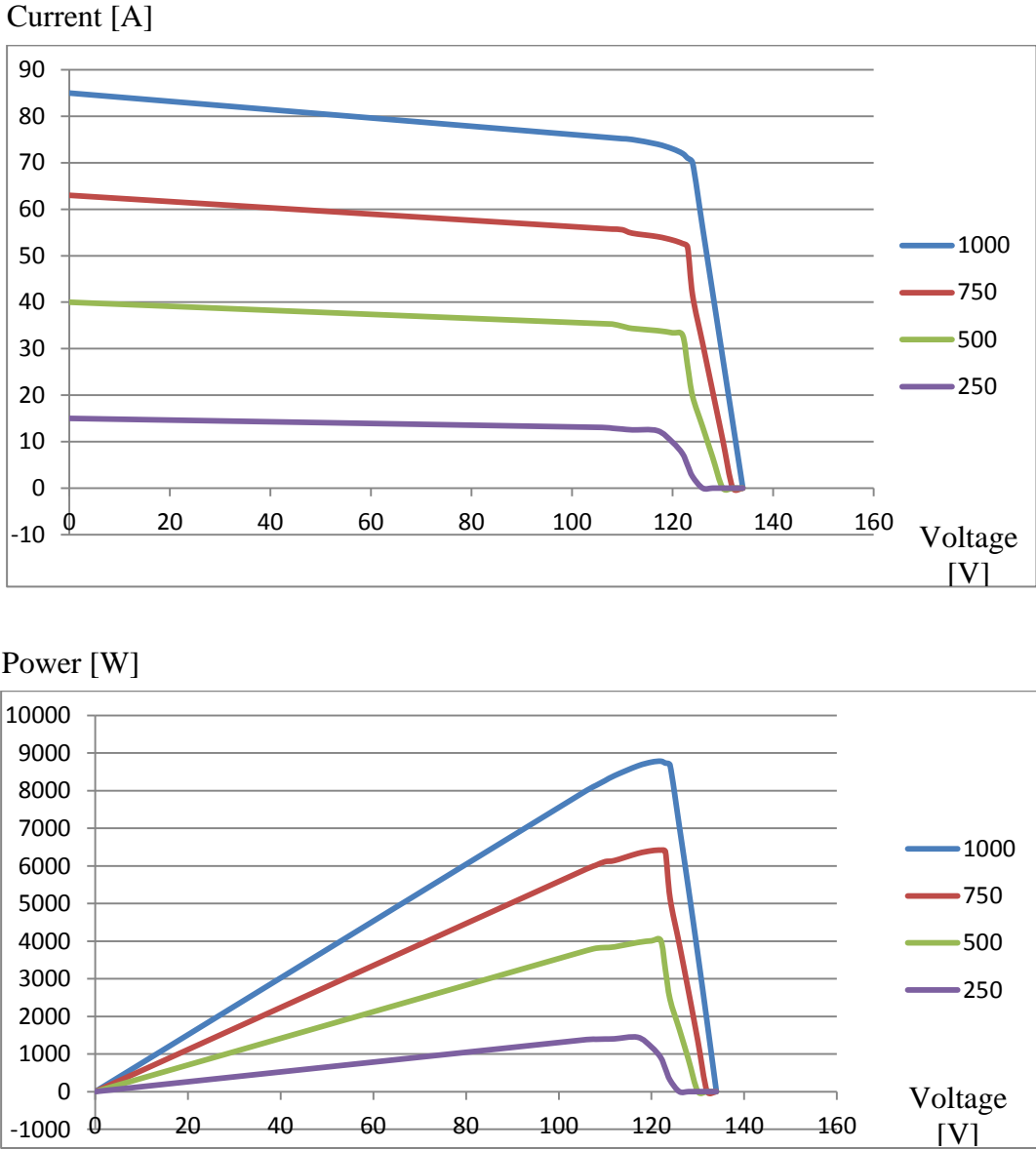
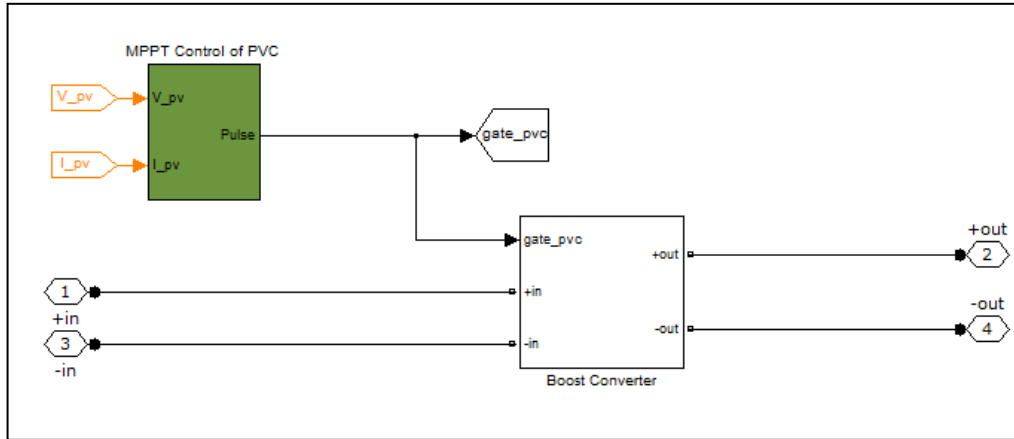


Figure 3.5 : Characteristics of modeled PV array.

### 3.1.4 Photovoltaic array charger model

Photovoltaic cells act as a DC source. Thus, it is decided to use a DC/DC converter to adjust the voltage output level of the PV cells for the voltage level of battery bank. Generally voltage level of PV cells is low, so that the voltage output must be increased. Here, a boost converter is used for this purpose. Thus, the photovoltaic array charger (PVC) is basically a boost converter using an MPPT control method,

which in this case is the incremental conductance method. This method was explained earlier in the work.



**Figure 3.6 :** General structure of PVC.

This control tries to move the operation point to MPP, where  $dP/dV = 0$ . On the other hand the condition of the operation point can be written as follows:

$$dP/dV = d(V*I)/dV = (V*dI)/dV + I = 0 \quad (4.1)$$

This can be rewritten as:

$$dI/dV + I/V = 0 \quad (4.2)$$

The implementation of the algorithm can be seen in Figure 3.7.

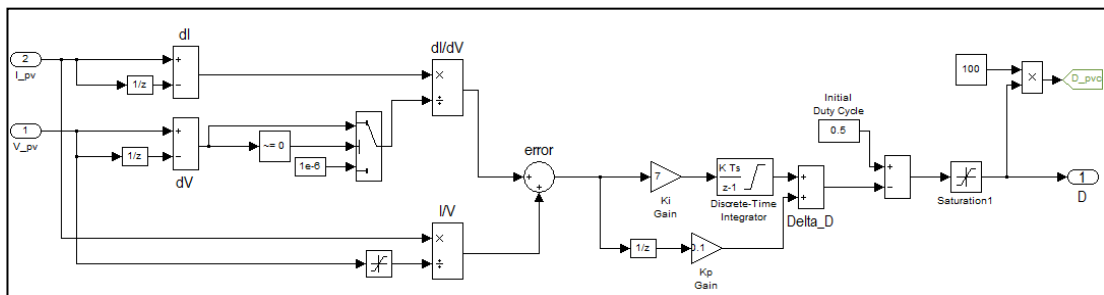


**Figure 3.7 :** MPPT controller of PVC.

Therefore the method first calculates the values of  $dI$  and  $dV$  and uses the equation above to calculate the MPP. The equation can also be defined as the error from operation point. The error is processed with a PI controller and the deviation of the

duty cycle is calculated. The output signal of the MPPT controller, duty cycle  $D$ , is sent to a pulse generator which regulates the gate of the switching element.

### 3.1.5 Wind turbine model

The wind power generation is modeled with wind turbine block set and synchronous machine which is used as generator. Both of these blocks can be found in SimPowerSystems library. In this work no pitching control is applied, thus the pitch angle is set to be constant at zero. The wind turbine block produces a mechanical power according to the given wind speed which is transmitted to the generator, where the electrical energy is generated.

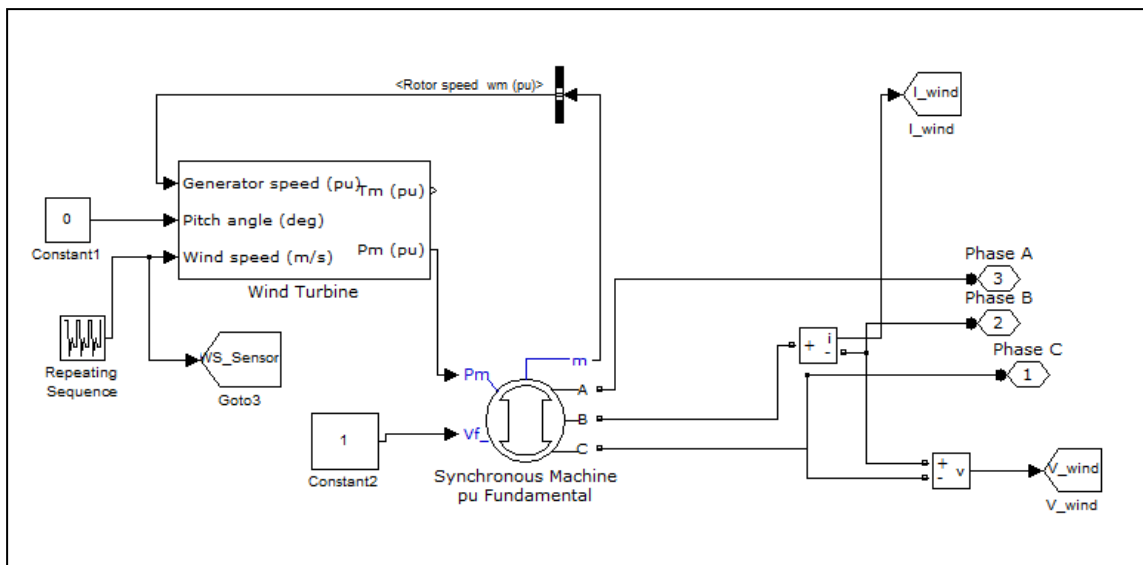


**Figure 3.8 :** Wind Turbine Model.

The following parameters are chosen for the wind energy conversion step of the model:

Nominal Parameters of Wind Turbine: 14.5 kW, 12 m/s Base Wind Speed,

Nominal Parameters of Generator: 42.09 Nm, 560 Vdc, 3000 RPM, Synchronous Machine (SG)

The characteristics of wind turbine are given in Figure 3.9. As it can be seen from the figure the generated power at any constant wind speed varies with the speed of the generator shaft, which creates a need for MPPT algorithm to be used for the controller of the wind turbine charger.

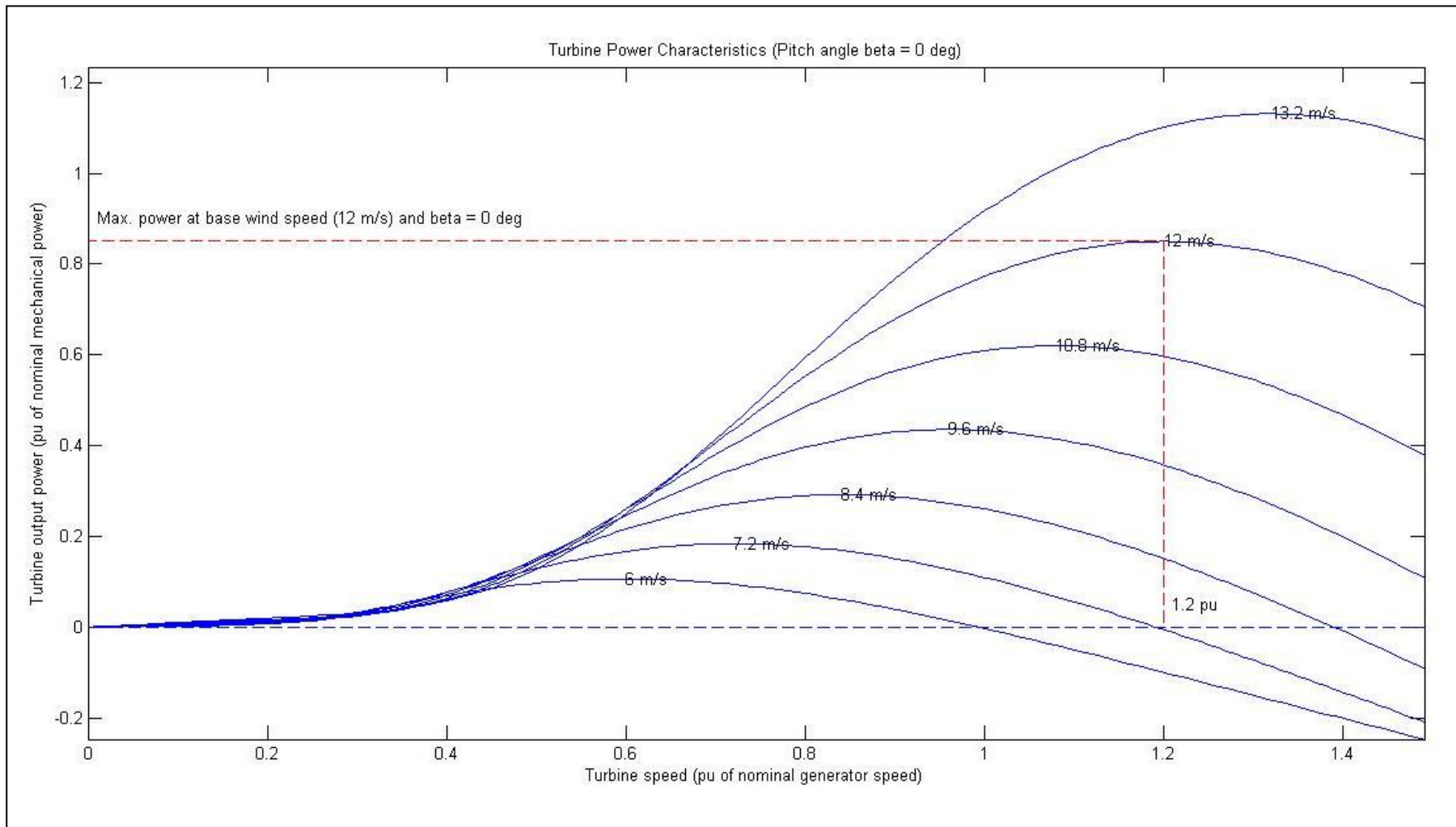


**Figure 3.9 :** Wind turbine characteristics.

### 3.1.6 Wind turbine charger model

Most of the wind turbines produce electrical energy at high voltage levels compared the voltage levels of the battery banks that are planned to use in this work. Thus, here a buck converter, also known as step-down converter, is used to decrease the voltage to a level suitable for the batteries. The peak voltage of the wind turbine is nearly 565 volts, thus the voltage output of the wind energy conversion branch must be decreased for the charging and storing process. For this purpose a buck converter is used with MPPT algorithm, which is a P&O algorithm mentioned earlier. The WTC and the application of MPPT method can be seen in Figure 3.10 and Figure 3.11.

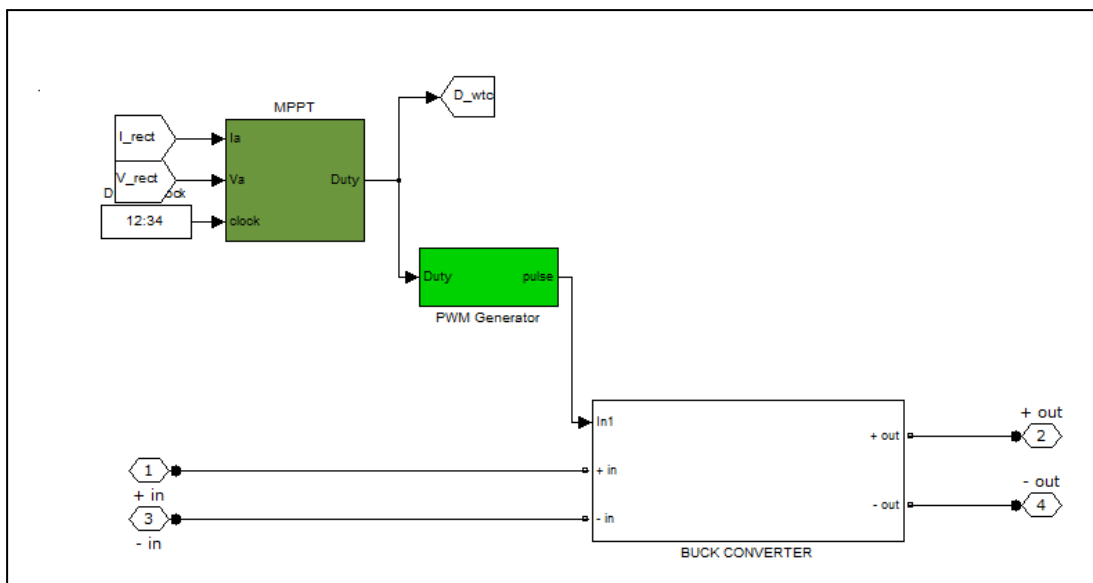


Figure 3.10 : Wind turbine charger model.

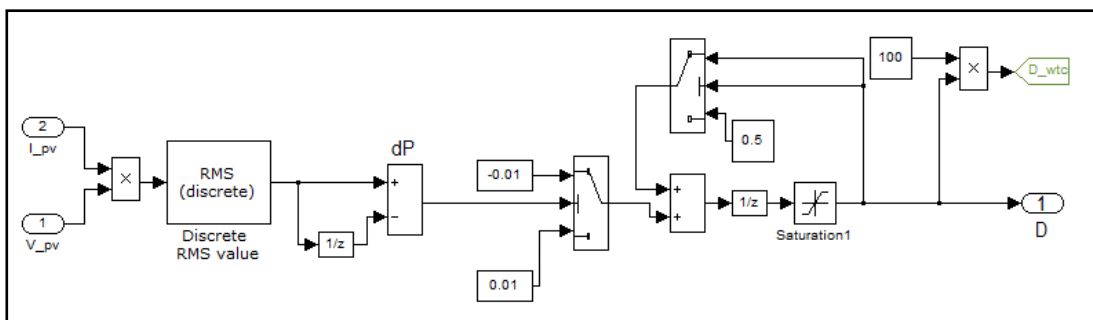


Figure 3.11 : MPPT controller of WTC.

### 3.1.7 Load side charger model

Load side charger (LSC) is again a boost converter, which is using the same control method as the GSC mentioned earlier. The difference from PVC is the control strategy. The LSC can either try to keep a stable charging current value or it can try



to keep a constant charging voltage. The controller regulates the output voltage of the boost converter so that it charges the load with 100 amperes. It also has a load cut off switch that is used to disconnect the LSC from load when it is not needed.

### 3.1.8 Battery model

The battery block from SimPowerSystems library is used for storage and load components of the system. Load is the battery bank that are used for storing electrical energy produced from renewable energy sources and the load is the electrical vehicle to be charged. The nominal voltage and the capacity of the storage is chosen to be 200 volts and 150 Ah, while the nominal voltage and the capacity of the load is set to be 300 volts and 75 Ah. The storage battery is chosen to have a bigger capacity than the load.

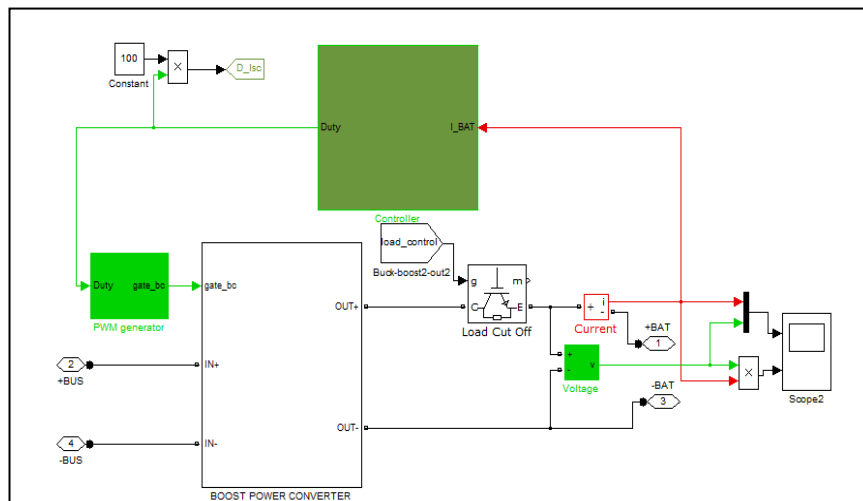


Figure 3.12 : General structure of LSC.

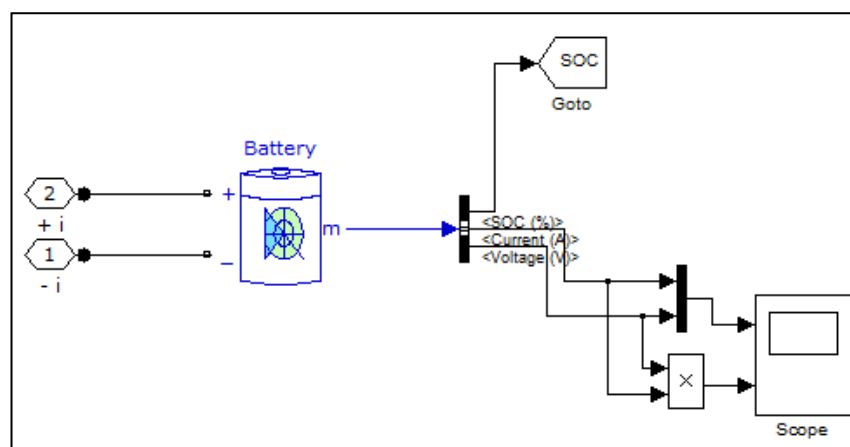


Figure 3.13 : Battery Model.

### 3.1.9 Calculation of DC/DC converter parameters

In order to maintain the DC/DC converters to function as planned, it is essential to be careful while choosing the inductance and capacitor values of these converters. At chapter 3 the equations for this purpose were given. These equations are derived from the ripple values and CCM boundaries. As it can be seen from these equations, the needed parameters are mostly duty cycle  $D$ , load resistance  $R$ , switching frequency  $f$ , voltage ripple  $V_r$ , and output voltage  $V_o$ . Below, a table summarizing the calculation of these values is given. The parameters  $D$  and  $R$  for extreme cases are taken into account, which gives the maximum values of the  $C_{min}$  and  $L_b$ . The inductance and capacitor values of converters must be equal to or bigger than the values calculated at the table.

**Table 3.1 :** Calculation of DC/DC converter parameters.

Component	Equations	Parameters	Results
<b>GSC (Cuk Converter)</b>	$L_{b1} = \frac{(1-D)R}{2Df}$ $L_{b2} = \frac{(1-D)R}{2f}$ $C_{min} = \frac{(1-D)V_o}{8V_r D L_2 f^2}$	$D=0.525$ $R=V_{out}/I_{out}$ $=354/37.5=9,44 \Omega$ $f= 10 \text{ kHz}$ $V_r=10 \text{ V}$	$L_{b1} \geq 4,27 \times 10^{-4} \text{ H}$ $L_{b2} \geq 2,242 \times 10^{-4} \text{ H}$ $C_{min} \geq 1,79 \times 10^{-3} \text{ F}$
<b>PVC (Boost Converter)</b>	$L_b = \frac{(1-D)^2 DR}{2f}$ $C_{min} = \frac{DV_o}{V_r R f}$	$D=0,70$ $R=V_{out}/I_{out} = 350/5=70\Omega$ $f= 10 \text{ kHz}$ $V_r=1 \text{ V}$	$L_b \geq 7,35 \times 10^{-4} \text{ H}$ $C_{min} \geq 3,5 \times 10^{-4} \text{ F}$
<b>WTC (Buck Converter)</b>	$L_b = \frac{(1-D)R}{2f}$ $C_{min} = \frac{(1-D)V_o}{8V_r L f^2}$	$D=0.95$ $R=V_{out}/I_{out}$ $=350/3=116.7 \Omega$ $f= 10 \text{ kHz}$ $V_r=1 \text{ V}$	$L_b \geq 1,46 \times 10^{-4} \text{ H}$ $C_{min} \geq 1,5 \times 10^{-4} \text{ F}$
<b>LSC (Boost Converter)</b>	$L_b = \frac{(1-D)^2 DR}{2f}$ $C_{min} = \frac{DV_o}{V_r R f}$	$D=0.34$ $R=V_{out}/I_{out}$ $=353/37.5=9.413 \Omega$ $f= 20 \text{ kHz}$ $V_r=1 \text{ V}$	$L_b \geq 3,48 \times 10^{-5} \text{ H}$ $C_{min} \geq 6.36 \times 10^{-4} \text{ F}$

### 3.1.10 Possible cases

When the operation of a system interpreted, all possible cases must be considered. The system must respond to all cases that have the possibility to occur. First of all, the parameters that define the cases must be determined. In this work, there are three main parameters that define the cases; charging demand by an EV, the state of the storage and the availability of the renewable energy sources (RES). According to the states of these parameters, different cases are formed. Table 3.2 shows the summary of all the possible cases. The assessments of the input parameters are explained in detail below:

- RES: The system has two renewable energy sources; sun and wind. If one or both of these sources are available for renewable energy production the input parameter RES has the value “1”. If none of these sources are available then this parameter has the value “0”.
- Storage: The system has a battery bank used as storage for energy produced from renewable energy sources. If this storage has energy to supply the load the parameter Storage has the value “1”.
- Charge: This parameter has the value “0”, when there is no demand for charge. The fast charging demand is defined by the value “1”. The parameter has the value “2”, when there are renewable energy sources available and no fast charge is required. This means that the EV will be charged with MPPT algorithms, extracting the maximum amount of power available from the renewable energy sources.

As it can be seen from the Table 3.2, there are eight main cases and two additional cases, which caused by the MPPT Charging demand. All cases will be explained in detail at next chapter. There is also two other conditions affecting the Case 6 and Case 7 that will be additionally handled. These conditions are that the storage is fully charged and that the storage is completely empty.

### 3.1.11 System controller

Previously, all possible cases were given; the system controller must be able to recognize these cases and respond accordingly. The system controller consist of 4 parts as it can be seen from the Figure 3.13; there is the main controller at the center and three subsystems that evaluate the parameters which define the possible cases

mentioned at Chapter 3.7. These subsystems are; wind cut-in & cut-off speed check, PV array irradiation check and storage evaluation.

Wind turbines generate electrical energy between certain speed limits. The lower limit is called cut-in wind speed, which defines the minimum wind speed that wind turbine is able to produce energy. The upper limit is the cut-off speed, which states the maximum wind speed that wind turbine will produce electrical energy. If the wind speed is higher than cut-off speed, the blades of the wind turbine is stopped, due to fact that higher wind speeds may cause the wind turbine be damaged. Figure 3.14 shows the wind cut-in & cut-off speed check subsystem. This subsystem controls the wind speed and decides if the wind speed is reasonable for energy generation. If the wind speed is suitable for energy production the output signal of the subsystem is equal to “1”. Here, the cut-in speed is defined to be 2,5 m/s and the cut-off speed is defined to be 24 m/s.

**Table 3.2 :** Possible cases.

Case	RES	Storage	Charge
(1)	0	0	0
(2)	0	0	1
(3)	0	1	0
(4)	0	1	1
(5)	1	0	0
(6)	1	0	1
(7)	1	1	0
(8)	1	1	1
(9)	1	0	2
(10)	1	1	2

The solar irradiation check subsystem decides if the solar irradiation level is able to produce energy. Here these subsystems set the output signal equal to “1” for irradiation values higher than 300 W/m<sup>2</sup>.

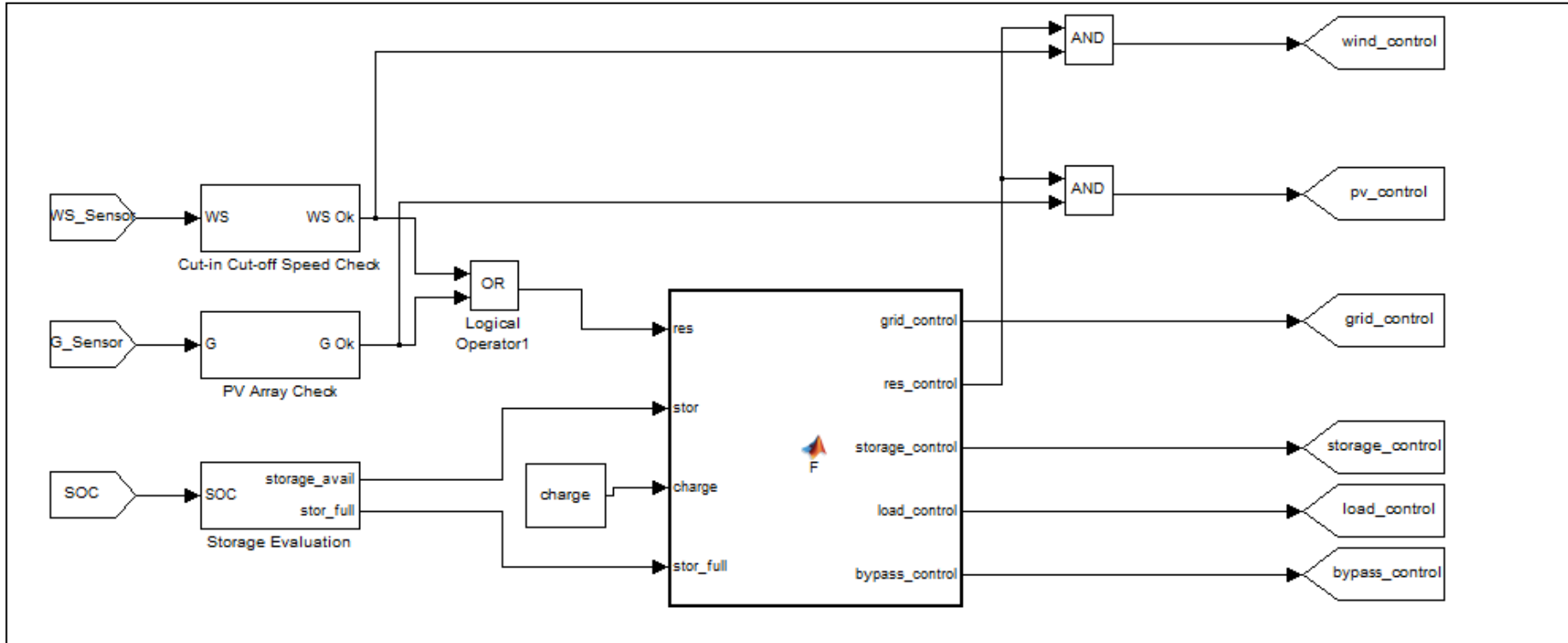


**Figure 3.14** : General overview of control system.

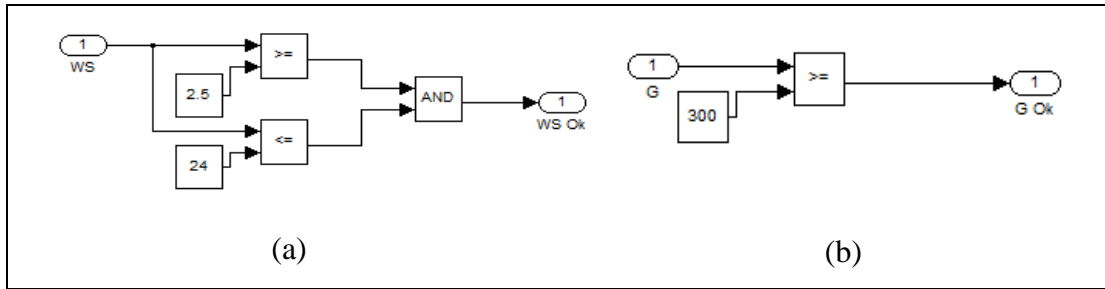


**Figure 3.15 :** (a) Wind cut-in & cut-off speed check subsystem (b) solar irradiation check subsystem.

The third subsystem is the storage evaluation, which decides if the battery bank used as storage is available to supply energy to load and it also warns the system when the battery bank is fully charged. Each battery type has a minimum state of charge (SOC) level allowed. If the SOC value is lower than the minimum level, the lifetime of the battery is decreased. Thus, the SOC value of the battery should never be allowed the drop under the minimum level. This subsystem provides that if the SOC value drops to the dangerous level, called “Stor\_low\_limit” at Figure 3.16, it must be decreased to a certain safe level, called “Stor\_high\_limit” at Figure 3.16, using any energy source available. For the simulation these levels are set to 40% and 45%. As it is seen at Figure 3.15 the strategy for this emergency condition is that any available energy source steps in as backup to feed the storage, when the SOC level drops the lower level. It keeps supplying energy until the SOC level is bigger than the defined upper limit; this behavior is illustrated with red line at Figure 3.15.

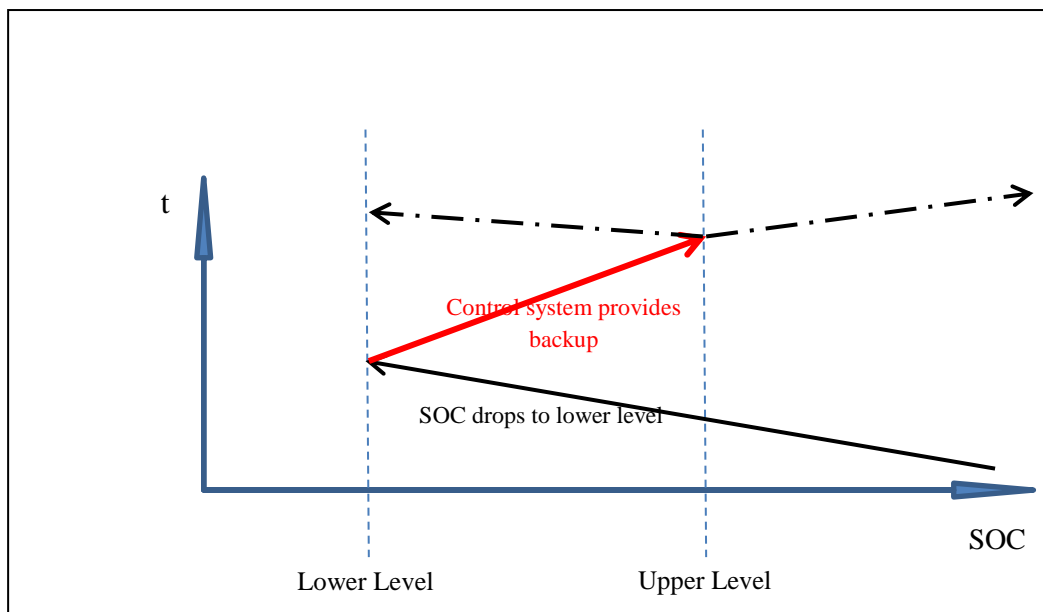


**Figure 3.16 :** Emergency condition.

Figure 3.16 shows the storage evaluation subsystem. The part in orange responsible for checking the availability of the storage including the strategy for emergency condition mentioned above. The part in green frame is only for checking if the storage is full. It sets the signal equal to “1” when the storage is fully charged.

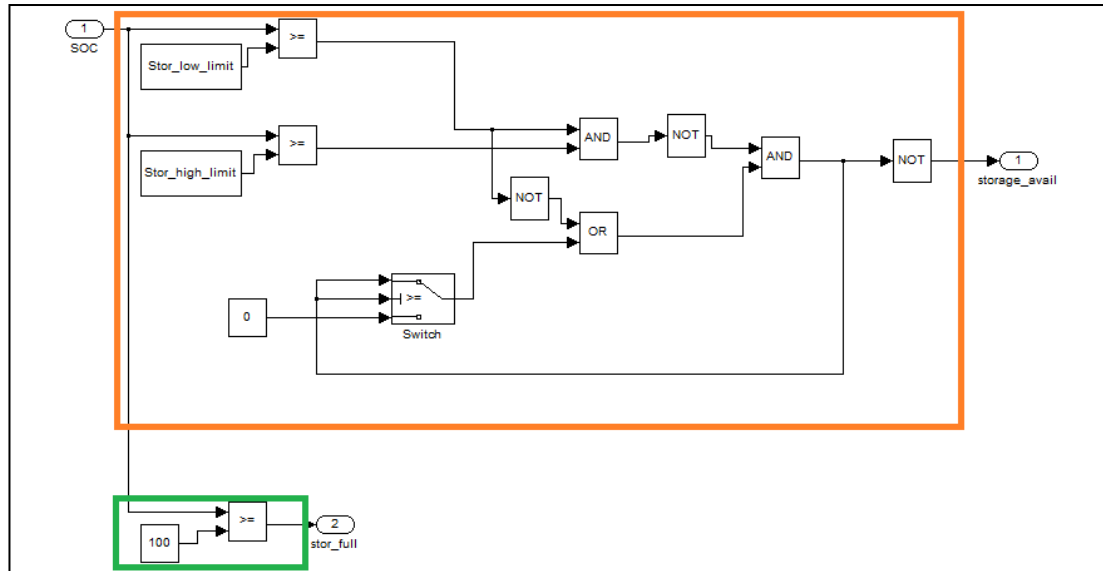


**Figure 3.17 :** Storage evaluation subsystem.

These three subsystems regulate the parameters that are the inputs of the main controller. Below all possible cases are explained in detail and required actions for each case is defined:

- In Case 1, there are no renewable energy sources available, charging is not demanded and the storage is below minimum critical level which means that the storage must be increased to safety level. Thus, the grid steps in to charge the storage to this level, meaning that the grid breaker must be closed. The other components need to be turned off.
- In Case 2, there are no renewable energy sources available and the storage is below minimum critical level whereas fast charging is demanded by an EV. Considering that the demanded charging strategy is fast charge, the user of the EV needs an immediate charge and the priority is given to the charging of the EV. Thus, the grid steps in to meet the fast charge demand and ignores that the SOC of storage is below minimum critical level. Therefore, the grids side charger directly charges the EV, while the load side charger is bypassed using the bypass breaker, meaning that grid breaker and bypass breaker must be closed by setting these control signals equal to “1”.

- Case 3 represents the situation where the battery is above critical level, no charging is demanded and no renewable energy sources are available. All of the control signals are equal to “0” because of the fact that there are no actions needed to be taken.
- In Case 4 renewable energy sources are unavailable, whereas fast charging is demanded and storage is above critical level. In this case the required energy is supplied from the storage and the load (EV) is charged by load side charger. Therefore, only the control signals “grid” and “load” are set to be “1”.
- In Case 5, one or both of renewable energy sources is/are available, no charging is demanded and the storage is below minimum critical level. Therefore, the system takes action to increase the SOC level of the storage by using the available renewable energy sources, meaning that control signals “res” and “storage” are set to be “1”.
- Case 6 represents the situation where one or both of renewable energy sources is/are available and fast charging is demanded whereas the SOC of the storage is below critical level. Similar to Case 2, the priority is given to the charging of the EV. The control signals, “res”, “storage” and “load” is set to “1”, meaning that the energy needed for fast charging will be supplied by the available renewable energy sources and the storage, despite the fact that the SOC of the storage is below the critical level.
- In Case 7, one or both or renewable energy sources is/are available, and the SOC of the storage is above critical level, whereas there is no charging demand. In this case, the renewable energy sources will supply the storage until it is fully charged. For this, the control signals “res” and “storage” are set to be “1”, meaning that the wind turbine generator breaker and storage breaker are closed.
- In Case 8, a fast charging is demanded, SOC of storage is above critical level and renewable energy sources are available. Therefore similar to Case 6, the required energy will be supplied from both renewable energy sources and storage. Therefore control signals “res”, “storage” and “load” are set to be “1”.



- Case 9 is one of the additional two cases where a MPPT charging is demanded when renewable energy sources are available to produce energy, meaning that the user of the EV doesn't need an immediate charge. In this case the storage is below critical level. Considering that the user of the EV doesn't need immediate charge, the priority is given to the storage and renewable energy sources are used to supply the storage and increase the SOC value to the safety level. Therefore, control signals "res" and "storage" are set to be "1".
- Case 10 is the other condition with MPPT charging. In this case the storage value is above critical level: renewable energy sources are used to charge the load directly and control signals "res" and "bypass" are set to be "1".

Table 3.3 gives a brief summary of the cases mentioned above. Also, in order to generate the main control algorithm with ease, the cases summarized at Table 3.3 are transferred to the shape of an algorithm tree given at Figure 3.17.

**Table 3.3 :** Control signals for possible cases.

Case	RES	Storage	Charge	grid	res	storage	load	bypass
(1)	0	0	0	1	0	1	0	0
(2)	0	0	1	1	0	0	0	1
(3)	0	1	0	0	0	0	0	0
(4)	0	1	1	0	0	1	1	0
(5)	1	0	0	0	1	1	0	0
(6)	1	0	1	1	1	0	0	1
(7)	1	1	0	0	1	1	0	0
(8)	1	1	1	0	1	1	1	0
(9)	1	0	2	0	1	1	0	0
(10)	1	1	2	0	1	0	0	1

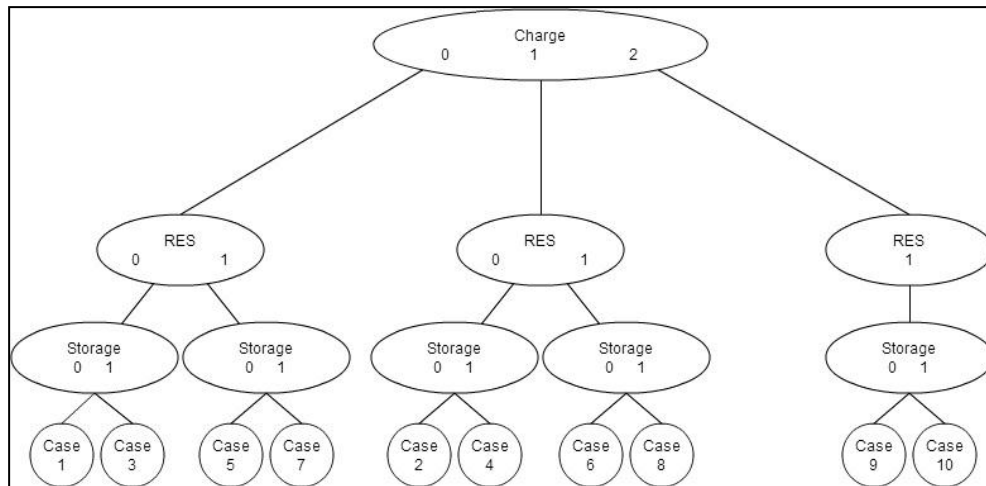


**Figure 3.18 :** Control logic figured as a tree.

As it can be seen from the Table 3.3, the output signals of the Case 5 and Case 7 are same, while the output signals of the Case 6 and Case 8 are the same. Therefore, a simplification for these cases in control algorithm can be made, meaning that the state of the storage doesn't need to be check for these cases. The control algorithm is implemented with an embedded function block, which uses the MATLAB coding syntax. The MATLAB code of this function is given below.

```
function [grid_control, res_control, storage_control, load_control,
bypass_control] = F(res,stor,charge, stor_full)
persistent A;

if (charge==0)
    if (res==0)
        if (stor==0)
            A=[1 0 1 0 0];
        else
            A=[0 1 1 0 0];
        end
    else
        if (stor_full==0)
            A=[0 1 1 0 0];
        else
            A=[0 0 0 0 0];
        end
    end
elseif (charge==1)
    if (res==0)
        if(stor==0)
            A=[1 0 0 0 1];
        else
            A=[0 0 1 1 0];
        end
    else
        if (stor==0)
            A=[1 1 0 0 1];
        end
    end
end
```

**Figure 3.19 :** MATLAB code of controller.

```

        else
            A=[0 1 1 1 0];
        end
    end
else
    if (stor==0)
        A=[0 1 1 0 0];
    else
        A=[0 1 0 0 1];
    end
end

grid_control=A(1);
res_control=A(2);
storage_control=A(3);
load_control=A(4);
bypass_control=A(5);

```

**Figure 3.19 (contd.) : MATLAB code of controller.**

### 3.2 System Simulation

Now that the design and the modeling of the system are done, the system will be examined by running the simulation for each case. However, there are many parameters such as solar irradiation, wind speed, SOC of storage and SOC of EV, which should be changed to different values in order to check the system reliability. Considering that there are already 10 cases to be checked, applying different parameters for each case will create too many scenarios, which will overcrowd the study. Hence, a few scenarios will be created in order to examine each case. These scenarios will contain more than one case, so that the transition between cases can be seen.

It should also be noted that the simulation will be run for a very short time, 0.45 seconds, due to fact that the system involves too many components. The sample time of the simulation is  $3 \times 10^{-6}$  seconds; such a small value was compulsory to choose because of the high switching frequencies used within the converters. Thus, it is impossible to run the simulation for a long period using normal computers.

The results will be discussed over the scopes showing the current ( $I_{grid}$ ,  $I_{stor}$ ,  $I_{EV}$ ,  $I_{pv}$ ,  $I_{wind}$ ) and power measurements ( $W_{grid}$ ,  $W_{stor}$ ,  $W_{EV}$ ,  $W_{pv}$ ,  $W_{wind}$ ) of each component and the SOC values of storage batteries ( $SOC_{stor}$ ) and EV ( $SOC_{EV}$ ).

### 3.2.1 Scenario 1

In this scenario it is aimed to observe three cases; the scenario will start with “Case 4”, meaning that the storage batteries are over the minimum limit and a fast charging is demanded by the user, whereas there are no renewable energy sources available. Thus, the storage batteries will supply the needed power for EV charging. After a while the SOC level of the storage batteries will drop to the minimum level and a transition to the “Case 2” will be observed. The scenario will end with “Case 1”, when no more charging is demanded from the system. For this setup following parameters are chosen:  $G=250 \text{ W/m}^2$ ,  $V_{\text{wind}}=2\text{m/s}$ ,  $\text{SOC}_{\text{storage}}=20.001\%$ ,  $\text{SOC}_{\text{EV}}=70\%$  and a charging is demanded from the beginning to the 0.30 seconds.

The Figure 3.19 shows the results. At the beginning, while there is available energy in the storage batteries, the needed energy is provided by these batteries (pink curves). In the present case the SOC of EV is 70%, meaning that the LSC adjust the voltage so that the current drawn by EV (cyan curve) is equal to 37.5 Amperes. In the figures displayed in this section, a positive value of current or power means that energy is drawn from the component, whereas negative values of these parameters mean that energy is supplied to the component. As it can be seen from the figure, the charging current for EV reaches -37.5 Amperes nearly at 0.04 seconds. After a while, nearly at 0.075 seconds, the SOC value of storage batteries drops to the critical level. Thus, from now on the grid (yellow curve) supplies the required energy for the charging process of EV. The last transition happens at 0.30 seconds, when the fast charging is no more demanded by the user. Now, the grid continues to supply energy, however this time it is used to supply 100 Amperes to the storage batteries, which are under critical level.

### 3.2.2 Scenario 2

The Scenario 2 starts with “Case 6”: in this case one or more renewable energy sources are available and a fast charging is demanded, however the storage batteries are under the minimum limit. In this case the priority will be given to the EV charging and the required energy will be provided by the available renewable energy source and the grid together. After a while the charging demand will be removed and a transition to “Case 5” will be observed, where the available renewable energy

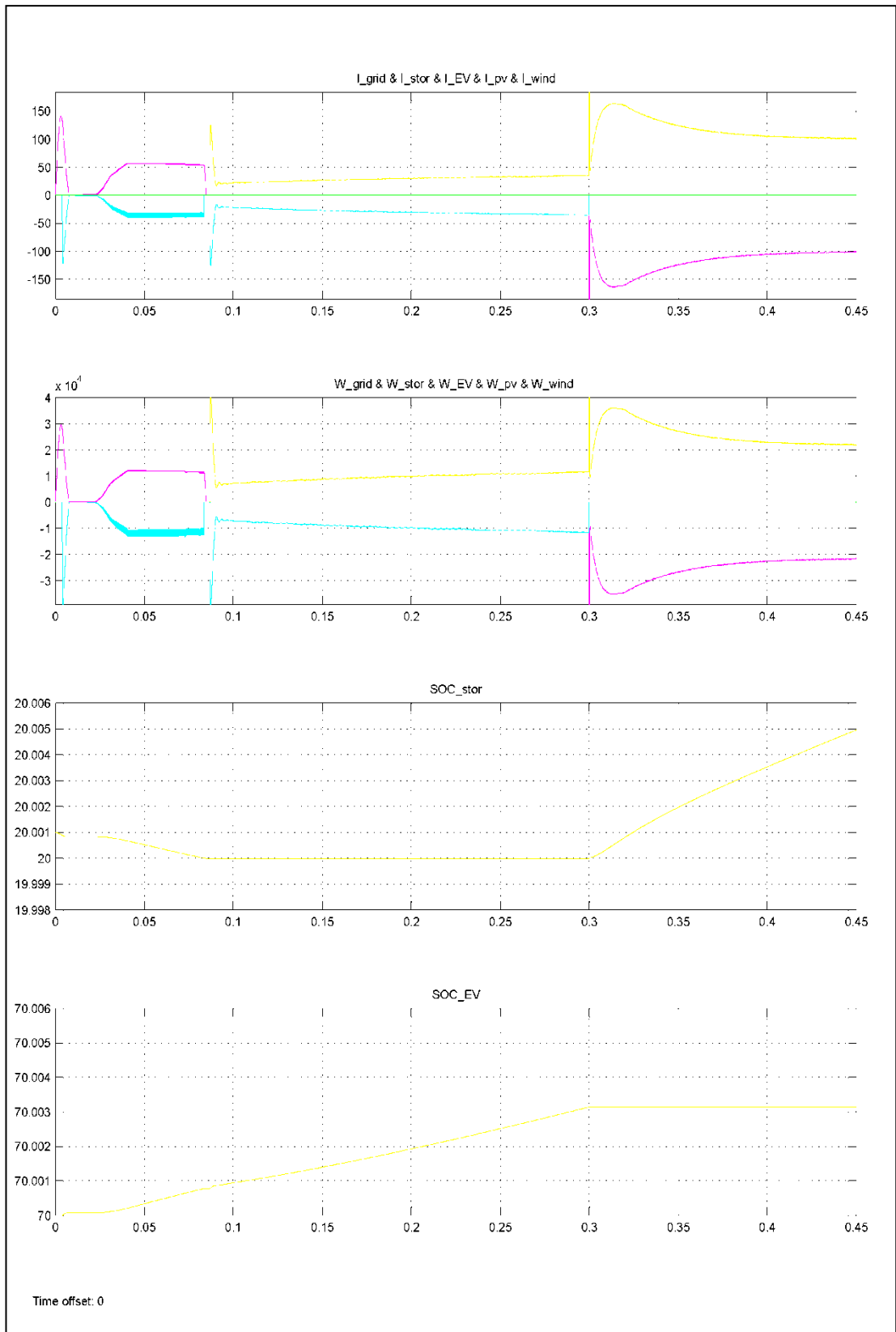


**Figure 3.20 : Results for scenario 1.**

sources will provide the energy to increase the SOC of storage batteries to the safe level. For this setup following parameters are chosen:  $G=1000 \text{ W/m}^2$ ,  $V_{\text{wind}}=12\text{m/s}$ ,  $\text{SOC}_{\text{storage}}=19\%$ ,  $\text{SOC}_{\text{EV}}=99.95\%$  and a fast charging is demanded from the beginning to the 0.15 seconds.

As it can be seen from the Figure 3.20, first the grid supplies the energy needed for the charging process. The SOC of EV is 99.95%, which means that 37.5 Amperes will be drawn from the system according to the charging algorithm. As the current drawn from the grid increases, the voltage of the PVC rises so that it provides energy (red curve) for the system at nearly 0.9 seconds. At 0.15 seconds, there is no more a charging demand. Thus the renewable energy sources provide energy for the storage batteries (pink curve). As it can be seen from the figure, the PVC is able to provide energy at nearly 0.16 seconds, whereas the WTC is able to provide energy (green curve) later at nearly 0.24 seconds. As it can be understood from the power curves, the MPPT algorithms enable the system to extract the maximum amount of available power from the renewable energy sources.

### 3.2.3 Scenario 3

This scenario consists of “Case 8” and “Case 7”. At the beginning, the storage batteries are above the minimum level, there are available renewable energy sources and a fast charge is required. In this case, the storage batteries and available renewable energy sources will provide the needed energy for the fast charge. After a while, the charging demand will be removed and the renewable energy sources will be stored in storage batteries for later uses. For this setup following parameters are chosen:  $G=615 \text{ W/m}^2$ ,  $V_{\text{wind}}=0 \text{ m/s}$ ,  $\text{SOC}_{\text{storage}}=90\%$ ,  $\text{SOC}_{\text{EV}}=10\%$  and a charging is demanded from the beginning to the 0.15 seconds.

The results are presented in Figure 3.21. At first, storage batteries alone provide the needed power (pink curve) for the charging alone, until the PVC is able to provide power (red curve) approximately at 0.07 seconds. After this point, the current drawn from the storage batteries decreases, so that the current provided to the EV stays at 100 Amperes.

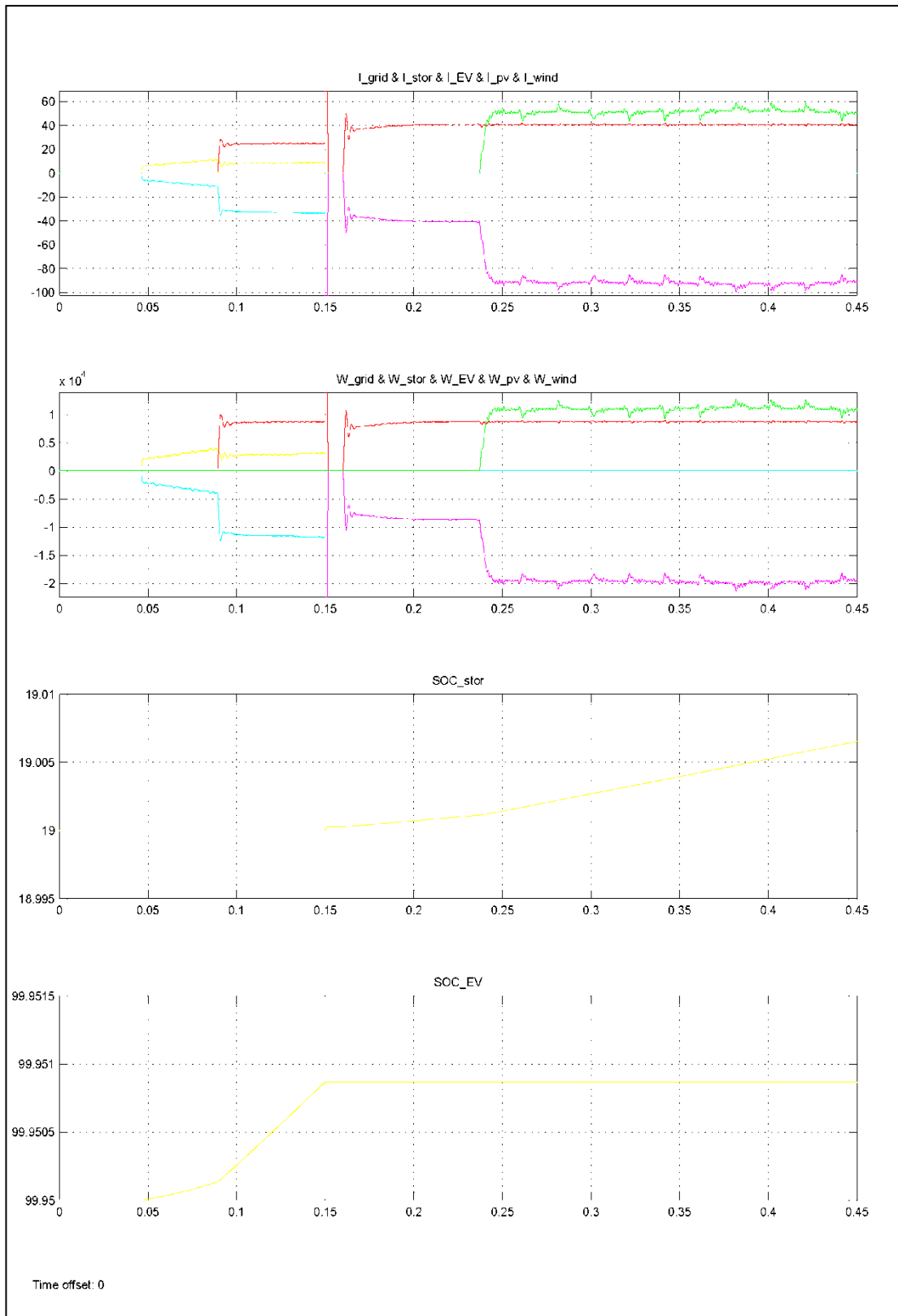


**Figure 3.21 : Results for scenario 2.**

In this scenario the wind speed is below cut-in speed, so that the WTC is unable to provide energy. The transition to Case 7 happens, when the charging demand is removed at 0.15 seconds. From now on the solar energy is channeled only to the storage batteries. As it is seen, the current and power values of storage batteries have a negative value, meaning that energy is provided to this component and the SOC value starts to increase after the transition.

### 3.2.4 Scenario 4

In this scenario the last two case, “Case 9” and “Case 10”, will be observed. At the beginning the “Case 10” will be observed, where the storage batteries are under the minimum limit, there are renewable energy sources available and so called “MPPT Charging” is required. This means that the EV user is in no hurry to charge the vehicle so that the priority will be given to the storage batteries: the renewable energy sources will provide energy for charging the storage batteries. After a while the storage batteries will reach to the safe level and the scenario will switch to the “Case 10”, where the MPPT charging of the EV will start.

For this setup following parameters are chosen:  $G=1000 \text{ W/m}^2$ ,  $V_{\text{wind}}=13 \text{ m/s}$ ,  $\text{SOC}_{\text{storage}}=19.998\%$ ,  $\text{SOC}_{\text{EV}}=1\%$  and MPPT charging is demanded for all the time. Additionally, the minimum SOC level and safe SOC level of storage batteries are set to very close values so that the transition from Case 9 to Case 10 can be observed within such short simulation time. These values are:  $\text{Stor\_low\_limit}=20\%$  and  $\text{Stor\_high\_limit}=20.0001\%$ . The Figure 3.22 shows the results for Scenario 2. As it can be seen, at first the generated power from the renewable energy sources is delivered to the storage batteries, which are below the critical level. The PVC starts the provide energy (red curve) at nearly 0.06 seconds, while the WTC is able to deliver energy (green curve) at approximately 0.22 seconds. As it is seen, the power delivered to the storage batteries are equal to the sum of power delivered by WTC and PVC. Once the SOC of storage batteries reaches to the safe level, defined as 20.001% for this scenario, the transition from Case 9 to Case 10 can be observed. From now on the storage batteries are in safety level and the power is directed to the EV (cyan curve). As it is seen in figure first the SOC value of storage increases and after nearly 0.022 seconds the SOC of EV starts to increase. As it is observed in the figures, there are some sudden bounces in the currents. These are assumed to be



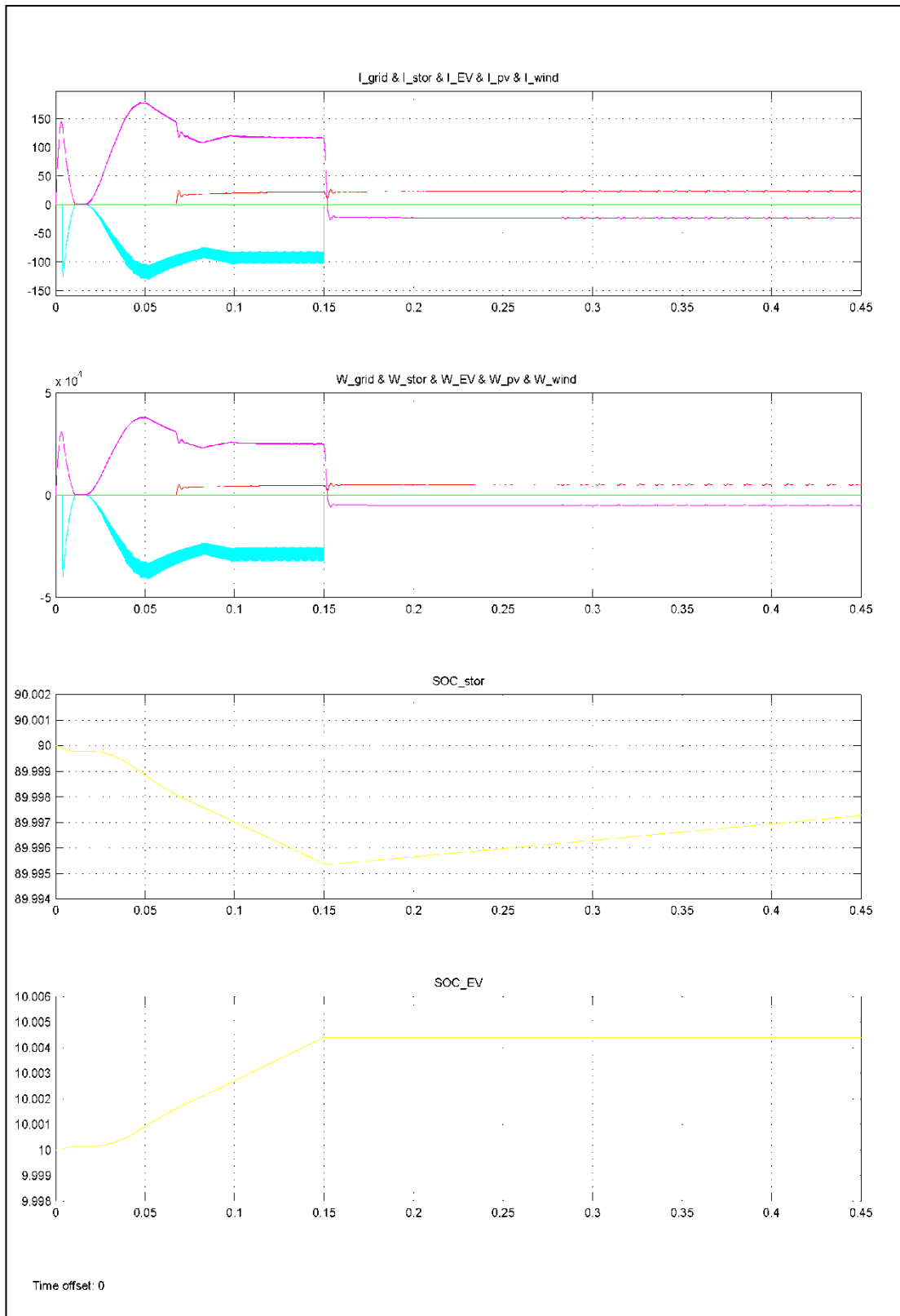


**Figure 3.22 : Results for scenario 3.**

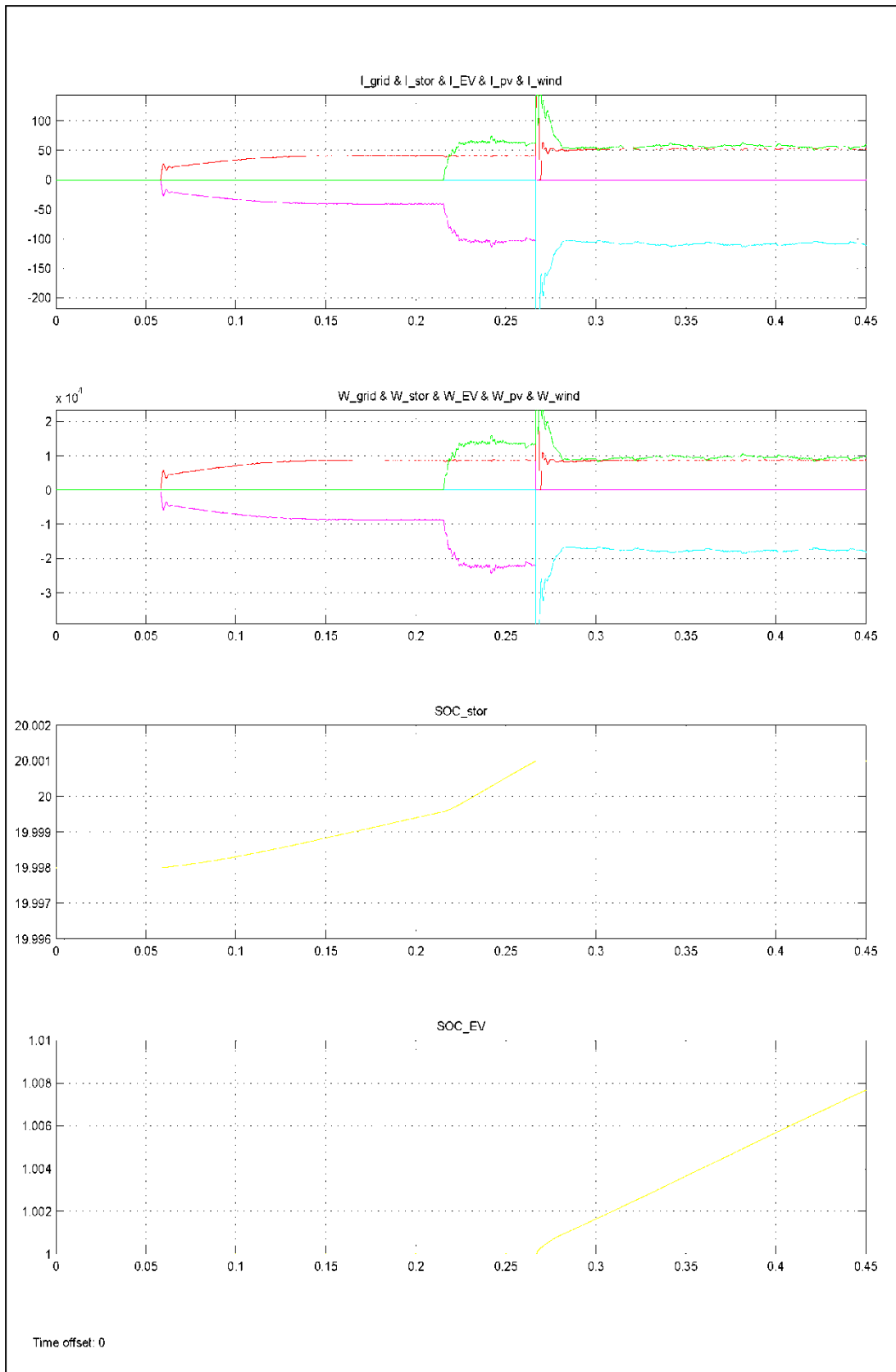


**Figure 3.23** : Results for scenario 4.

neglectable due to the fact that these bounces occur for very short periods. It should also be noted that some of these are considered to be caused by the simulation and they may be dependent on the solver configuration parameters of Simulink.



#### 4. CONCLUSION

Depending on the facts and statistics that were represented at earlier chapters of this thesis, it seems that the EVs are going to be an essential part of future. Although there are lots of challenges to overcome, related with battery technology and charging infrastructure, the efforts for this purpose seems to be worth dealing with. One other important challenge is the effects of the EVs on the current grid network, in case the penetration of these vehicles increases as expected. Thus, the topics of smart grids, distributed energy generation and the idea of using renewable energy sources for supplying the needed energy for EVs have been intensely studied.

This thesis offers an environment friendly way to supply the needed charging energy for EVs. The designed charging system uses two renewable energy sources, sun and wind, equipped with a battery bank so that the electric vehicles can be charged with the energy generated on spot. The system is also supported with the grid network, which supplies energy in emergency cases. The designed system works in the limits of Level 2 DC Charging Standards. The ability of the system either to provide a fast charge or to provide a “MPPT Charging” makes it preferable especially for both residential use and work area use.

As seen in the simulation chapter, the designed system is able to provide the needed energy in all considered possible cases. These cases are represented in four scenarios. The “Case 3” is not mentioned in simulation part due to fact that this case doesn’t require any action from the system.

As future work similar systems benefiting from bidirectional converters might be offered. Such a system would allow the electric vehicles to be used as energy storages and it would enable the vehicle to grid applications. This could also result in a decrease for the size of storage batteries, which would also decrease the costs as the battery is one of the expensive components of such systems.

Another suggestion for future work is that an application of supercapacitor can be implemented for the system. Supercapacitors have much higher capacities and

energy densities than regular capacitors, so that it is able to use these components in fast charging stations. In such works, the whole storage batteries or a part of them might be replaced with supercapacitors.

## REFERENCES

- [1] **International Energy Agency** (2011). *Key World Energy Statistics*, Paris. Date retrieved: 10.10.2012, address: [http://www.iea.org/publications/freepublications/publication/key\\_world\\_energy\\_stats.pdf](http://www.iea.org/publications/freepublications/publication/key_world_energy_stats.pdf)
- [2] **Republic of Turkey Energy and Natural Resources** (2010). Enerji ve Tabii Kaynaklar Bakanlığı 2010-2014 Stratejik planı, Date retrieved: 10.10.2012, address: [http://www.enerji.gov.tr/yayinlar\\_raporlar/ETKB\\_2010\\_2014\\_Stratejik\\_Planı.pdf](http://www.enerji.gov.tr/yayinlar_raporlar/ETKB_2010_2014_Stratejik_Planı.pdf)
- [3] **Republic of Turkey Energy and Natural Resources** (2012). Date retrieved: 10.10.2012, address: [http://www.enerji.gov.tr/EKLENTI\\_VIEW/index.php/raporlar/raporVeriGir/71073/2](http://www.enerji.gov.tr/EKLENTI_VIEW/index.php/raporlar/raporVeriGir/71073/2)
- [4] **Republic of Turkey Energy and Natural Resources** (2012). *Dünya'da ve Türkiye'de Enerji Görünümü*. Date retrieved: 10.10.2012, address: [http://www.enerji.gov.tr/yayinlar\\_raporlar/Dunyada\\_ve\\_Turkiyede\\_Enerji\\_Gorunumu.pdf](http://www.enerji.gov.tr/yayinlar_raporlar/Dunyada_ve_Turkiyede_Enerji_Gorunumu.pdf)
- [5] **European Commission** (2010). *Europe 2020 Strategy Executive Summary*. Date retrieved: 10.10.2012, address: <http://ec.europa.eu/research/era/docs/en/investing-in-research-european-commission-europe-2020-2010.pdf>
- [6] **Renewable Energy Policy Network for 21<sup>st</sup> Century** (2012). *Renewables 2012 Global Status Report*. Date retrieved: 10.10.2012, address: [http://www.ren21.net/Portals/0/documents/Resources/%20GSR\\_2012%20highres.pdf](http://www.ren21.net/Portals/0/documents/Resources/%20GSR_2012%20highres.pdf).
- [7] **International Energy Agency** (2011). *World Energy Outlook 2011*, Paris. 9789264124134.
- [8] **Manfred, M., Caputo, P., and Costa, G.** (2010). Paradigm Shift in Urban Energy Systems Through Distributed Generation: Methods and Models. *Applied Energy*, Vol. 88, pp. 1032-1048.
- [9] **Andersen, P. H., Mathews, J. A., and Rask, M.** (2009). Integrating Private Transport into Renewable Energy Policy: The Strategy of Creating Intelligent Recharging Grids for Electric Vehicles. *Energy Policy*, Vol. 37, pp. 2481-2486.
- [10] **Ozaki, R., and Sevastyanova, K.** (2010). Going Hybrid: An Analysis of Consumer Purchase Motivations. *Energy Policy*, Vol. 39, pp. 2217-2227.
- [11] **Becker, T. A., Sidhu, I., and Tenderich, B.** (2009). Electric vehicles in the United States: A new model with forecasts to 2030, *Center for Entrepreneurship & Technology (CET)*.
- [12] **Amoroso, F. A., and Cappuccino, G.** (2011). Impact of Charging Efficiency Variations on the Effectiveness of Variable-rate-based Charging

Strategies for Electric Vehicles. *Journal of Power Sources*, Vol. **196**, pp. 9574-9578.

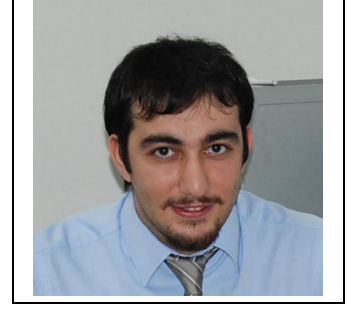
- [13] **Amoroso, F. A., and Cappuccino, G.** (2011). Advantages of Efficiency-Aware Smart Charging Strategies for PEVs. *Energy Conversion and Management*, Vol. **54**, pp. 1-6.
- [14] **Bajpai, P., and Dash, V.** (2012). Hybrid Renewable Energy Systems for Power Generation in Stand-Alone Applications: A review. *Renewable and Sustainable Energy Reviews*, pp. 2926-2939.
- [15] **Deshmukh, M. K., and Deshmukh, S. S.** (2006). Modeling of Hybrid Renewable Energy Systems. *Renewable and Sustainable Energy Reviews*, pp. 235-249.
- [16] **Messenger, R. A., and Ventre, J.** (2004). Photovoltaic Systems Engineering. CRC Press, USA.
- [17] **Bianchi, F. D., De Battista, H., and Mantz, R. J.** (2006). Wind Turbine Control Systems. Springer, Germany.
- [18] **Patel, M. R.** (1999). Wind and Solar Power Systems.: CRC Press, USA.
- [19] **Hocaoğlu, F. O., Gerek, Ö. N., and Kurban, M.** (2009). A Novel Hybrid (Wind–Photovoltaic) System Sizing Procedure. *Solar Energy*, Vol. **83**, pp. 2019-2028.
- [20] **Kaabeche, A., Belhamel, M., and Ibtiouen, R.** (2010). Sizing Optimization of Grid-Independent Hybrid Photovoltaic/Wind Power Generation System. *Energy*, Vol. **36**, pp. 1214-1222.
- [21] **Örs, M.** (2009). Maximum Power Point Tracking for Small Scale Wind Turbine with Self-Excited Induction Generator. *Journal of Control Engineering and Applied Informatics*, Vol. **11**, pp. 30-34.
- [22] **Ehsani, M., Gao, Y., and Emadi, A.** (2010). Modern Electric, Hybrid Electric and Fuel Cell Vehicles (2. ed.). CRC Press, USA.
- [23] **Chau, K. T., and Wong, Y. S.** (2002). Overview of Power Management in Hybrid Electric Vehicles. *Energy Conversion and Management*, Vol. **43**, pp. 1953–1968.
- [24] **Pistoia, G.** (2010). Electric and Hybrid Vehicles. Elsevier Academic Press.
- [25] **Nelson, R. F.** (2004). Charging Techniques for VRLA Batteries, in *Valve-Regulated Lead–Acid Batteries*, pp. 241-293, D. A. Rand, P. I. Moseley, J. Garche, and C. D. Parker, Elsevier Academic Press.
- [26] **Schalkwijk, W. A., and Scrosati, B.** (2002). Advances in Lithium-Ion Batteries. Kluwer Academic Publishers, Boston, USA.
- [27] **Liaw, B. Y., and Yang, X.-G.** (2001). Limiting Mechanism of Rapid Charging Ni-MH Batteries. *Electrochimica Acta*, Vol. **47**, pp. 875-884.
- [28] **Ikeya, T., Sawada, N., Murakami, J.-i., Kobayashi, K., Hattori, M., Murotani, N., et al.** (2002). Multi-Step Constant-Current Charging Method for an Electric Vehicle Nickel/Metal Hydride Battery with High-Energy Efficiency and Long Cycle Life. *Journal of Power Sources*, Vol. **105**, pp. 6-12.



- [29] **Svoboda, V., Doering, H., and Garche, J.** (2004). The Influence of Fast Charging on the Performance of VRLA Batteries. *Journal of Power Sources*, Vol. **144**, pp. 244-254.
- [30] **Zaghiba, K., Dontigny, M., Guerfi, A., Charest, P., Rodrigues, I., Mauger, A., et al.** (2010). Safe and Fast-Charging Li-ion Battery with Long Shelf Life for Power Applications. *Journal of Power Sources*, Vol. **196**, pp. 3949-3954.
- [31] **Rashid, M. H.** (2007). *Power Electronics Handbook* (2. ed.). Elsevier Academic Press, Florida, USA.
- [32] **Luo, F. L., Ye, H., and Rashid, M.** (2005). *Digital Power Electronics and Applications*. Elsevier Academic Press.
- [33] **Murray, R. M.** PID Control [Pdf Document]. Date retrieved: 12.08.2012, address: [http://www.cds.caltech.edu/~murray/books/AM05/pdf/am06-pid\\_16 Sep06.pdf](http://www.cds.caltech.edu/~murray/books/AM05/pdf/am06-pid_16 Sep06.pdf)
- [34] **Morales, D. S.** (2010). Maximum power point tracking algorithms for photovoltaic applications, *Master Thesis*, Aalto University, Aalto, Finland.
- [35] **Thongam, J. S., and Ouhrouche, M.** (2005). MPPT Control Methods in Wind Energy Conversion Systems, in *Fundamental and Advanced Topics in Wind Power*, R. Carriveau, InTech Press, Quebec, Canada.
- [36] **Galyen, R.** (2012). SAE Standards to Support Electro-Mobility. *Electric Vehicle Safety Technical Symposium*. Date retrieved: 12.09.2012, address: [http://www.nhtsa.gov/pdf/ev/First\\_SAE\\_Presentation-Bob\\_Galyen.pptx](http://www.nhtsa.gov/pdf/ev/First_SAE_Presentation-Bob_Galyen.pptx)
- [37] **Bohn, T.** (2012). Plug-in Electric Vehicle (PEV) Standards, Upcoming PEVs/Features, Charging System Overview. *Electric Vehicle Winter 2012 Quarterly Discussion Webinar*. Date retrieved: 12.09.2012, address: [http://www1.eere.energy.gov/cleancities/toolbox/pdfs/plug-in\\_electric\\_vehicle\\_standards.pdf](http://www1.eere.energy.gov/cleancities/toolbox/pdfs/plug-in_electric_vehicle_standards.pdf)
- [38] **Kissel, G.** (2009). SAE J1772™. Date retrieved: 12.09.2012, address: [http://www.midmichigansae.org/presentations/SAEFrankenmuth10\\_10\\_08.pptx](http://www.midmichigansae.org/presentations/SAEFrankenmuth10_10_08.pptx)
- [39] **Francfort, J.** (2010). Electric Vehicle Charging Levels and Requirements Overview. *Clean Cities December 2010 Webinar*. Date retrieved: 12.09.2012, address: 2012, [https://www1.eere.energy.gov/cleancities/toolbox/pdfs/ev\\_charging\\_requirements.pdf](https://www1.eere.energy.gov/cleancities/toolbox/pdfs/ev_charging_requirements.pdf)
- [40] **Kissel, G.** (2010). SAE J1772™ Update for IEEE Standard 1809 Guide. *Electric-Sourced Transportation Infrastructure Meeting*. Date retrieved: 12.09.2012, address: [http://grouper.ieee.org/groups/earthobservations/SCC/IEEE\\_SAE\\_J1772\\_Update\\_10\\_02\\_08\\_Gery\\_Kissel.pdf](http://grouper.ieee.org/groups/earthobservations/SCC/IEEE_SAE_J1772_Update_10_02_08_Gery_Kissel.pdf)
- [41] **Bernal Agustin, J. L., and Dufo Lopez, R.** (2009) Simulation and Optimization of Stand-Alone Hybrid Renewable Energy Systems. *Renewable and Sustainable Energy Reviews*, Vol. **13**, pp. 2111-2118.

- [42] **Fadee, M., and Radzi, M. A.** (2012). Multi-Objective Optimization of a Stand-Alone Hybrid Renewable Energy System by Using Evolutionary Algorithms: A review. *Renewable and Sustainable Energy Reviews*, Vol. **16**, pp. 3364-3369.
- [43] **Hafez, O., and Bhattacharya, K.** (2012). Optimal Planning and Design of a Renewable Energy Based Supply System for Microgrids. *Renewable Energy*, Vol. **45**, pp. 7-15.
- [44] **Erdinc, O., and Uzunoğlu, M.** (2012). Optimum Design of Hybrid Renewable Energy Systems: Overview of different approaches. *Renewable and Sustainable Energy Reviews*, Vol. **16**, pp. 1412-1425.
- [45] **Gupta, A., Saini, R. P., and Sharma, R. P.** (2011). Modelling of Hybrid Energy SystemdPart II: Combined dispatch strategies and solution algorithm. *Renewable Energy*, Vol. **36**, pp. 466-473.
- [46] **Kohsri, S., and Plangklang, B.** (2011). Energy Management and Control System for Smart. *Energy Procedia*, Vol. **9**, pp. 198-296.
- [47] **Jeong, K., Lee, W., Kim C.** (2005). Energy Management Strategies of a Fuel Cell/Battery Hybrid System Using Fuzzy Logics. *Journal of Power Sources*, Vol. **145**, pp. 319-326.
- [48] **Tofighi, A., and Kalantar, M.** (2011). Power Management of PV/Battery Hybrid Power Source via Passivity-Based Control. *Renewable Energy*, Vol. **36**, pp. 2440-2450.
- [49] **Benysek, G., and Jarnut, M.** (2012). Electric Vehicle Charging Infrastructure in Poland. *Renewable and Sustainable Energy Reviews*, Vol. **16**, pp. 320-328.
- [50] **Li-wei, W., and Dian-long, W.** (2012). Digital Charger Powersource for Electric Vehicle Based on TMS320LF2407A. *Procedia Engineering*, Vol. **29**, pp. 99-104.
- [51] **Gallardo-Lozano, J., Milanés-Montero, M. I., and Guerrero-Martínez, M. A.** (2012). Electric Vehicle Battery Charger for Smart Grids. *Electric Power Systems Research*, Vol. **90**, pp. 18-29.
- [52] **Birnie III, D. P.** (2009). Solar-to-vehicle (S2V) Systems for Powering Commuters of the Future. *Journal of Power Sources*, Vol. **186**, pp. 539-542.
- [53] **Suppes, G. J.,** 2005: Plug-in Hybrid with Fuel Cell Battery Charger. *International Journal of Hydrogen Energy*, Vol. **30**, pp. 113-121.
- [54] **Villa, J. L., Sallan, J., Llombart, A., and Sanz, J. F.** (2009). Design of a High Frequency Inductively Coupled Power Transfer System for Electric Vehicle Battery Charge. *Applied Energy*, Vol. **86**, pp. 355-363.

## **CURRICULUM VITAE**



**Name Surname:** Taha Nurettin GÜCİN

**Place and date of birth:** Elazığ – 19/05/1987

**Address:** Yalova University, Engineering Faculty,  
Kazım Karabekir Mah., Rahmi Üstel Cad. No:1,  
77100, Yalova - TURKEY

**E-Mail:** tngucin@yalova.edu.tr

### **Universities and Colleges attended:**

Istanbul Technical University, Electrical Engineering  
Department, 2010

RWTH Aachen, Electrical Engineering Department,  
Erasmus Student Exchange Program, 2007 – 2008

St. Georg Austrian College, 2006

### **Professional Experience and Rewards:**

Research and Teaching Assistant, Energy Systems  
Engineering Department, Yalova University, Since  
2010